



MÁSTER BIOTECNOLOGÍA BIOMÉDICA – UPV
Módulo IV: ENFERMEDADES CARDIOVASCULARES
(Patrocinio Cátedra Cardiovascular EVES / FERRER/ UPV)

 
Cátedra Empresa
"Cardiovascular EVES/FERRER"

Identificación de dianas terapéuticas. Síndrome de progeria de Hutchinson-Gilford

José María González-Granado

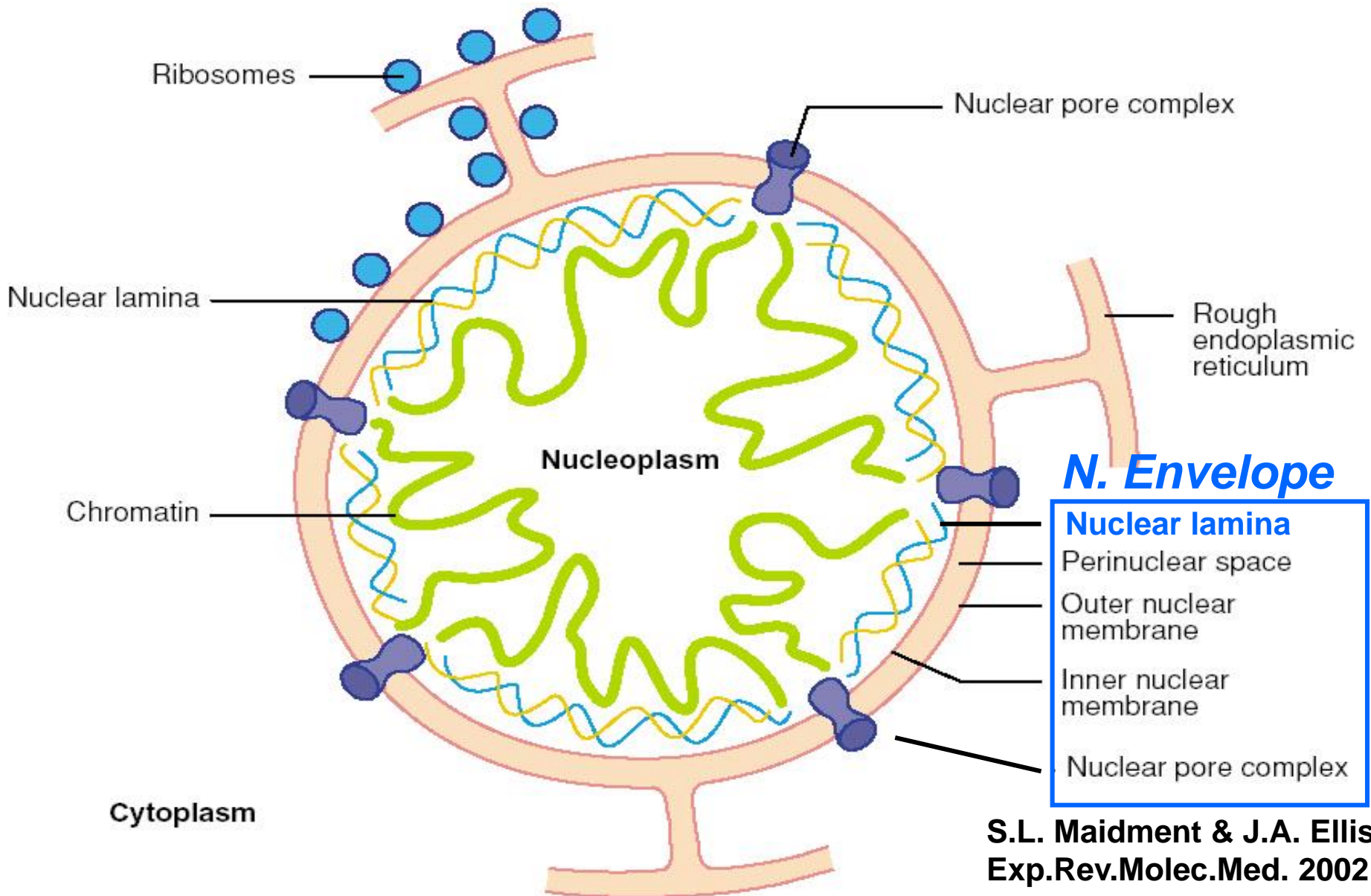
Instituto de Investigación Hospital 12 de Octubre (i+12)
Centro Nacional de Investigaciones Cardiovasculares (CNIC)



CFP Lamin A

By Dr. JM González

The major architectural components of the mammalian nuclear envelope



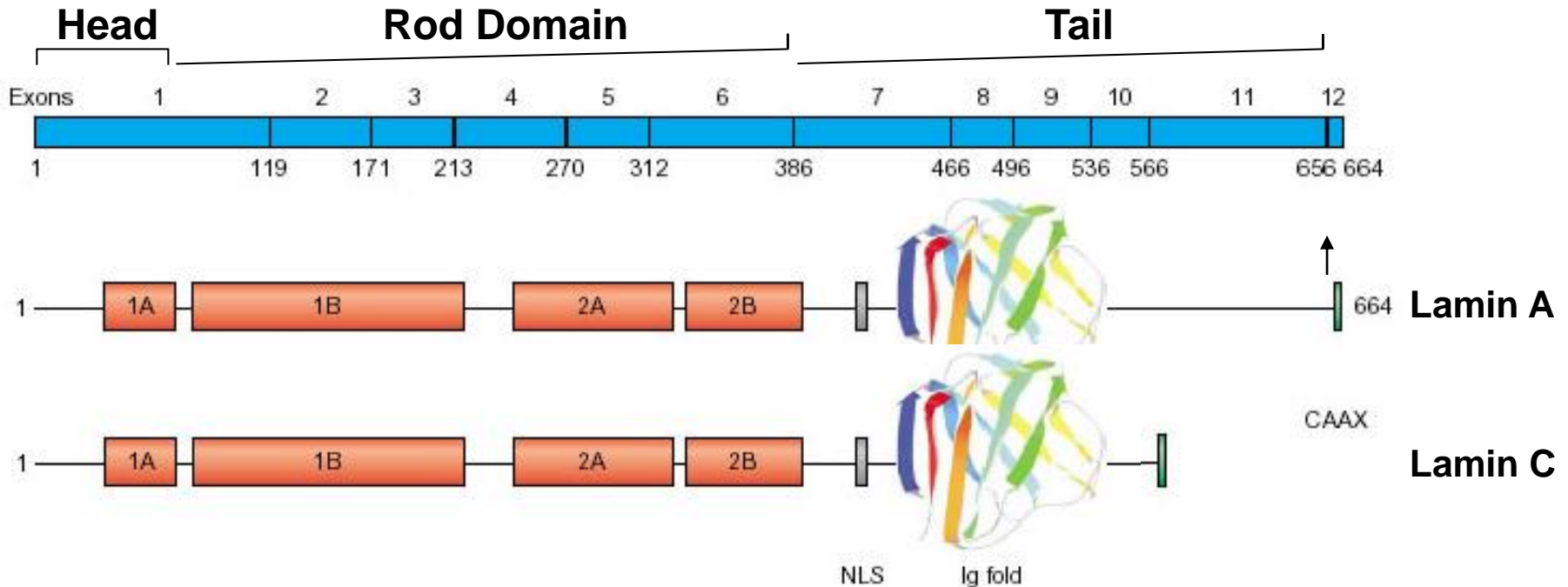
Lamin genes:

Lamin A/C (splicing variants *LMNA* gene)

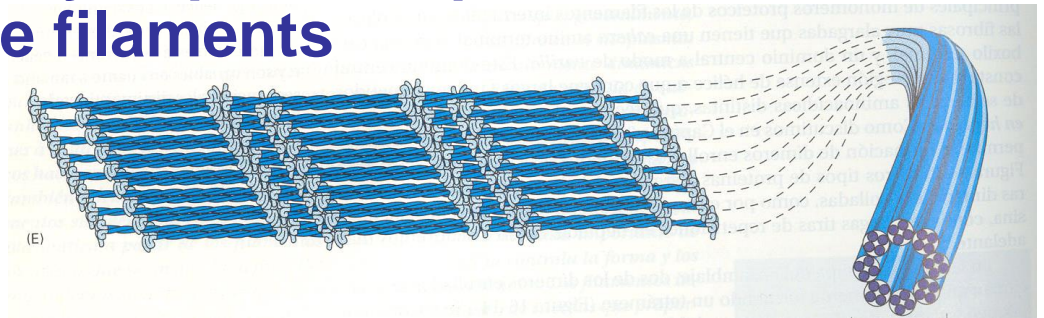
Lamin B1 (*LMNB1* gene)

Lamin B2-B3 (splicing variants *LMNB2* gene)

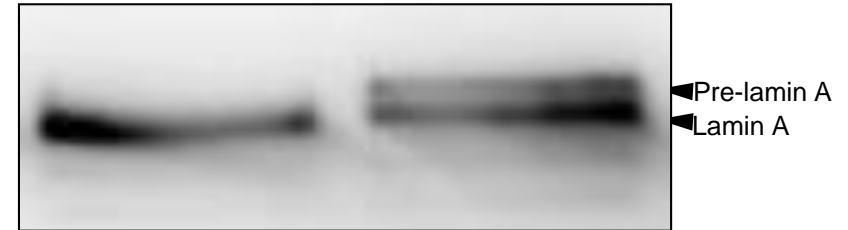
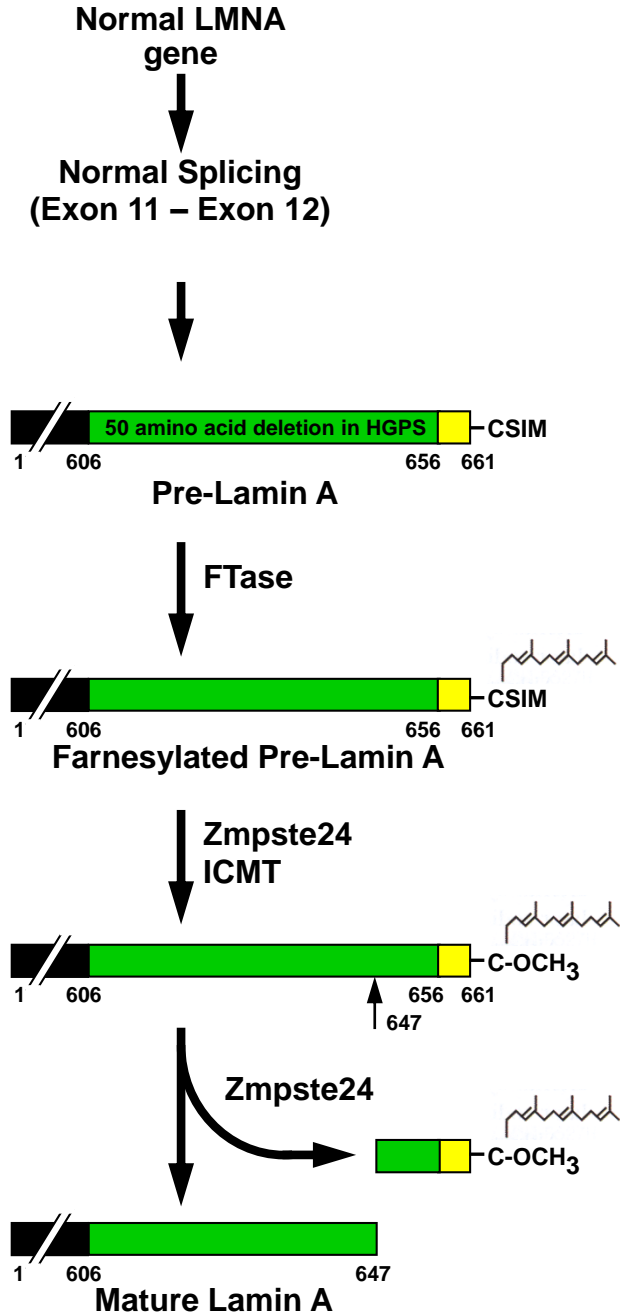
Lamin A and Lamin C (alternative splicing)



Lamin A/C are ubiquitously expressed proteins which form Type V intermediate filaments



Lamin A/C maturation



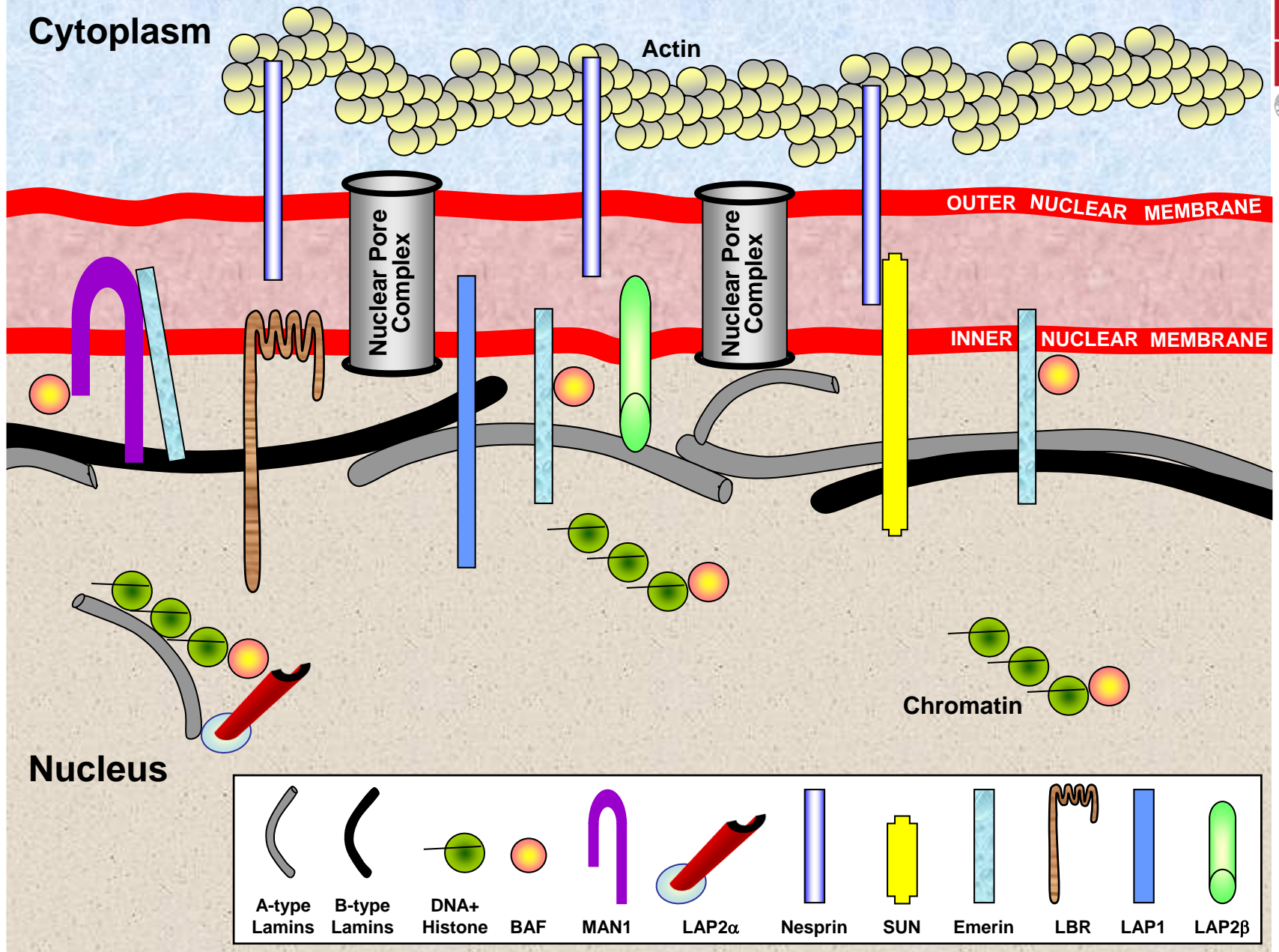
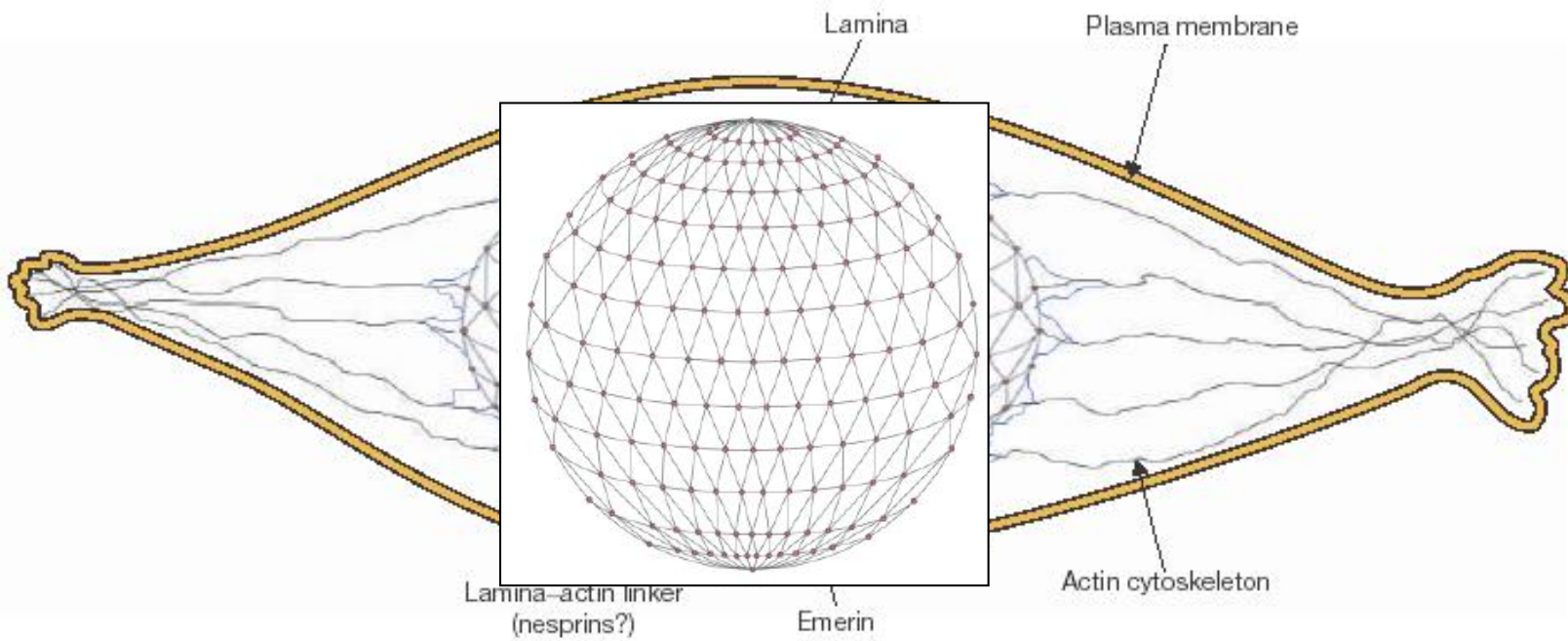


Figure 1 Schematic illustration of the mammalian nuclear envelope showing the localization of lamina and laminin-interacting proteins. Chromatin can interact with both nucleoplasmic and NE-anchored A-type lamins

LAMIN A/C

FUNCTIONS

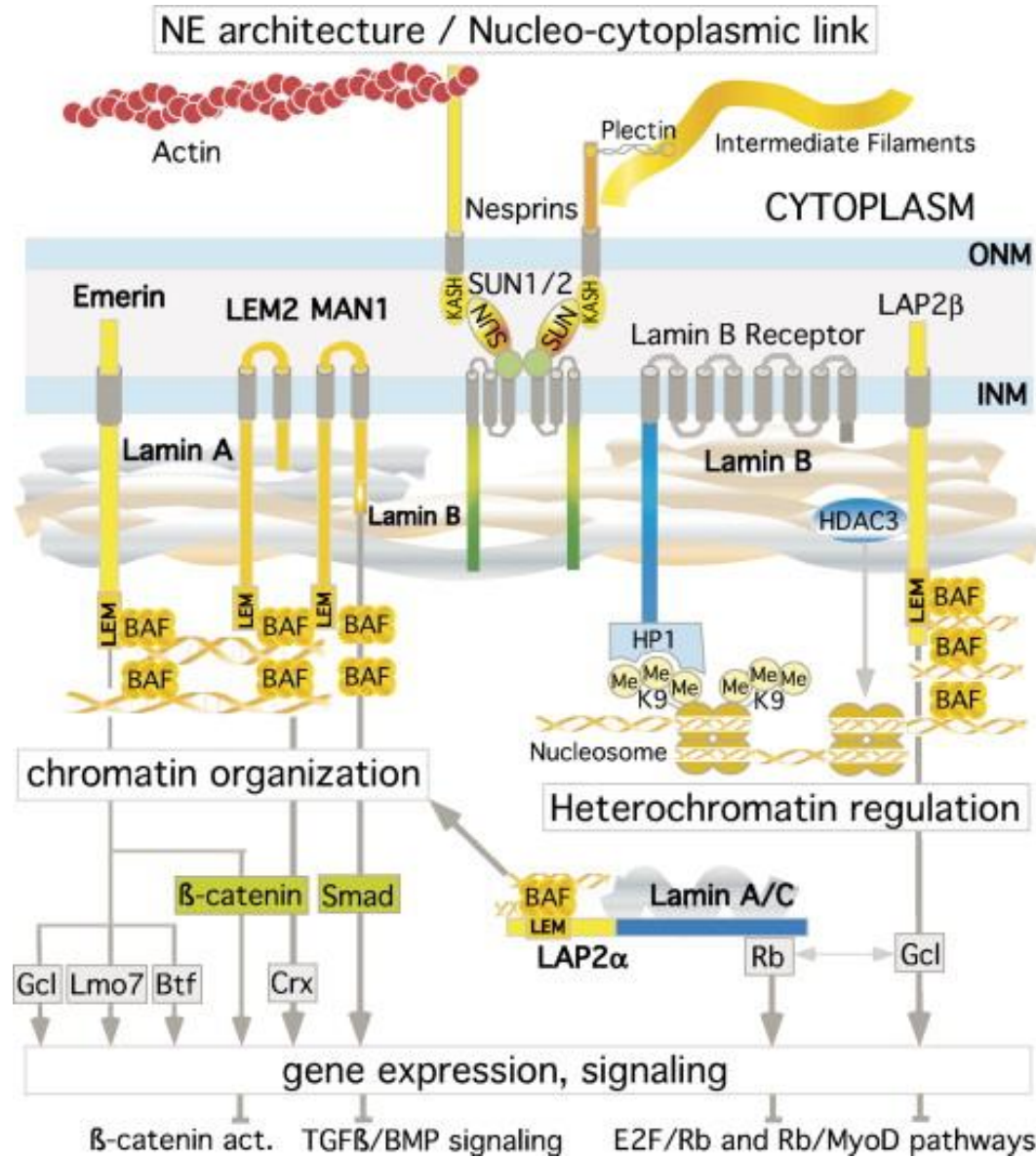
Structural



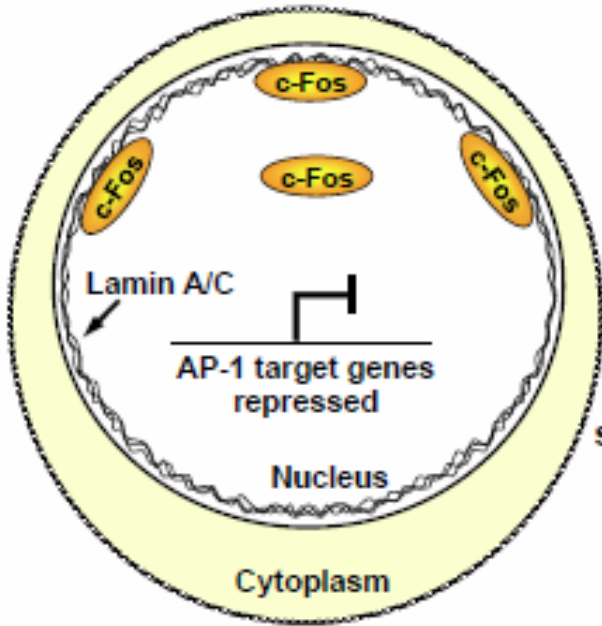
Nuclear positioning and cell migration

Hutchinson & Worman. *Nat. Cell Biol.* 6: 1062-1067. 2004

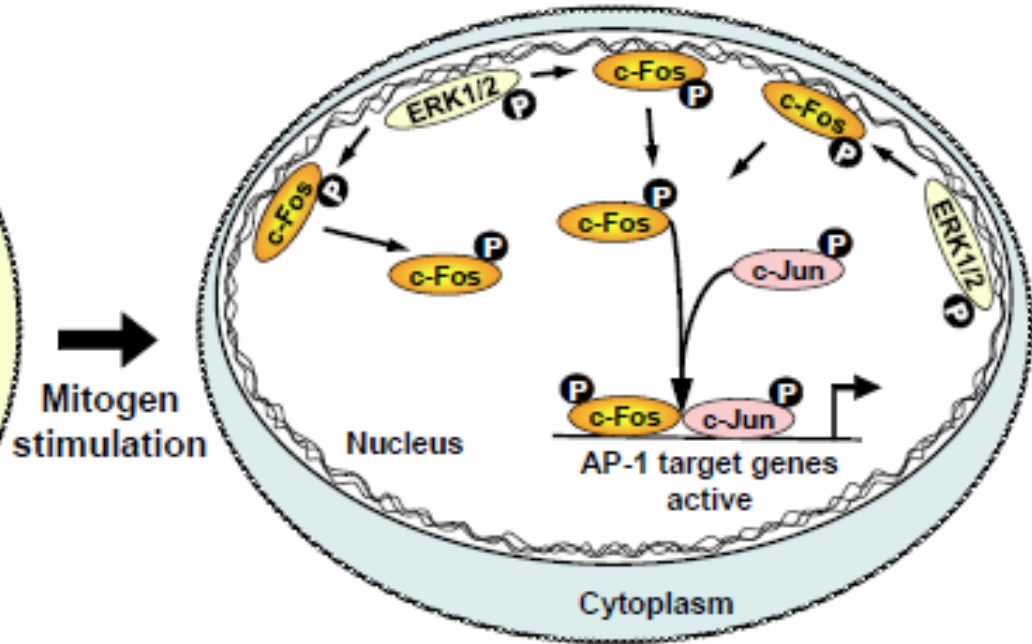
Chromatin organization, Gene expression, Signalling...




ERK1/2 signaling **OFF**
Serum-starved cell

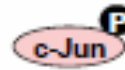


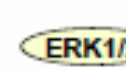
ERK1/2 signaling **ON**
Serum-stimulated cell (very early response)



Mitogen
stimulation

 Phospho-c-Fos

 Phospho-c-Jun

 Phospho-ERK1/2

Laminin A/C mutations linked to human diseases (laminopathies)

specific tissues

Striated Muscle **Emery–Dreifuss Muscular Dystrophy/AD-EDMD**
Dilated Cardiomyopathy/CMD1A
Limb-Girdle Muscular Dystrophy/LGMD1B

Muscle and Neurons **Charcot–Marie–Tooth disorder/AR-CMT2B1**

Adipose Tissue **Familial Partial Lipodystrophy**

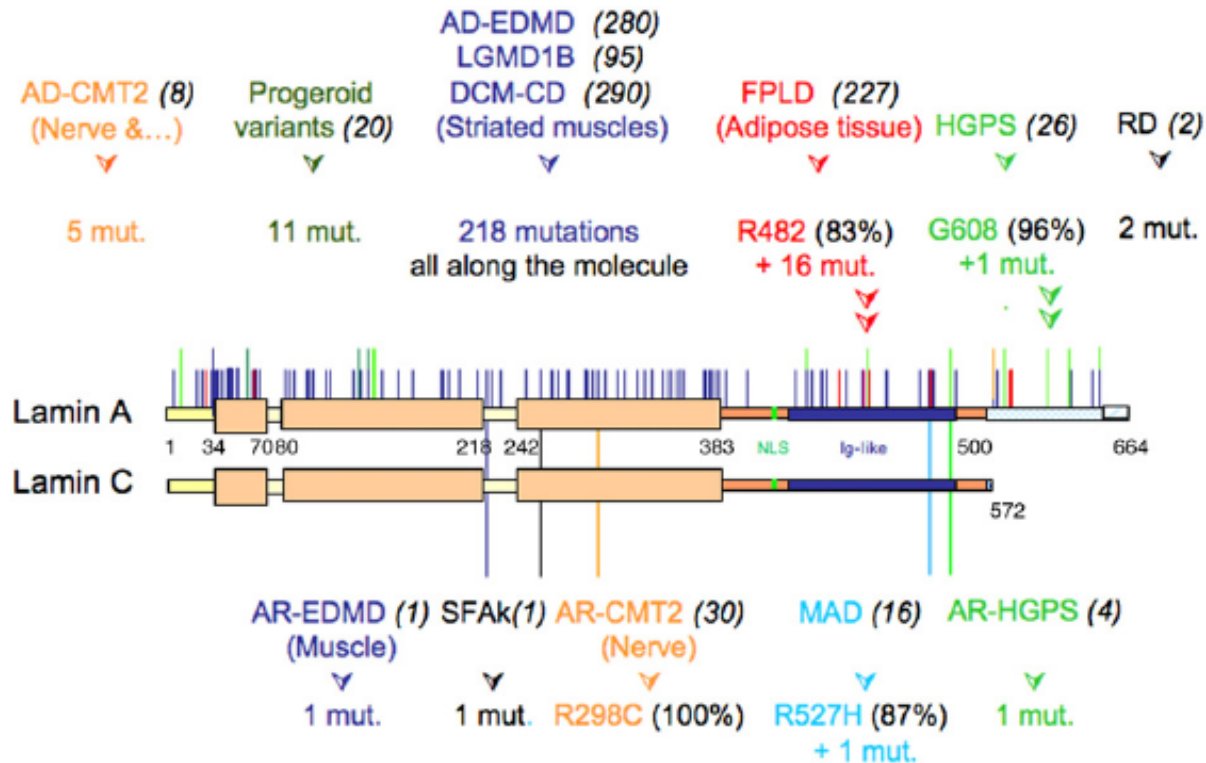
Adipocytes and Bone **Mandibuloacral Dysplasia**

**Human Progeroid Syndromes
affecting multiple tissues**

Hutchinson–Gilford Progeria Syndrome 
Atypical Werner's Syndrome
Restrictive Dermopathy

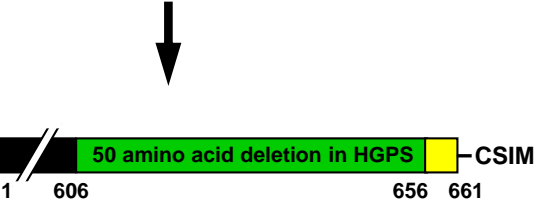
1 in 4×10^6 live births

How do different mutations in LMNA ,a protein expressed in most differentiated somatic cells, cause different tissue-specific disease phenotypes?



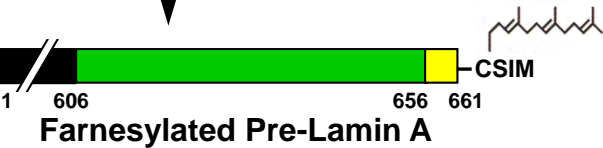
Hutchinson–Gilford Progeria Syndrome Human Fibroblast

Normal LMNA gene
 ↓
 Normal Splicing
 (Exon 11 – Exon 12)



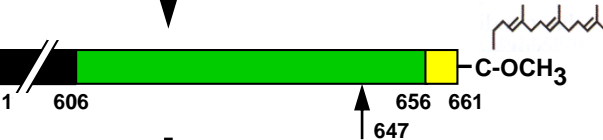
Pre-Lamin A

FTase



Farnesylated Pre-Lamin A

Zmpste24
ICMT



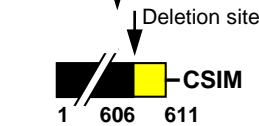
Zmpste24



Mature Lamin A

Mutant LMNA
 HGPS patient

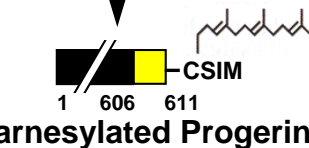
Aberrant Splicing
 Exon 11 – Exon 12
 Deletion of 150 Nucleotides
 Deletion of 50 amino acids



Pre-Progerin

(Cleavage site for Zmpste24 deleted)

FTase



Farnesylated Progerin

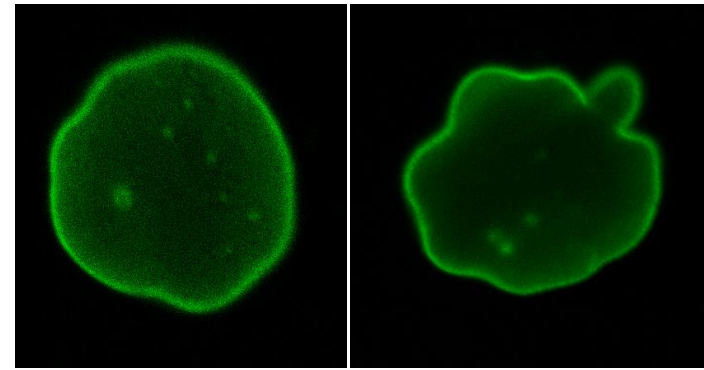
Zmpste24
ICMT



Mature Progerin

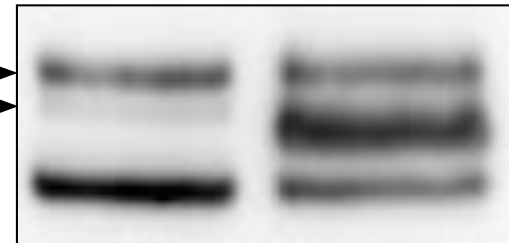
Control

HGPS



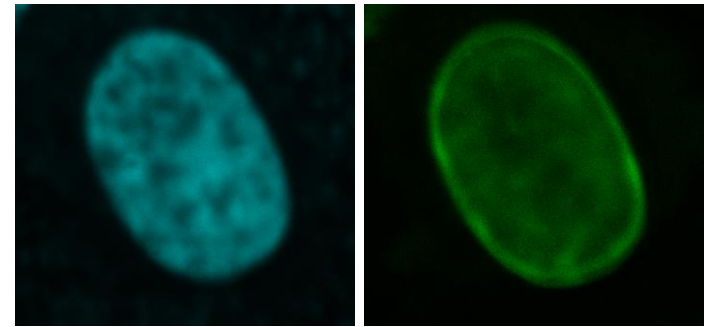
anti-Lamin A

Lamin A



Lamin A
 Progerin
 Lamin C

U2O2 transfected cells



Wild-type
 HA-Lamin A

HA-Progerin

TOPRO

anti HA

Hutchinson–Gilford Progeria Syndrome

- Premature ageing
- Alopecia
- Loss of subcutaneous fat
- Myocardial infarction or stroke by an average age of 13 years
- Premature atherosclerosis



- dramatic loss of vascular smooth muscle cells.
- increased fibrous material
- calcification
- breaks in elastin structure
- intimal thickening

Disease-causing mechanisms

Structural hypothesis { Reduced mechanical stiffness and increased fragility.

Defective mechanotransduction and enhanced cell death

Cell damage in mechanically stressed tissues

Nesprin

Gene Regulation Hypothesis

Chromatin organization and gene expression

Control of transcription factors

c-Fos

SREBP1c

SMADS

Cell Proliferation and Defective Differentiation Hypothesis

LAP2α

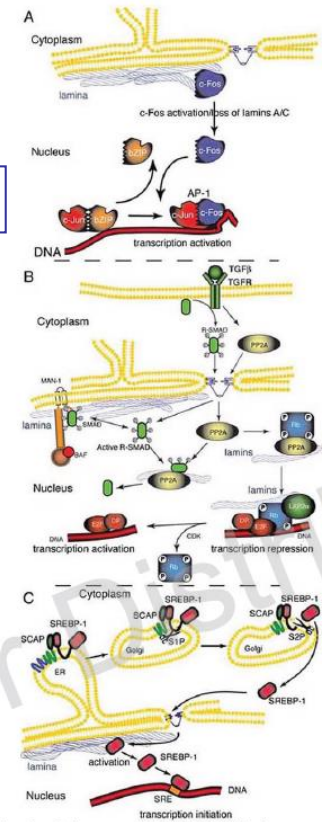
pRb

DNA-repair Hypothesis

p53

Prelamin A toxicity Hypothesis

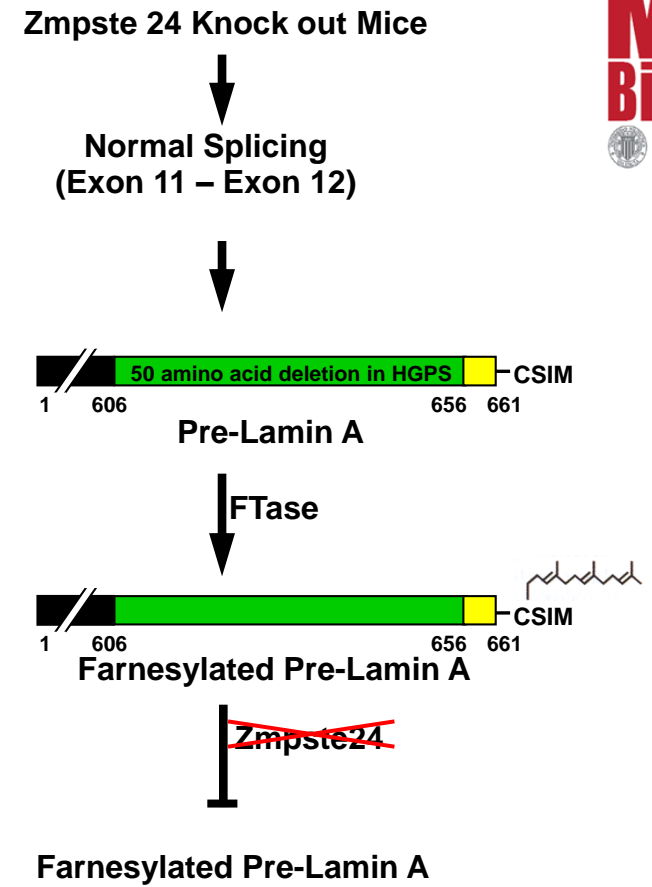
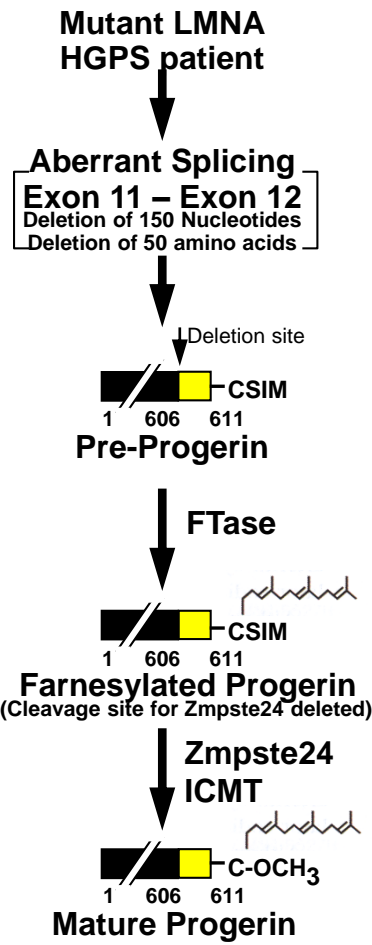
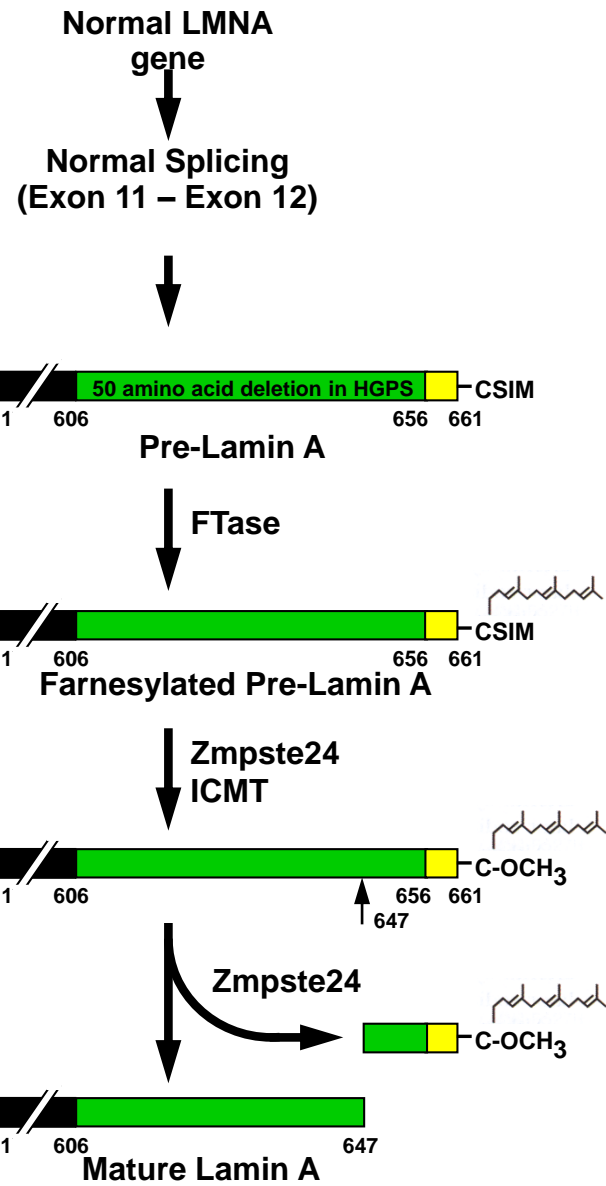
Senescence, telomere shortening, decreased capacity to propagate in subculture, and decreased repair capacity.



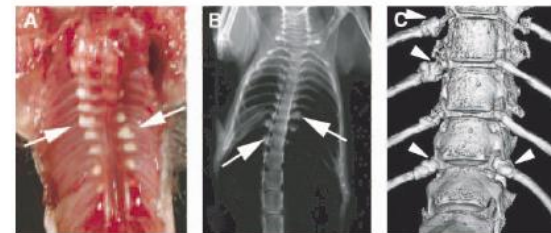
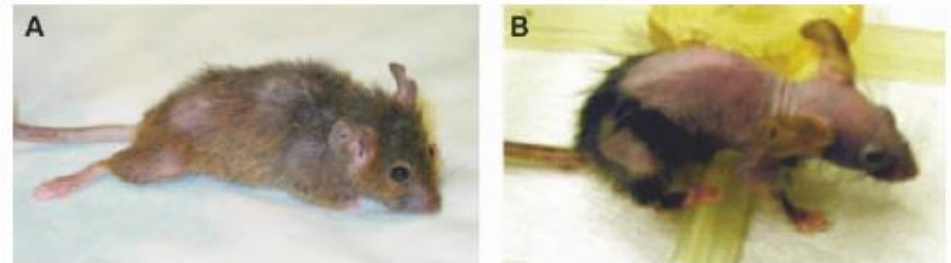
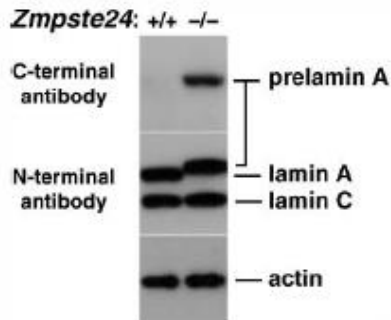
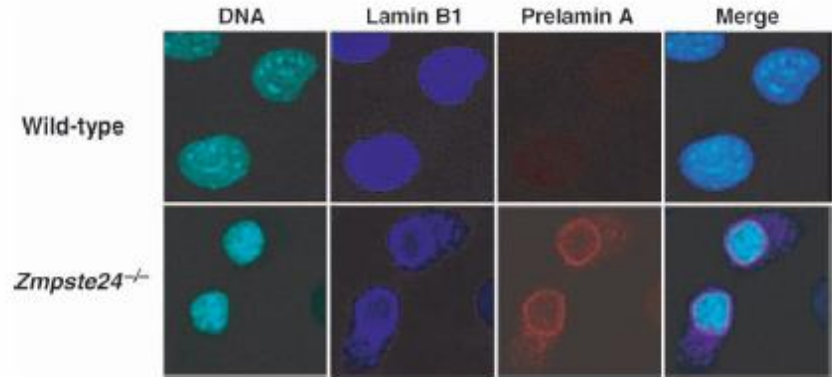
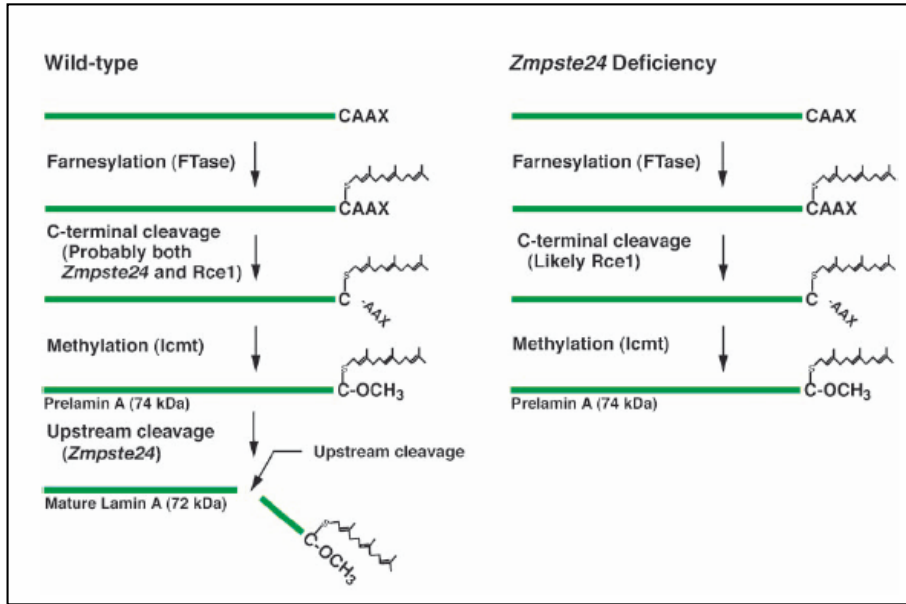
Summary of Mouse Models of Laminopathies

Mutation	Mutations introduced into Mouse Lamin genes		Ref
	Description	Phenotype	
<i>Lmna</i> ^{-/-}	Lamin A and C Null	Postnatal lethality associated with muscular dystrophy and cardiomyopathy	[19]
<i>Lmna</i> ^{N195K/N195K}	Mis-sense mutation	Postnatal death associated with cardiomyopathy	[25]
<i>Lmna</i> ^{H222P/H222P}	Mis-sense mutation	Postnatal death associated with muscular dystrophy and cardiomyopathy	[24]
<i>Lmna</i> ^{Δ9/Δ9}	Splicing mutation and inframe deletion of exon 9	Early postnatal lethality and a model for progeria	[54]
<i>Lmna</i> ^{HG/HG}	A-type lamins are replaced by Progerin	Heterozygotes die at 6 months with osteoporosis, alopecia. Homozygotes severely retarded postnatal growth, death at 3 weeks	[55]
<i>Lmna</i> ^{LOO/LOO}	Lamin C only mice with no Lamin A	Overtly normal	[58]
<i>Lmnb1</i> ^{-/-}	Gene trap insertion into <i>Lmnb1</i>	Perinatal lethal possibly due to respiratory failure	[62]
Mutations in proteins associated with Lamin A			
<i>Emd</i> ^{-/-}	Null	Mice overtly normal but with slightly retarded muscle regeneration	[21,23]
<i>Zmpste24</i> ^{-/-}	Null	Mice retain farnesylated pre-lamin A. They die at 6–7 months and have rib fractures, osteoporosis, muscle weakness	[69,74]
Transgenic Lines			
<i>Lmna</i> M371K	cDNA with missense mutation	Expressed in heart resulting in cardiomyopathy and early postnatal lethality	[26]
<i>Lmna</i> BAC G608G	hBAC with G606g base change	Mice show progressive loss of smooth muscle cells in medial layer of large arteries	[57]

Lmna^{G609G/G609G}

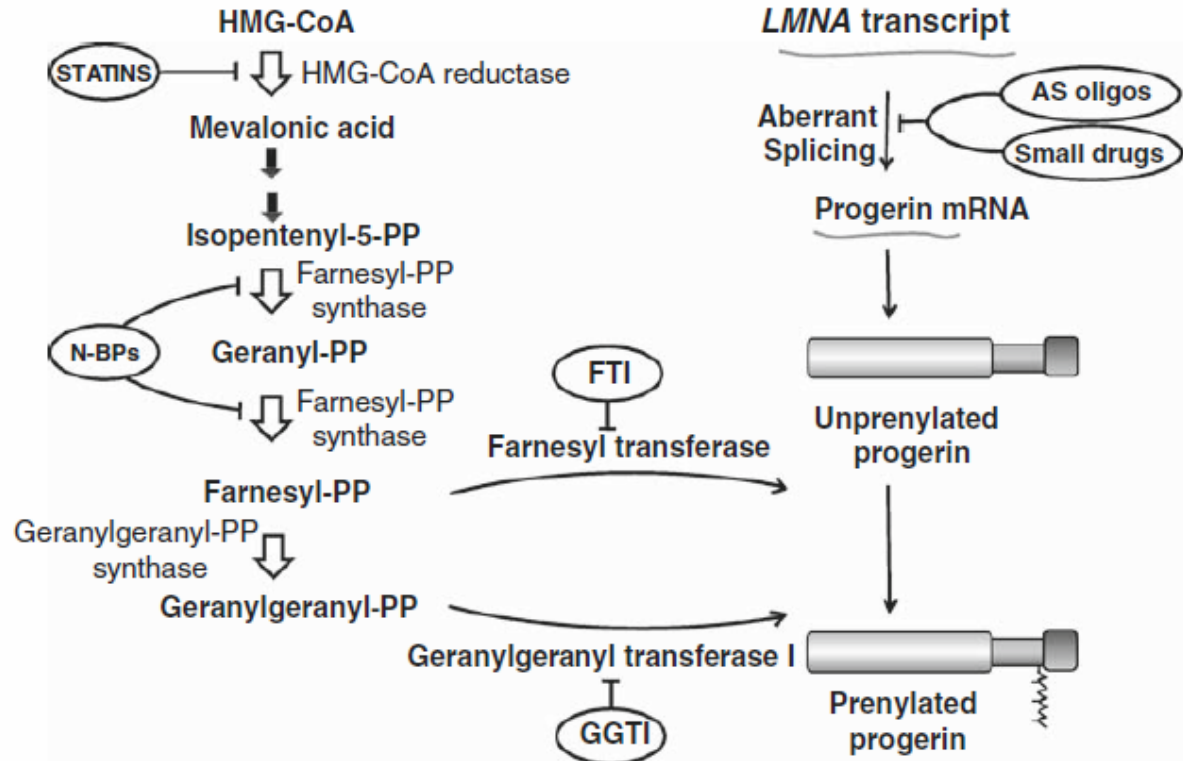


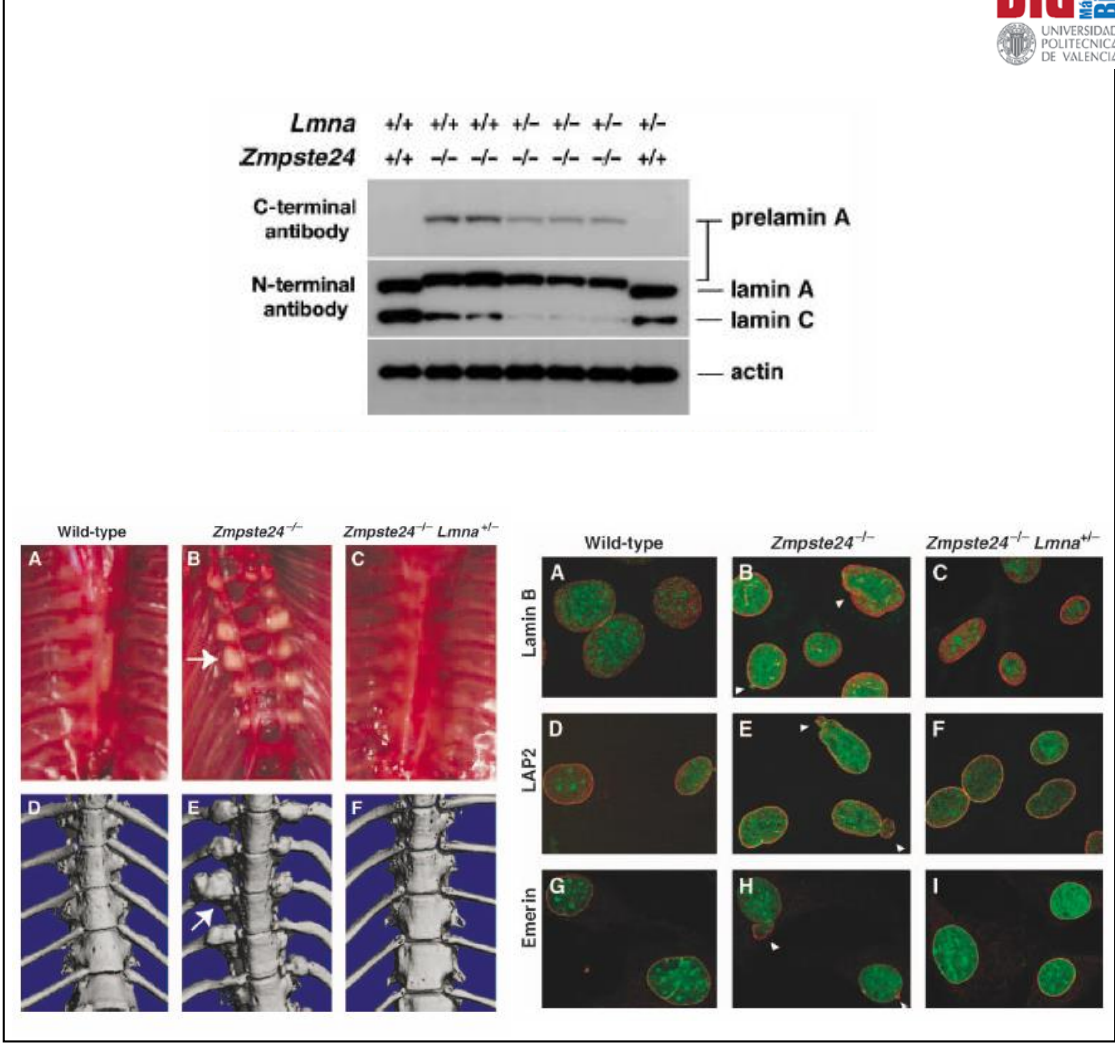
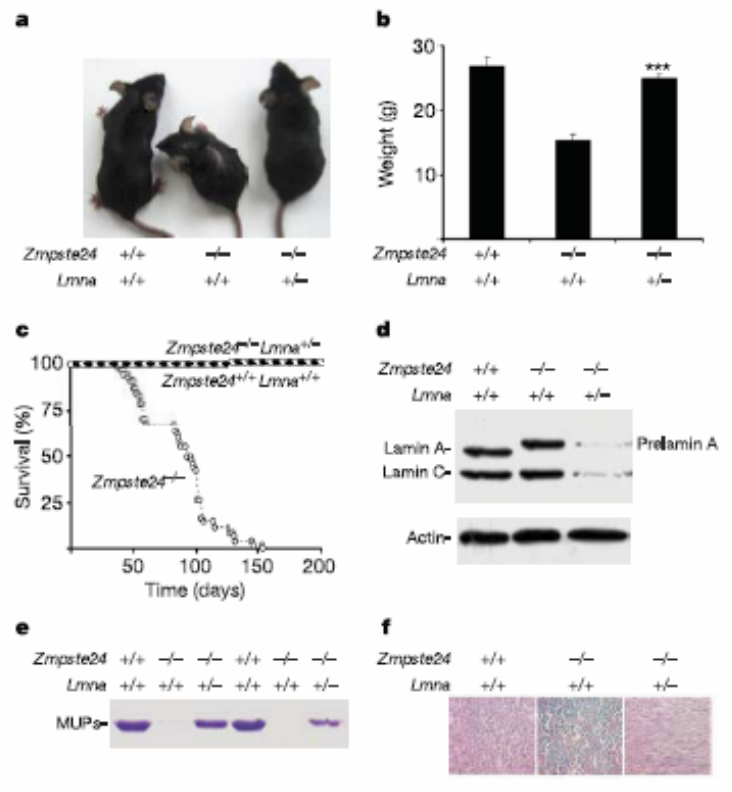
Zmpste24^{-/-}



Therapeutic approaches

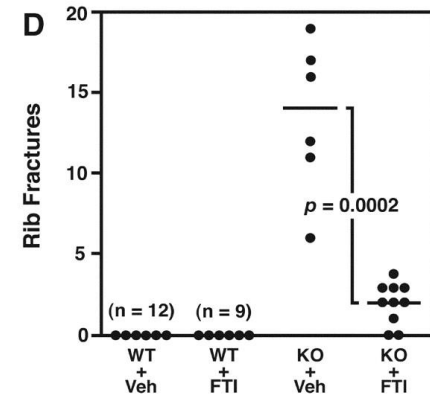
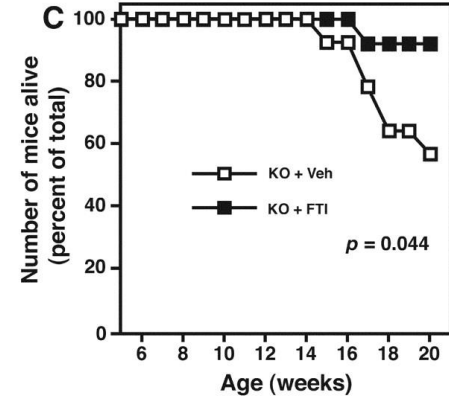
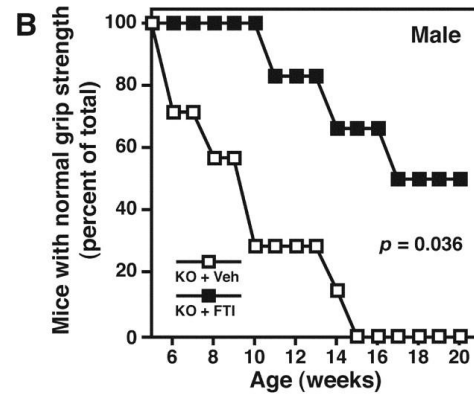
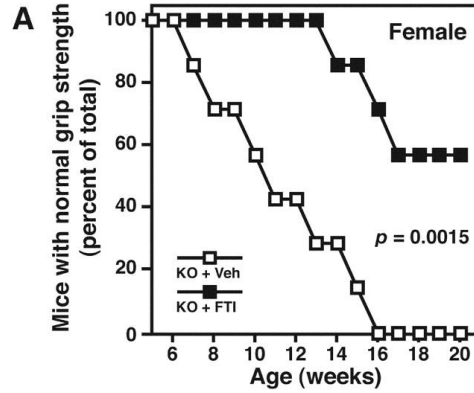
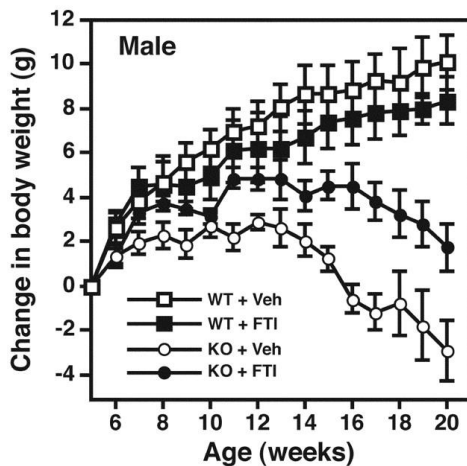
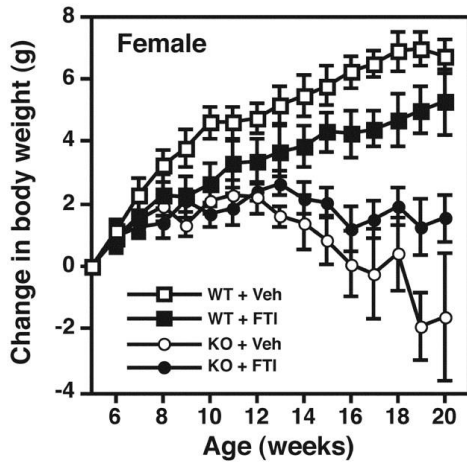
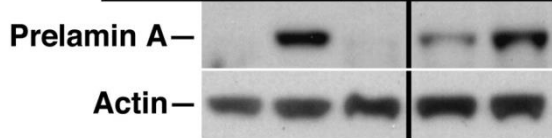
Fig. 2 Therapeutic options to prevent the accumulation of prenylated progerin. The possibilities discussed include compounds acting on the mevalonate pathway such as statins, and aminobisphosphonates (N-BPs), farnesyltransferase inhibitors (FTI), geranylgeranyltransferase inhibitors (GGTI), and agents designed to block the alternative splicing event that leads to progerin synthesis such as small drugs or specific antisense oligonucleotides (AS oligos)





Nature. 2005 Sep 22;437(7058):564-8.

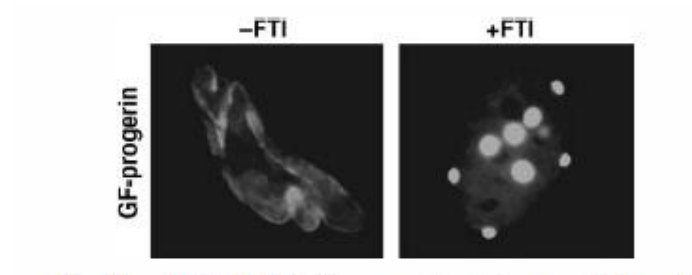
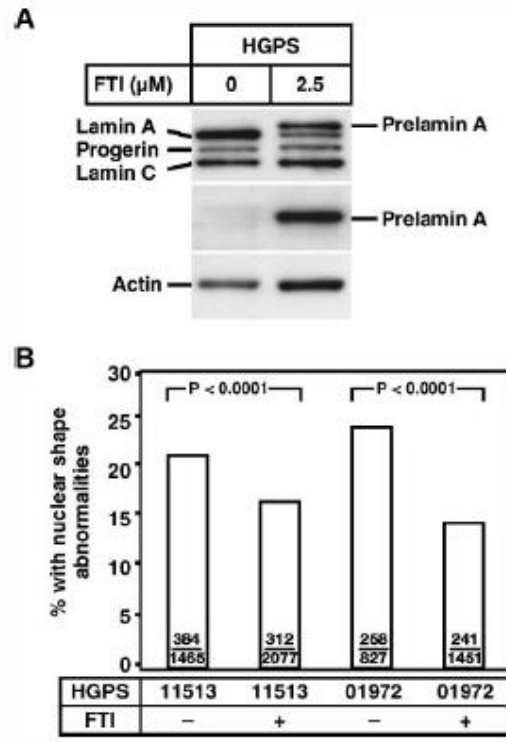
	cells		mouse tails		
FTI	-	+	-	+	+



Fong et al. Science 2006 (311)5767,1621 - 1623

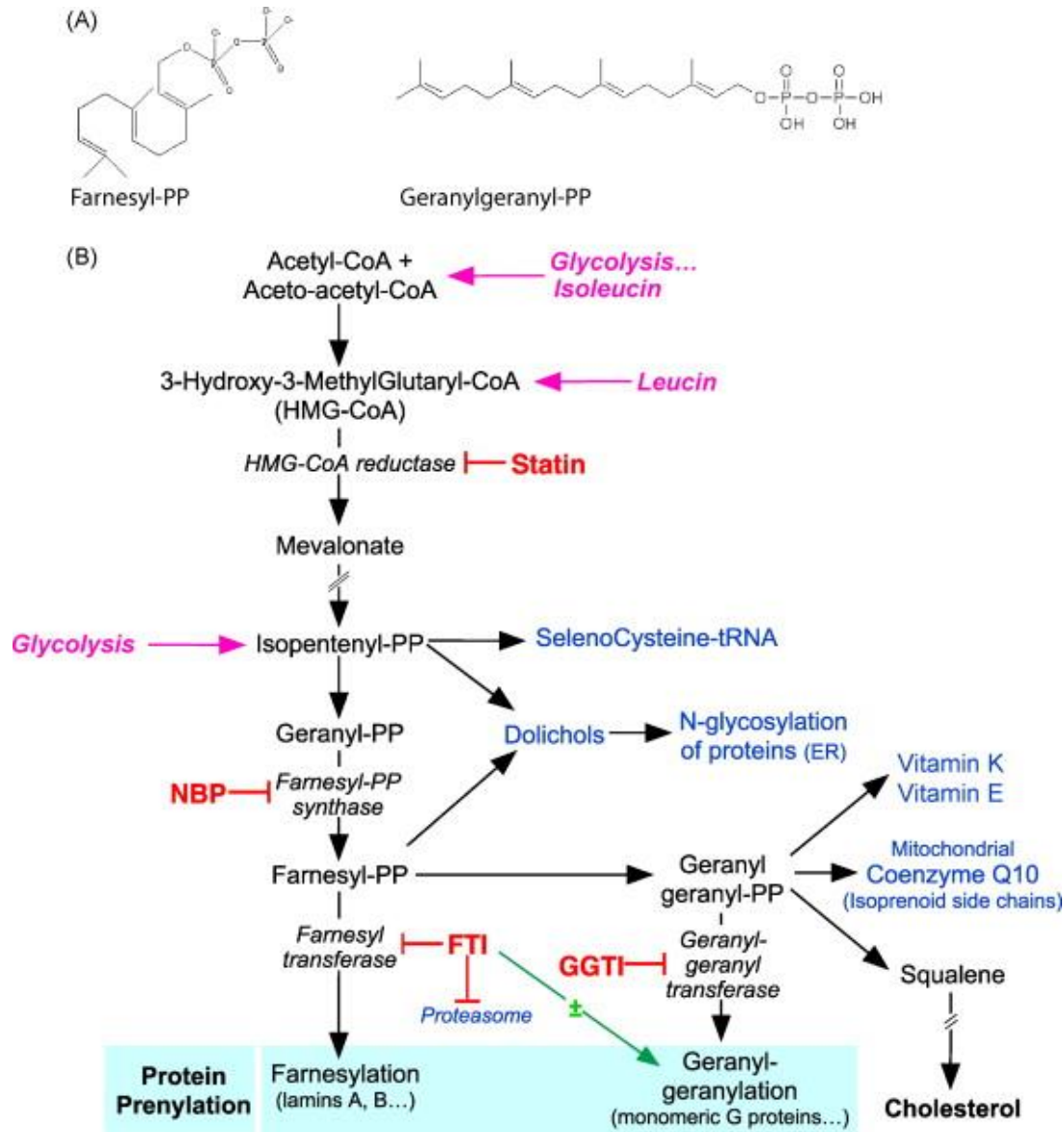
FTI treatment

FTI effects on HGPS fibroblast

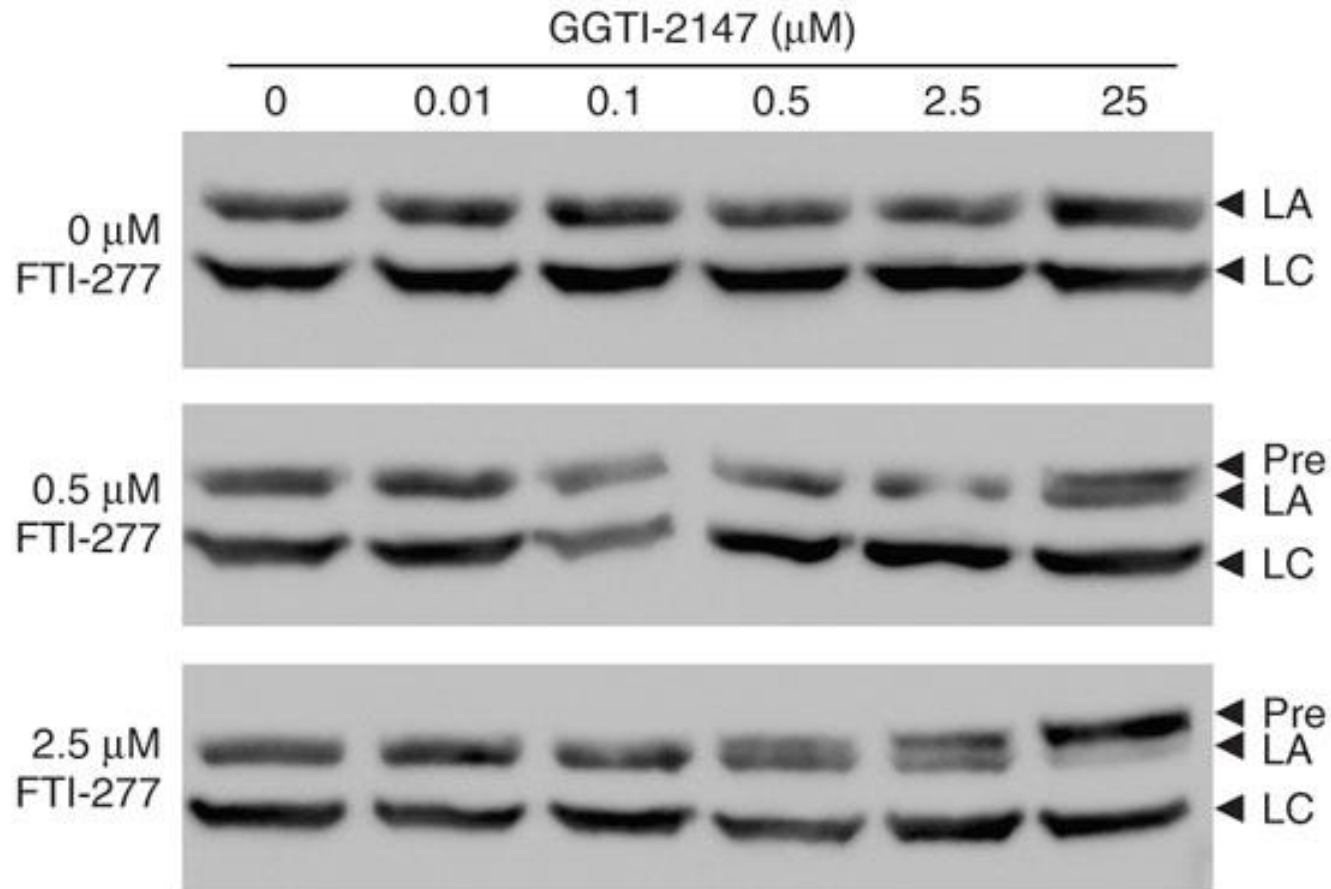


FTI treatment reverses the nuclear morphology alterations resulting from the expression of GFP-progerin

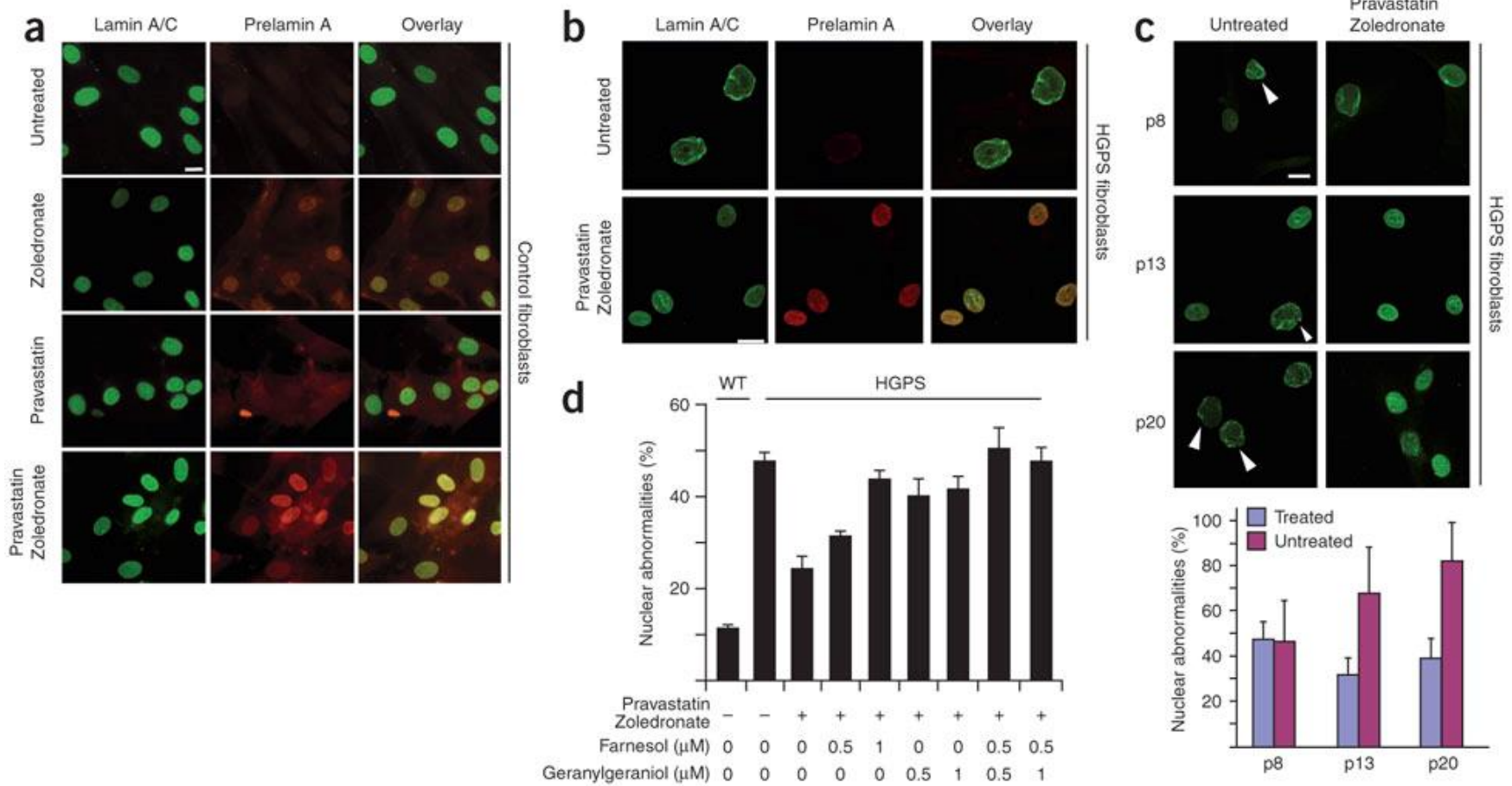
The effects of an FTI on the frequency of misshapen nuclei in human HGPS fibroblast

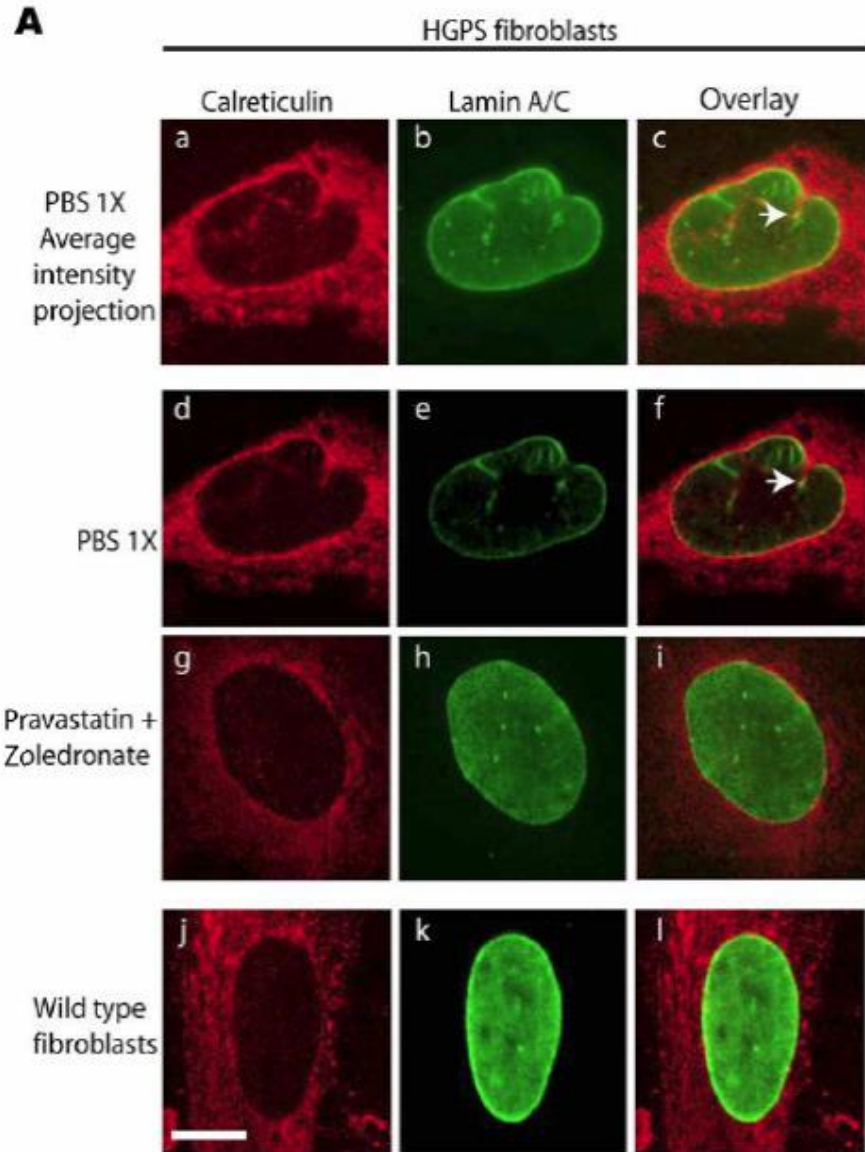


Combination of statins and aminobisphosphonates

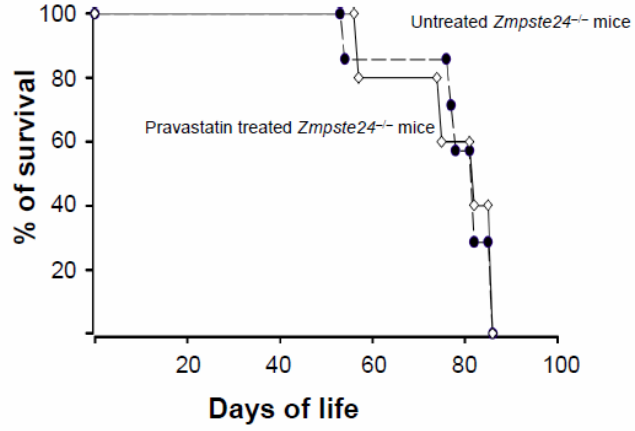


Synergistic effect of pravastatin and zoledronate on prelamin A accumulation in normal and HGPS fibroblast nuclei

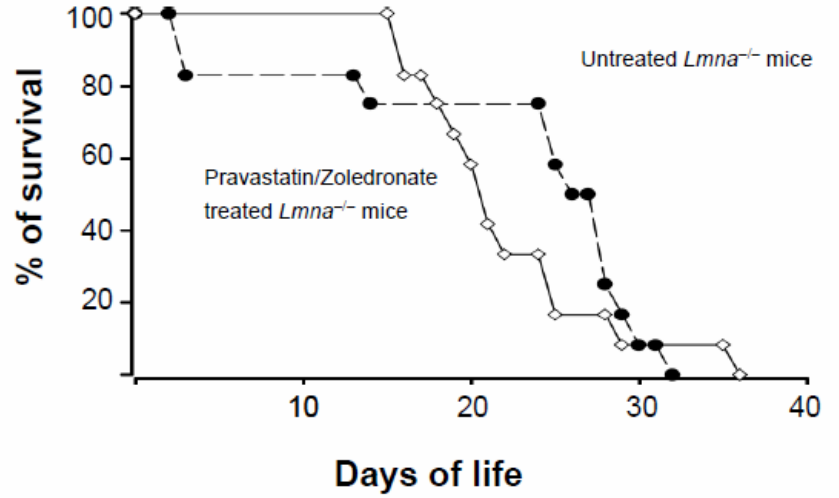
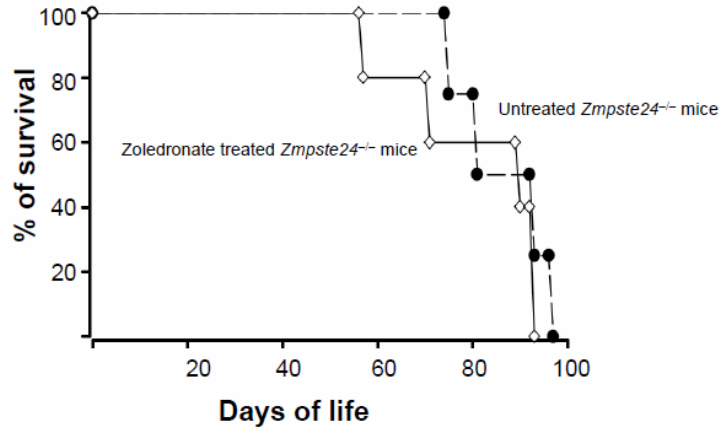




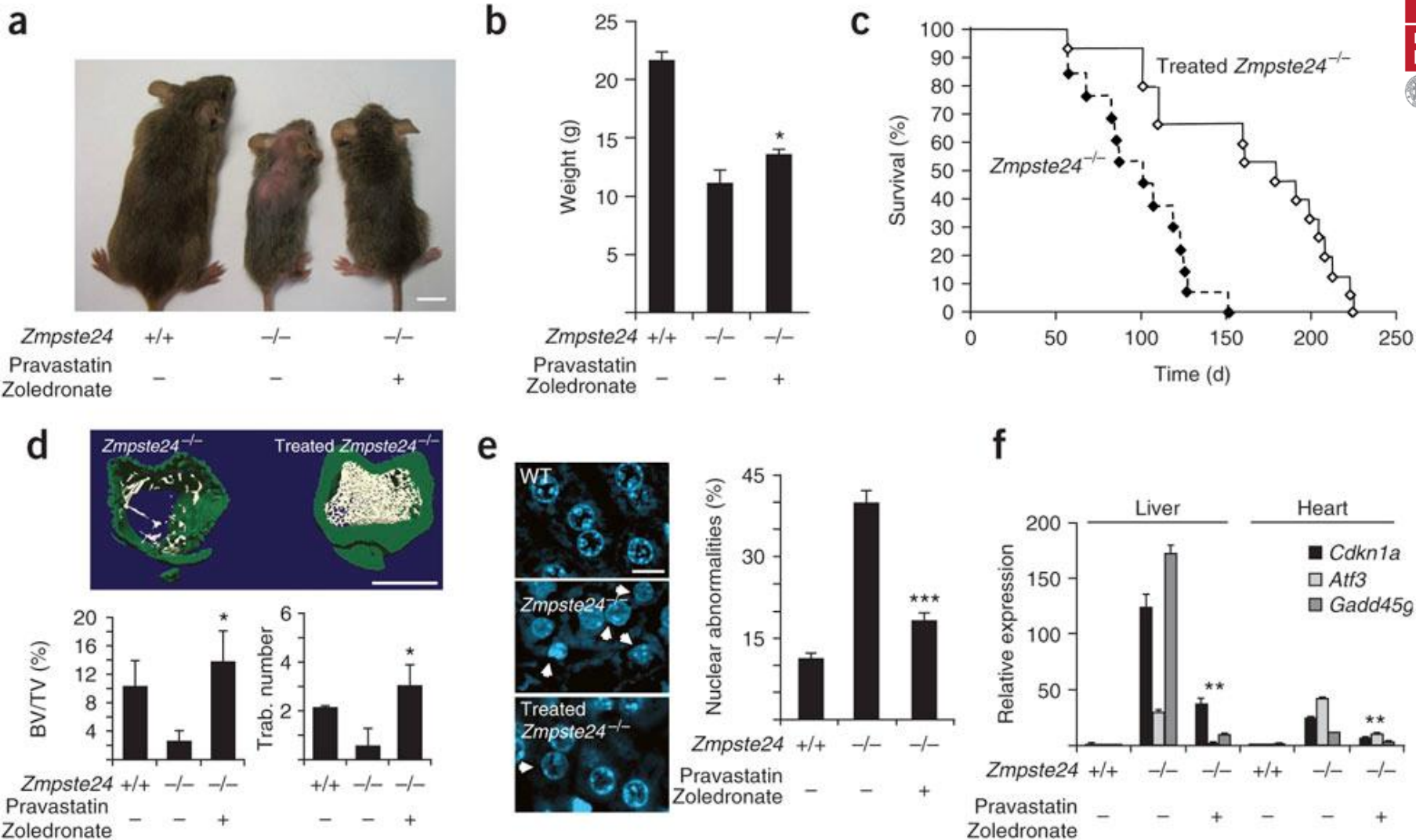
a



b



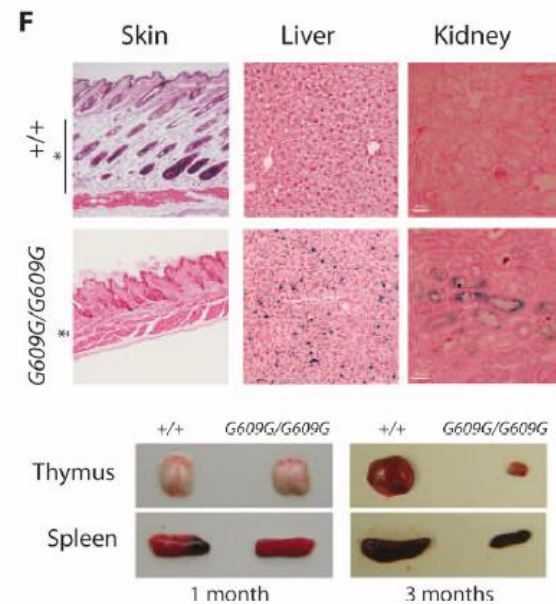
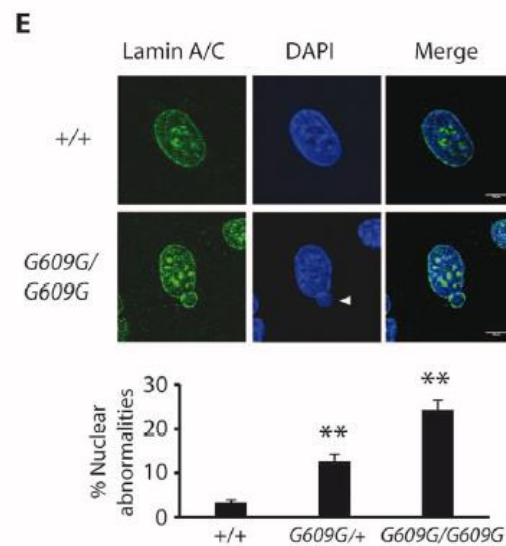
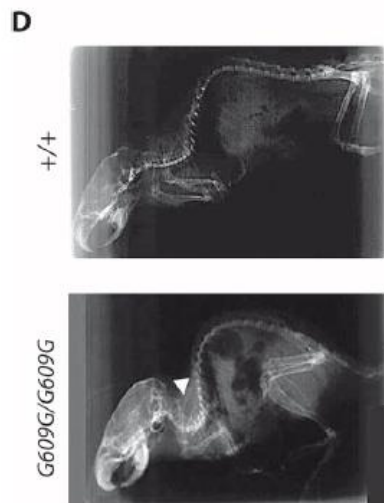
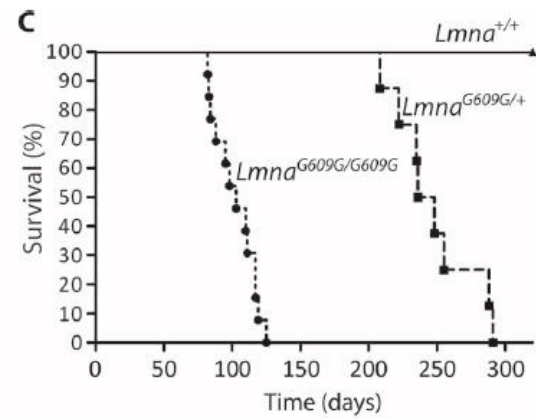
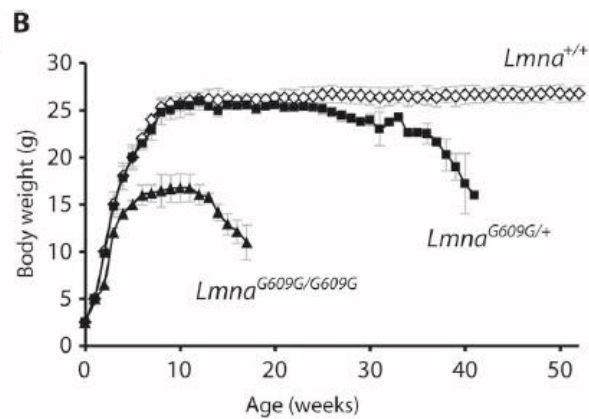
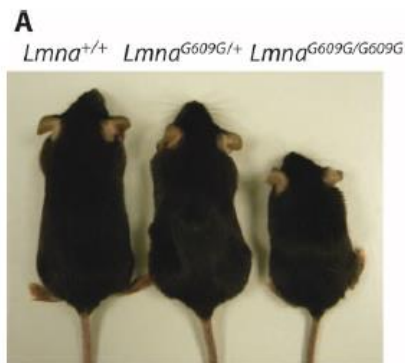
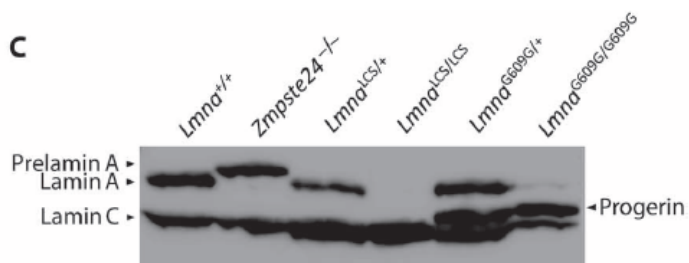
Combined treatment with statins and aminobisphosphonates ameliorates *Zmpste24*^{-/-} mouse progeroid phenotypes

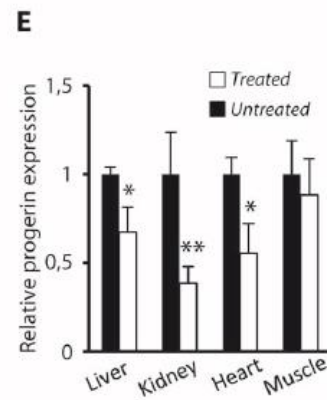
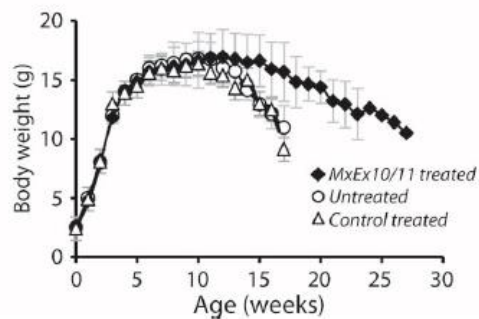
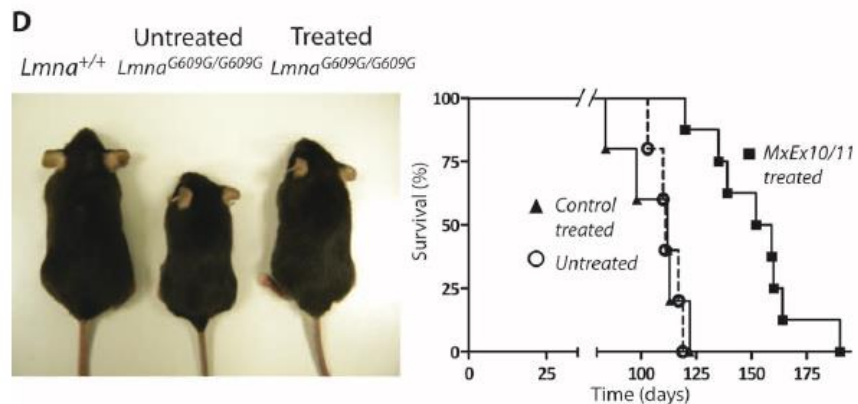
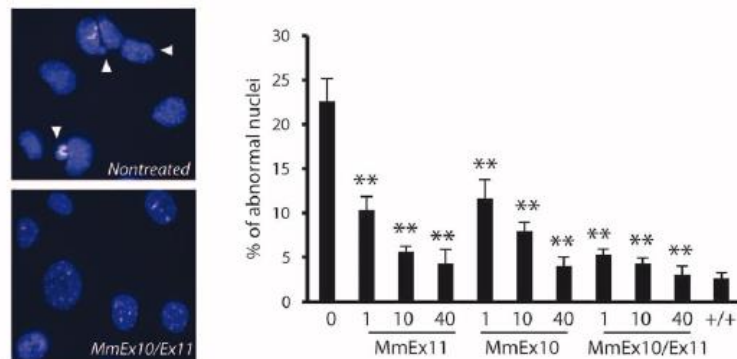
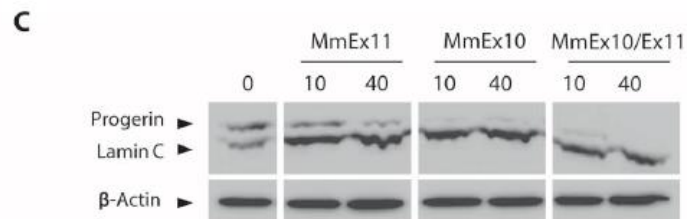
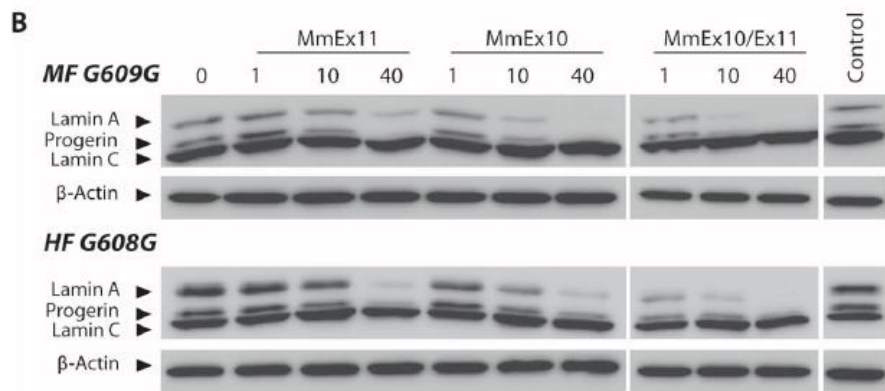
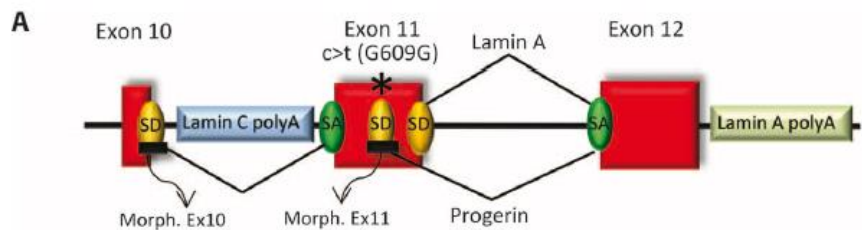


Splicing-Directed Therapy in a New Mouse Model of Human Accelerated Aging

Fernando G. Osorio,¹ Claire L. Navarro,² Juan Cadiñanos,^{1*} Isabel C. López-Mejía,³ Pedro M. Quirós,¹ Catherine Bartoli,² José Rivera,⁴ Jamal Tazi,³ Gabriela Guzmán,⁵ Ignacio Varela,¹ Danielle Depetris,² Félix de Carlos,⁶ Juan Cobo,⁶ Vicente Andrés,⁴ Annachiara De Sandre-Giovannoli,^{2,7} José M. P. Freije,¹ Nicolas Lévy,^{2,7} Carlos López-Otín^{1†}

Hutchinson-Gilford progeria syndrome (HGPS) is caused by a point mutation in the *LMNA* gene that activates a cryptic donor splice site and yields a truncated form of prelamin A called progerin. Small amounts of progerin are also produced during normal aging. Studies with mouse models of HGPS have allowed the recent development of the first therapeutic approaches for this disease. However, none of these earlier works have addressed the aberrant and pathogenic *LMNA* splicing observed in HGPS patients because of the lack of an appropriate mouse model. Here, we report a genetically modified mouse strain that carries the HGPS mutation. These mice accumulate progerin, present histological and transcriptional alterations characteristic of progeroid models, and phenocopy the main clinical manifestations of human HGPS, including shortened life span and bone and cardiovascular aberrations. Using this animal model, we have developed an antisense morpholino-based therapy that prevents the pathogenic *Lmna* splicing, markedly reducing the accumulation of progerin and its associated nuclear defects. Treatment of mutant mice with these morpholinos led to a marked amelioration of their progeroid phenotype and substantially extended their life span, supporting the effectiveness of antisense oligonucleotide-based therapies for treating human diseases of accelerated aging.





Trial Medications at a Glance

Pravastatin (marketed as Pravachol or Selektine) is a member of the drug class of statins. It is usually used for lowering cholesterol and preventing cardiovascular disease.

Zoledronic acid is a **bisphosphonate**, usually used as a bone drug for improving osteoporosis, and to prevent skeletal fractures in people suffering from some forms of cancer.

Lonafarnib is an **FTI** (Farnesyltransferase inhibitor), a drug that can reverse an abnormality in Progeria cells in the laboratory, and has improved disease in Progeria mice.

All 3 drugs block the production of the farnesyl molecule that is needed for progerin to create disease in Progeria

Pravastatin, Zoledronic acid and FTI clinical trial

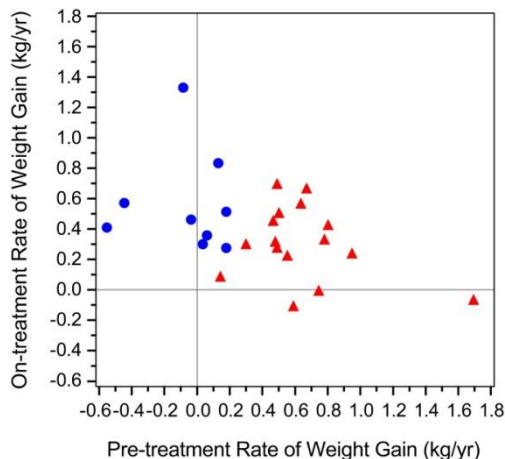


Table 1.

Patient characteristics at study entry

Characteristic	Mean	S.D.	Minimum	Median	Maximum
Age at enrollment (y)	7.0	3	3	7	16
Height-age (y)	3.4	1.6	1.0	3.0	7.0
Weight (kg)	10.4	2.7	6.6	9.5	17.6
Standing height (cm)	94.9	11.9	76.7	93.8	122.0
Standing height BMI	11.4	1.2	9.3	11.7	13.5
Z-scores for standing height*	-5.41	1.33	-7.34	-5.43	-3.47
Z-scores for weight*	-10.18	5.90	-33.69	-9.04	-5.30

Of the 25 participants, 11 (44%) were male, and 14 (56%) were female.

*Derived from age- and sex -adjusted reference values using 2000 Centers for Charts (41).

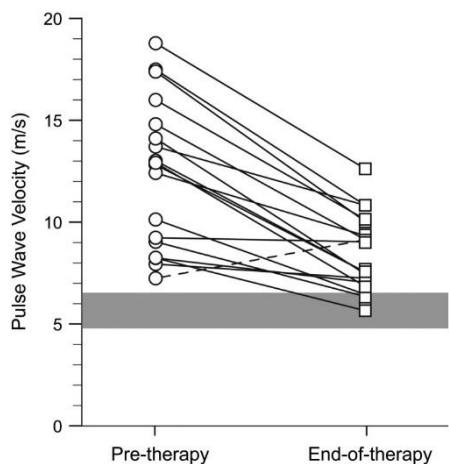


Table 3.

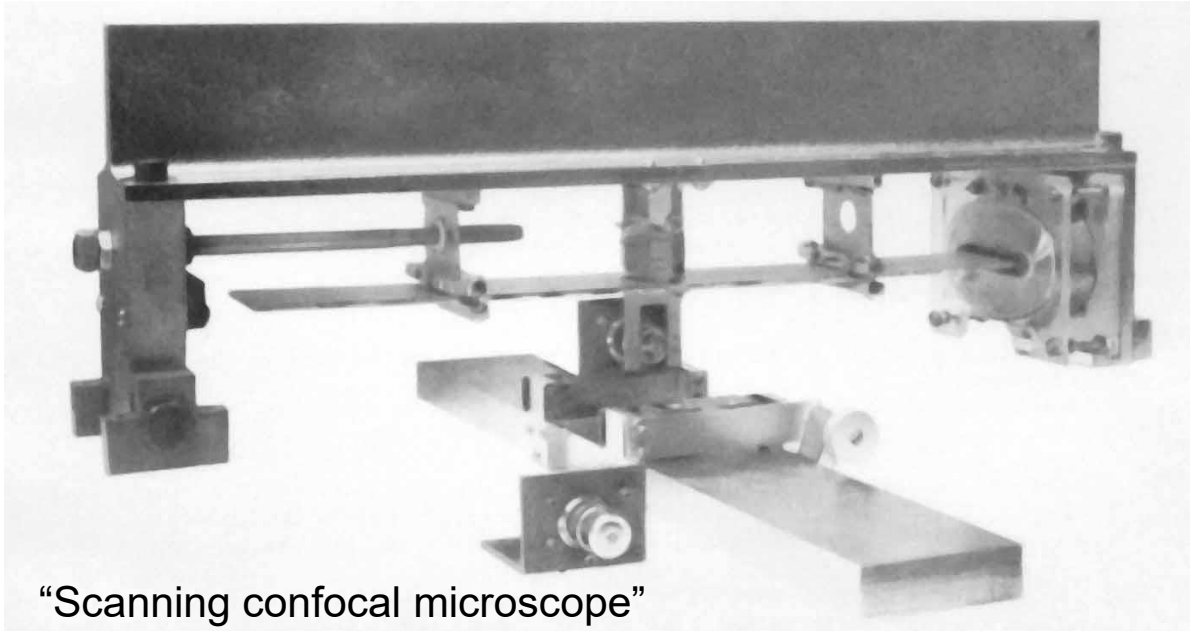
Effect of lonafamib on carotid artery density by ultrasound

Site	Percentile	Median density in pixels (range)			Control vs. HG(P)*
		Control (n = 55)	HG(P) (n = 22)	HG(E) (n = 22)	
Intima media	50	73.0 (28.0–156.0)	87.0 (15.0–242.0)	72.0 (2.0–140.0)	0.002
Adventitia luminal near wall	50	169.0 (95.0–237.0)	228.0 (61.0–254.0)	170.0 (70.0–252.0)	0.0004
Adventitia deep near wall	50	166.0 (34–254.0)	167.0 (30.0–254.0)	121.0 (12.0–215.0)	0.32

HG(E), HGPS end of therapy; HG(P), HGPS pretherapy.

*Based on Wilcoxon rank-sum test.

Microscopio confocal



“Scanning confocal microscope”
Prototipo de Marvin Minsky, 1955



Marvin Minsky, 1927

Dec. 19, 1961

M. MINSKY
MICROSCOPY APPARATUS
Filed Nov. 7, 1957

3,013,467

LIBRARY

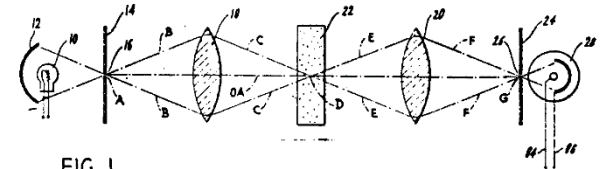


FIG. 1.

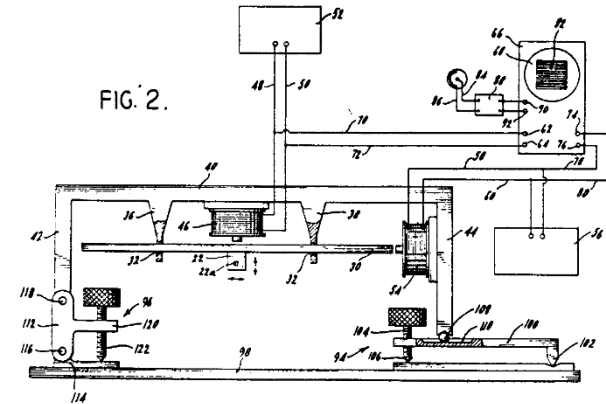


FIG. 2.

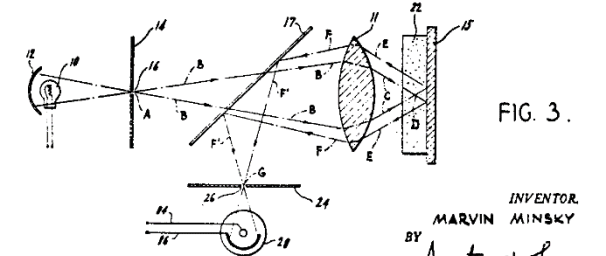
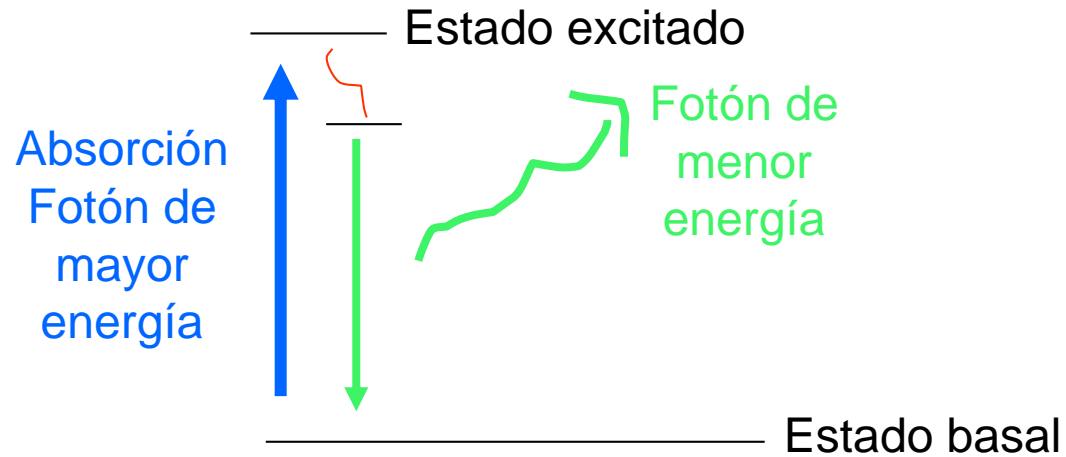


FIG. 3.

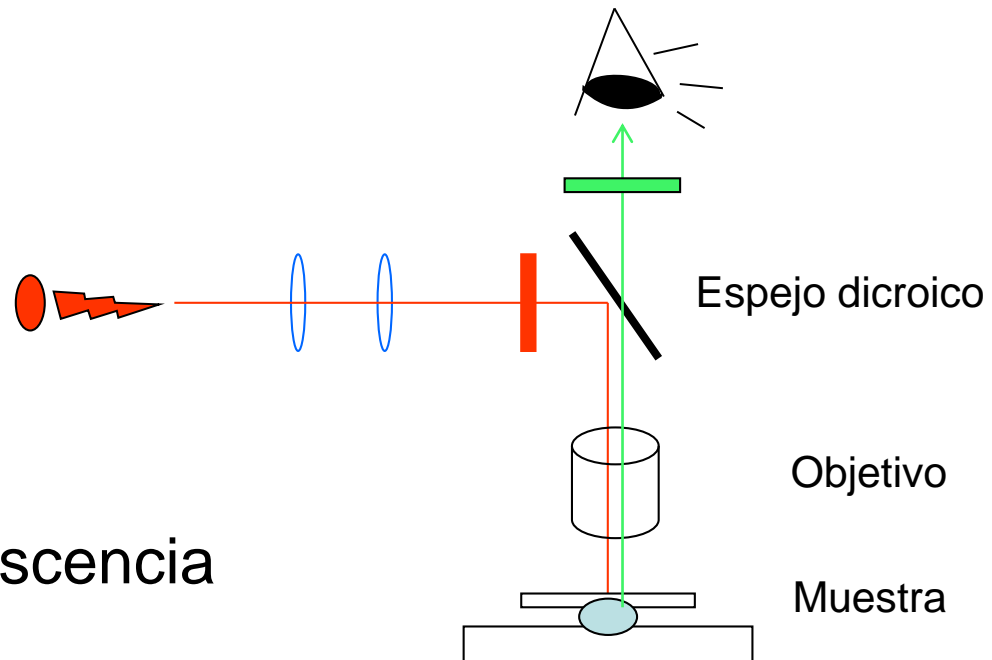
INVENTOR
MARVIN MINSKY
BY *Ametor & Levy*

Como funciona el microscopio confocal

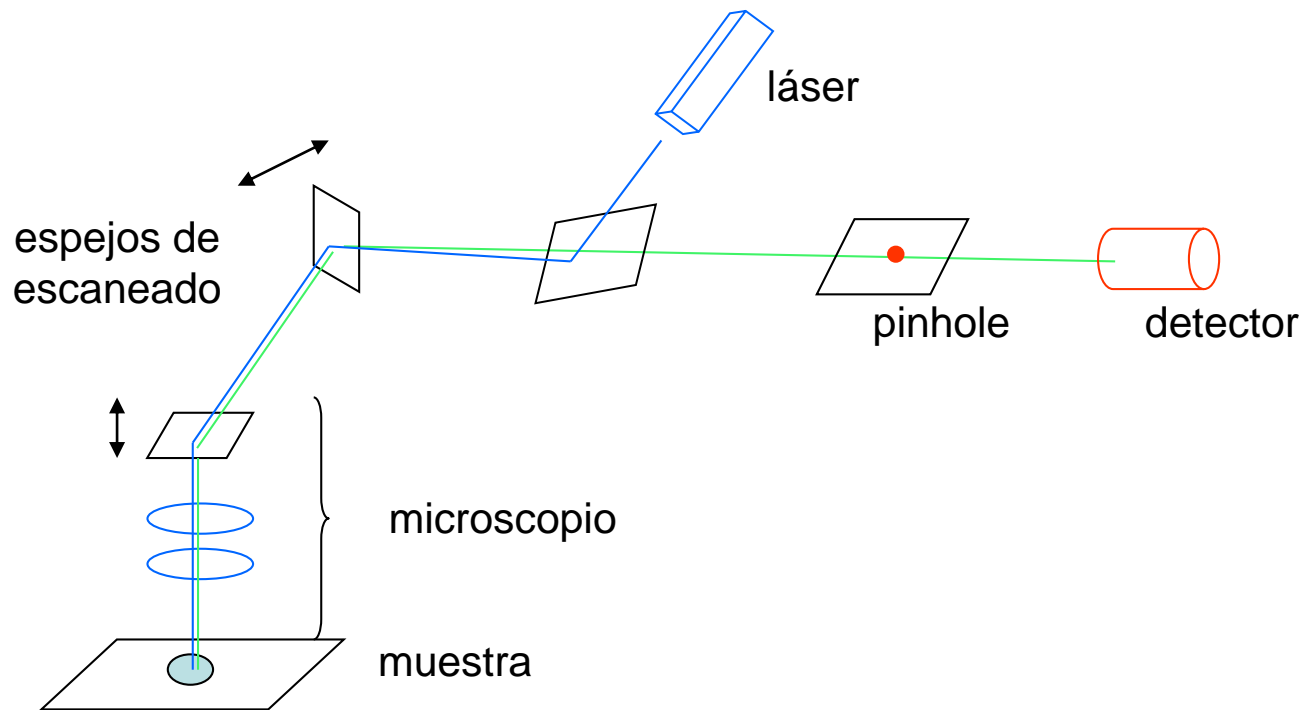
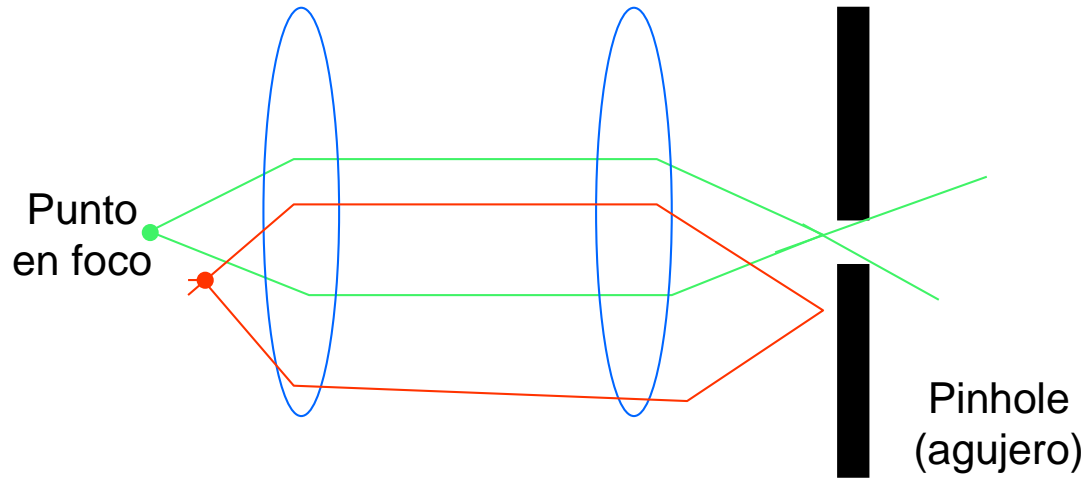
Fluorescencia

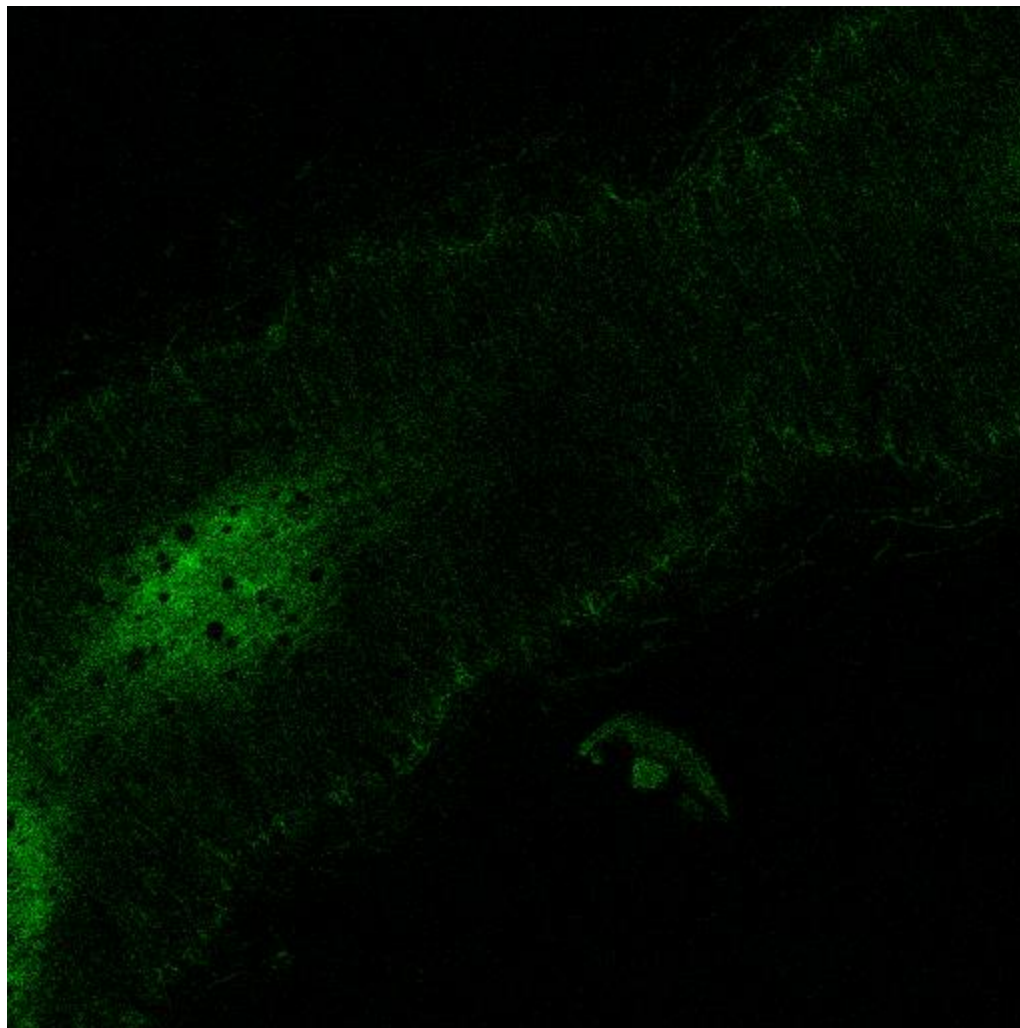
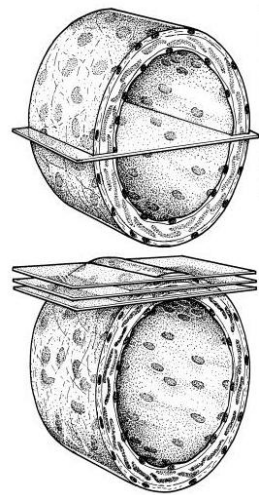


Microscopio de fluorescencia



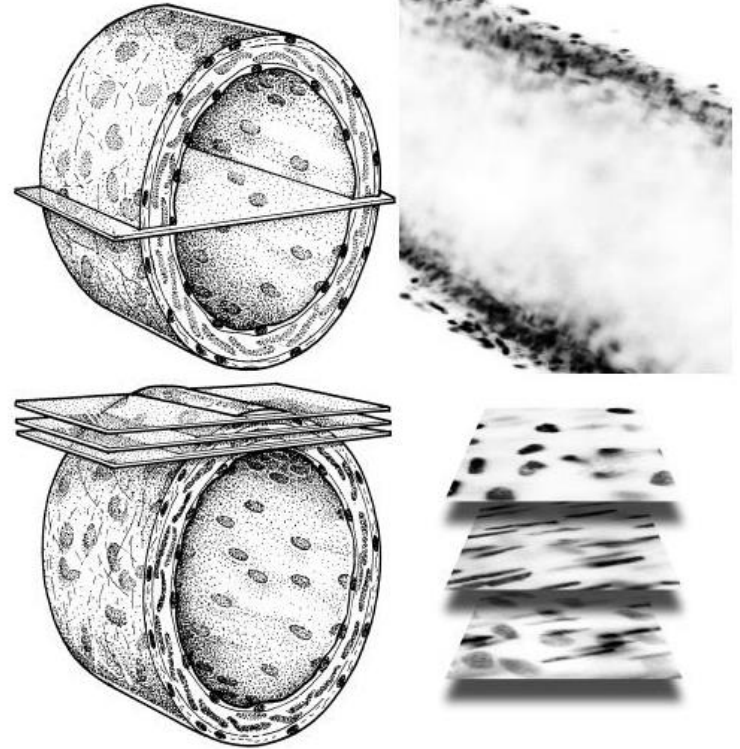
Microscopio confocal



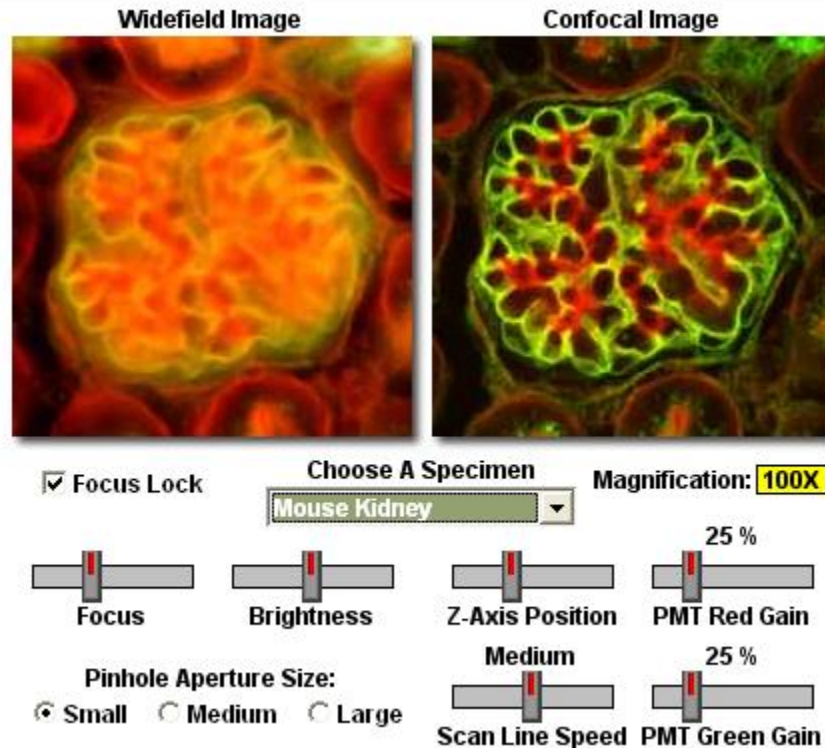


Ventajas

- Permite obtener secciones ópticas.
- Permite hacer reconstrucciones 3D.
- Permite hacer experimentos *in vivo*.
- No hay que hacer cortes histológicos
- Se pueden utilizar varios marcadores



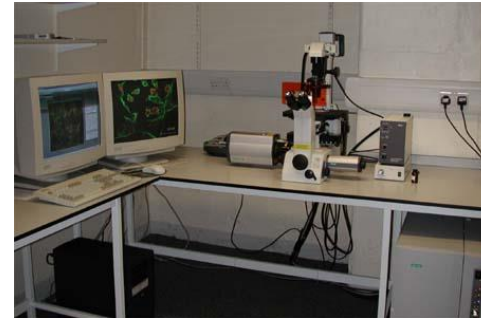
Diferencias microscopia confocal y de fluorescencia



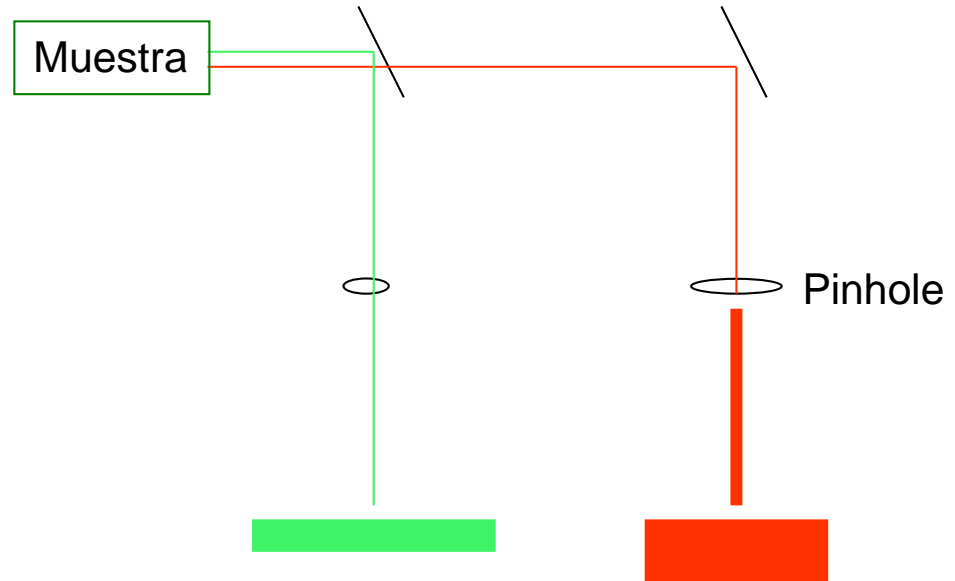
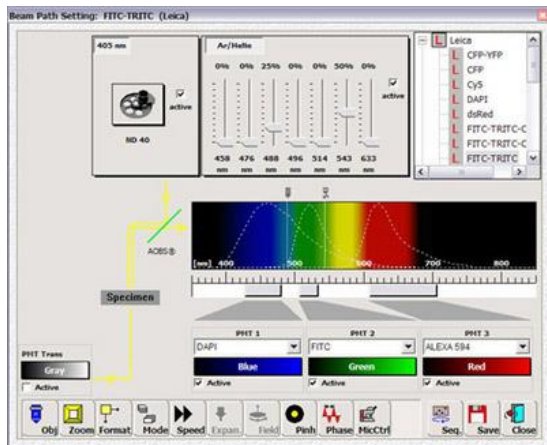
Tipos de microscopio confocal

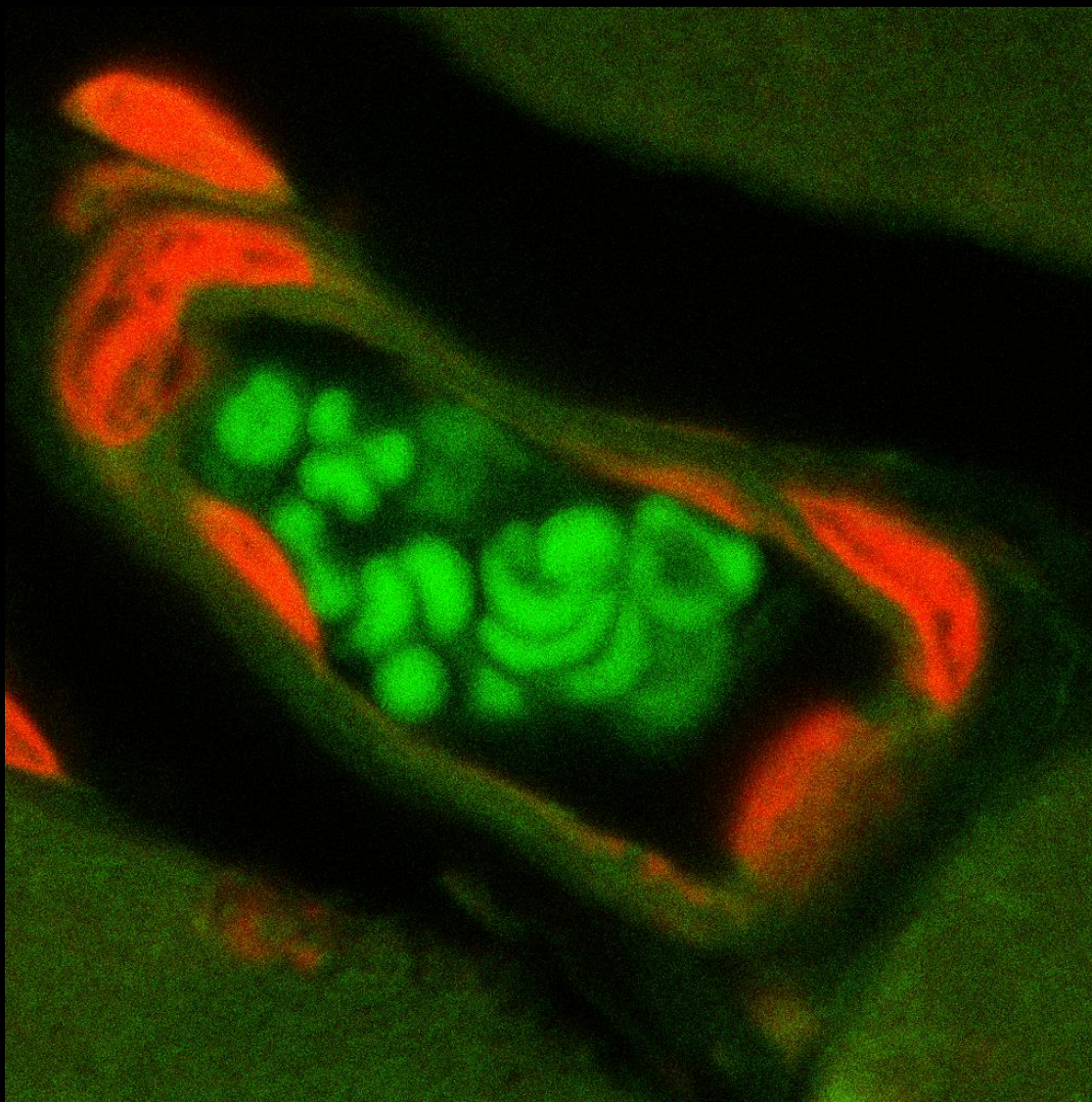


Espectral



Multipinhole

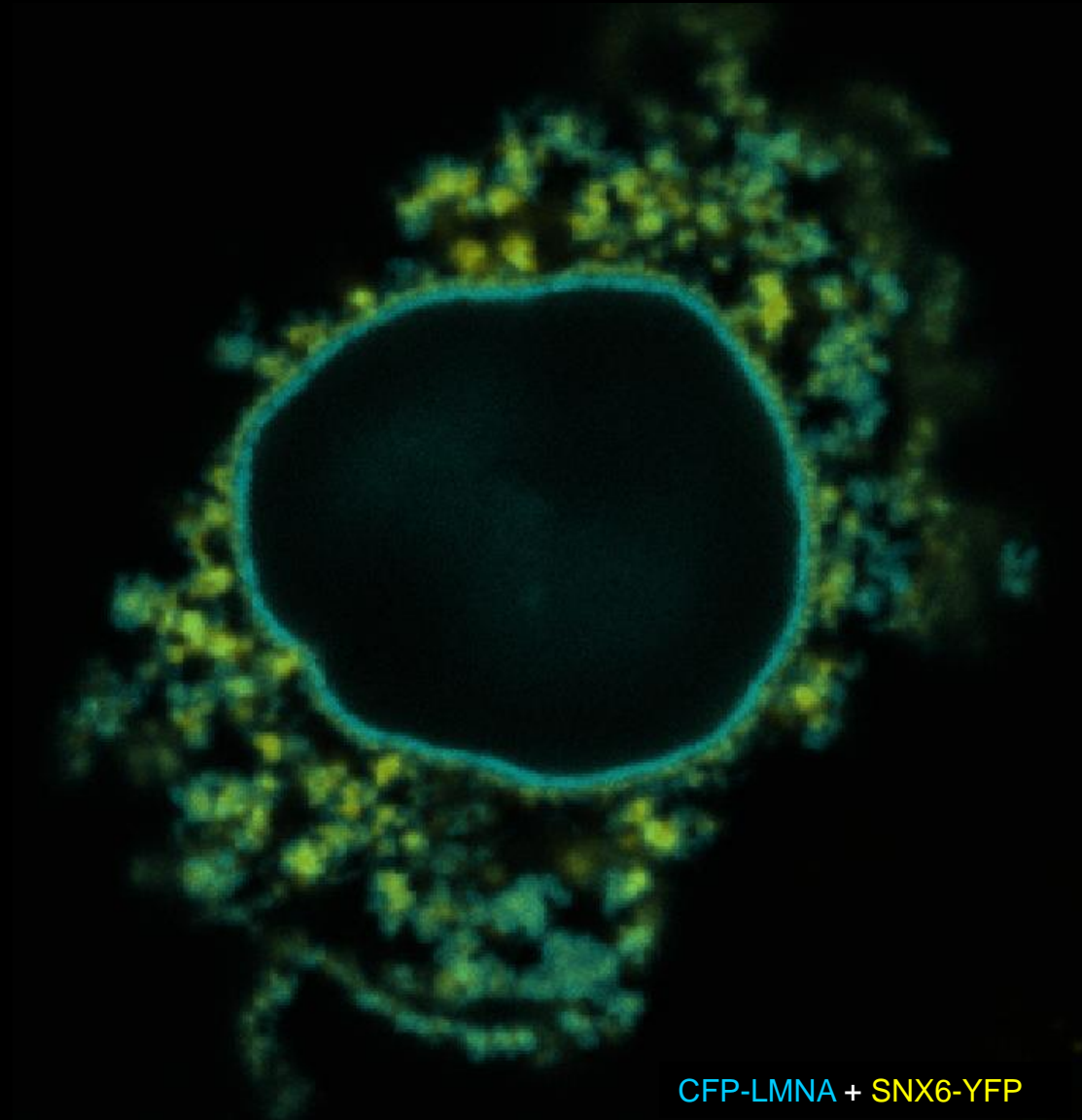


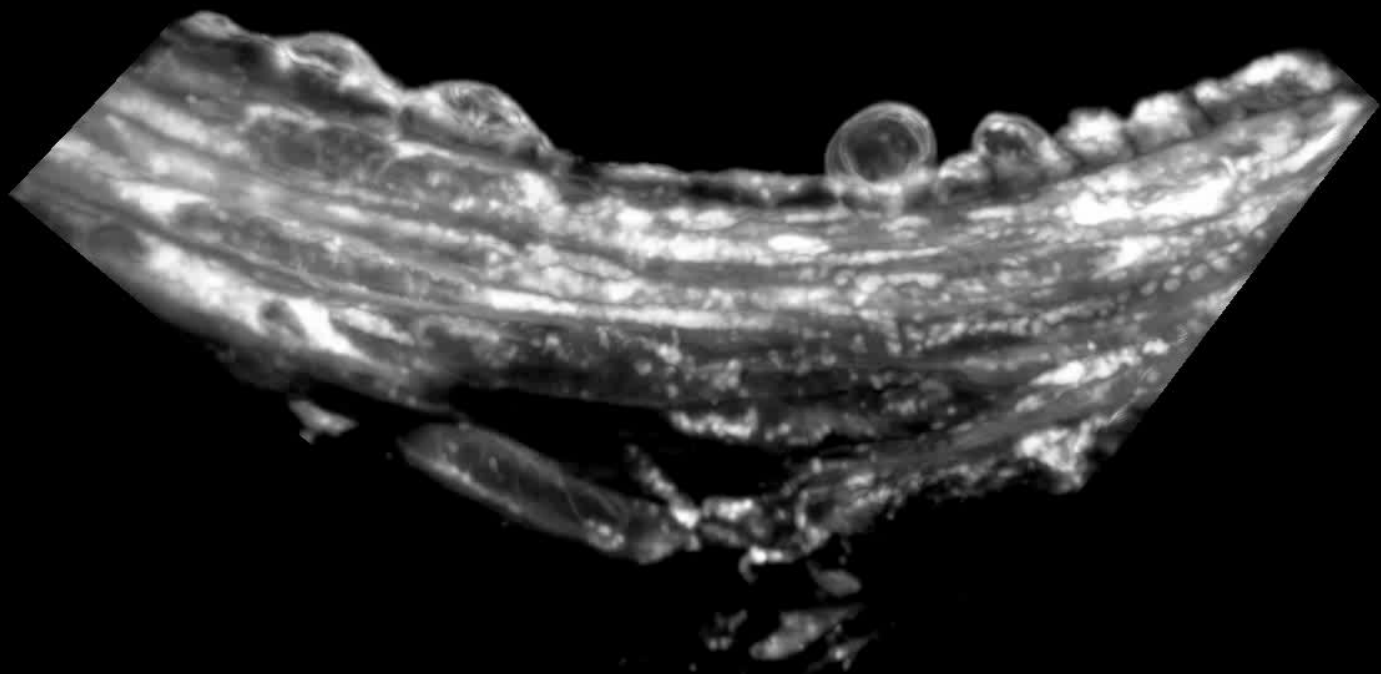


Autofluorescence-Erythrocytes

IP- nucleus

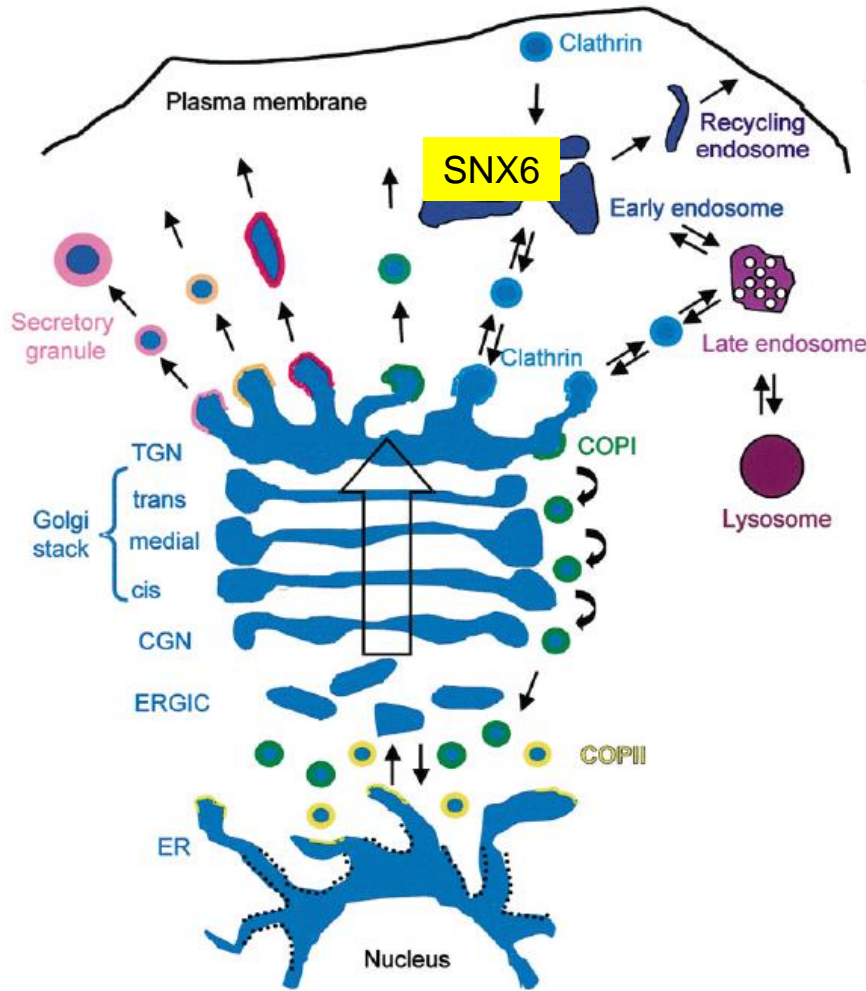
SNX6 overexpression affects lamin A distribution





10 μ m

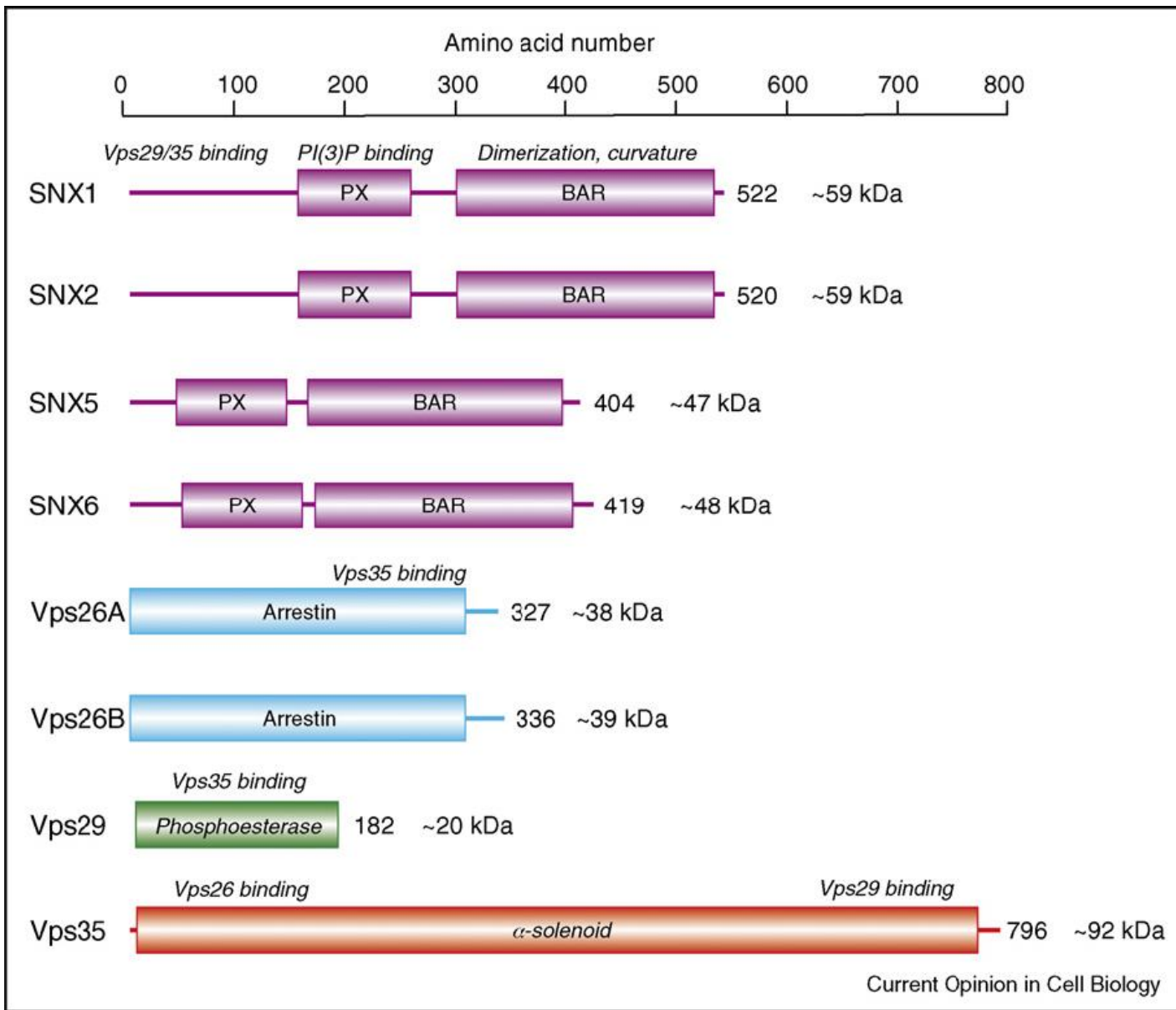
The secretory and endocytic pathways



Sorting Nexin 6 (SNX6)

SNX6 is a membrane-associated protein that is found in the **endosomes**.

SNX6 could be a component of the **retromer**, a complex of proteins related to the **recycling** of **transmembrane receptors** from endosomes to the trans-Golgi network



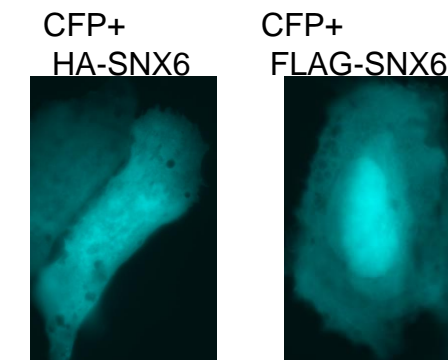
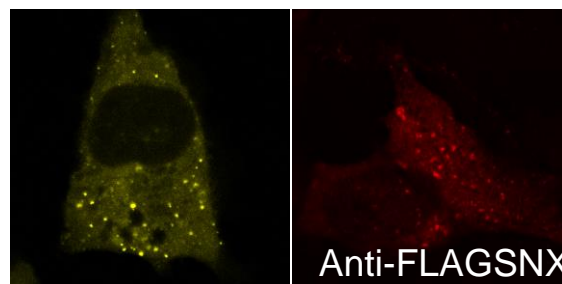
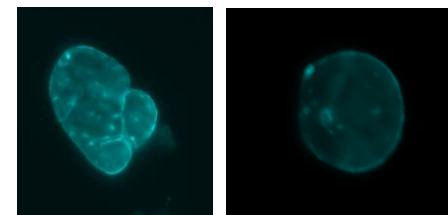
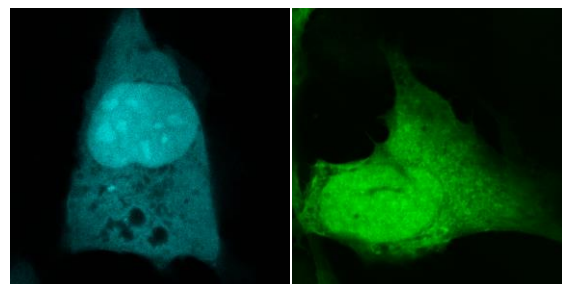
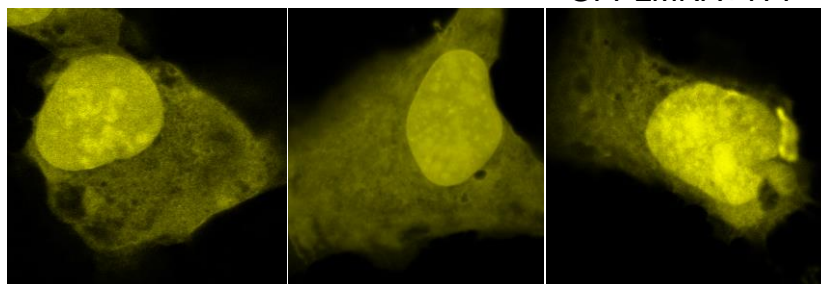
Lamin A

SNX6

CFPLMNA+YFP HA-LMNA+YFP GFPLMNA+YFP

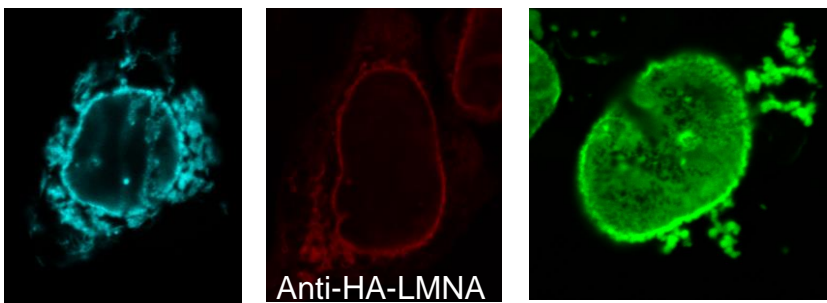
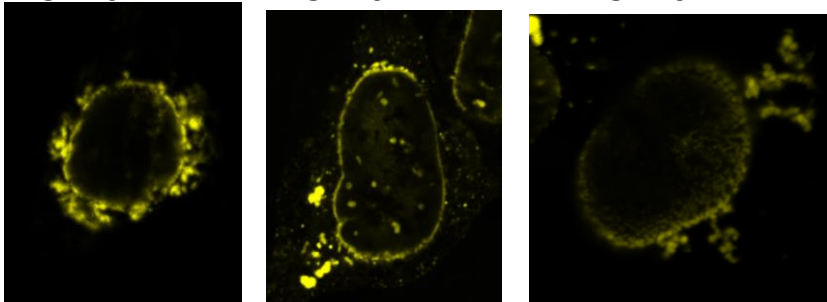
CFP+SNX6YFP GFP + FLAG-SNX6

CFPLMNA+ FLAG CFPLMNA+ HA

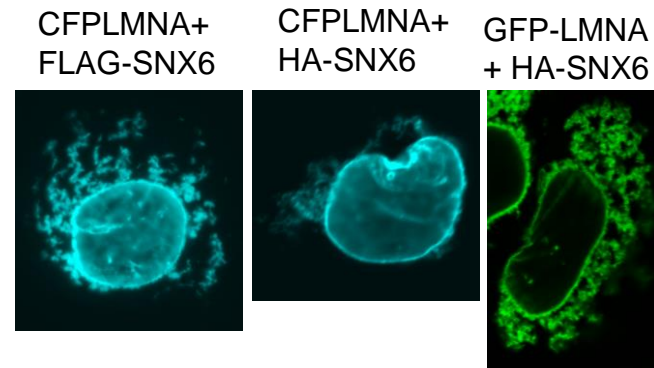


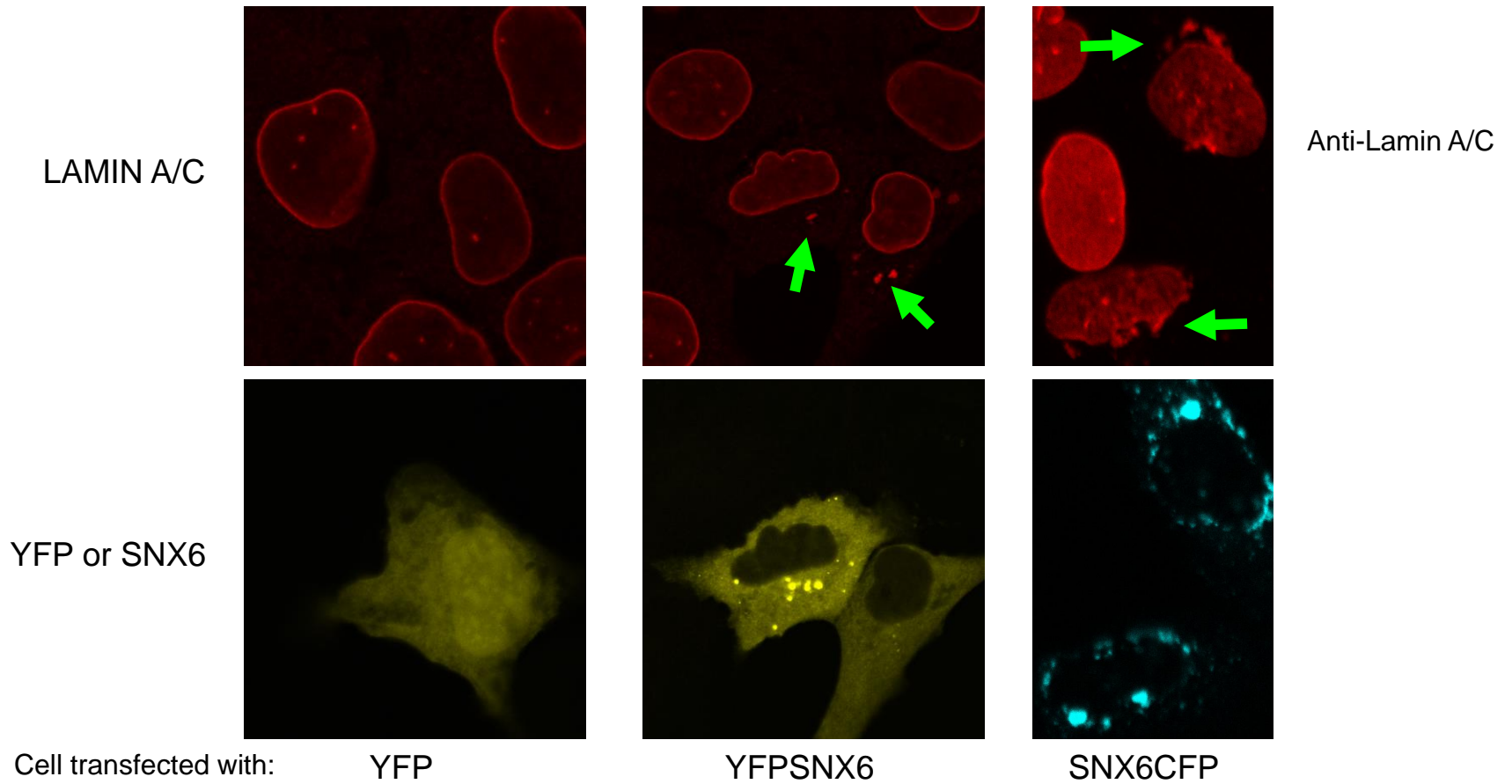
CFPLMNA+ SNX6YFP HA-LMNA+ SNX6YFP GFP-LMNA+ SNX6YFP

SNX6 overexpression affects lamin A distribution



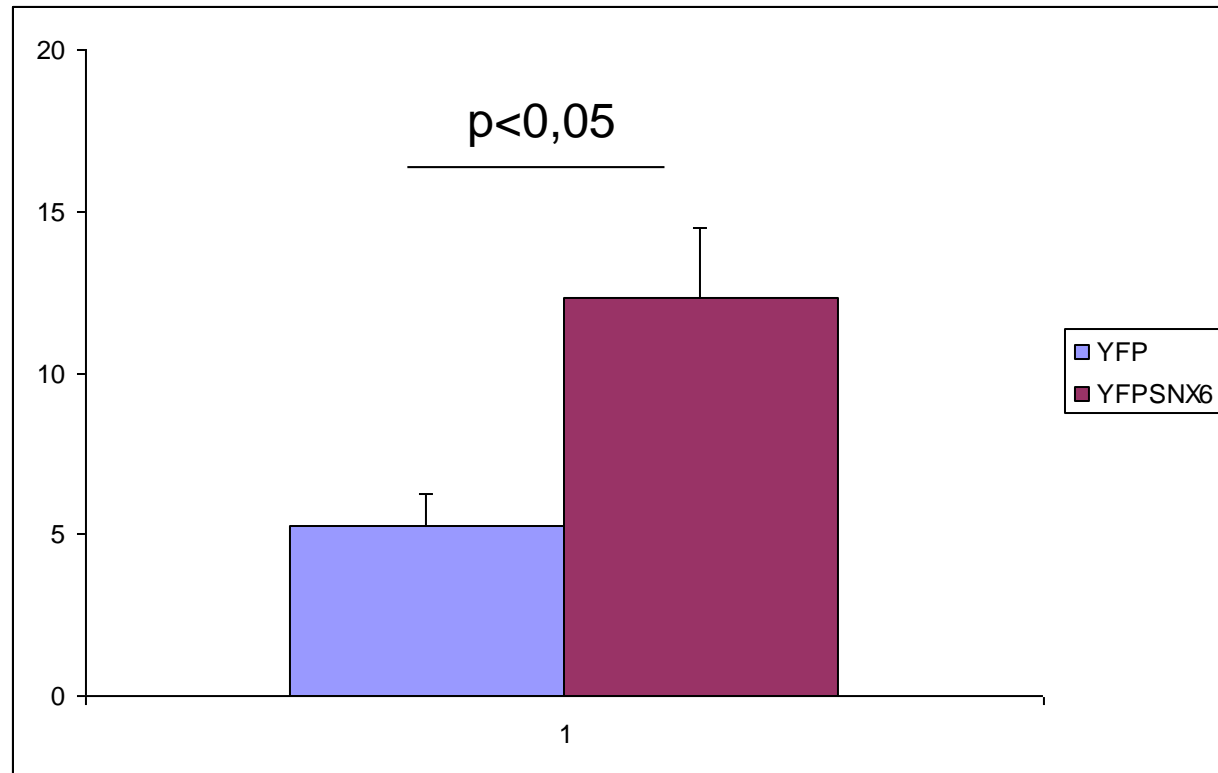
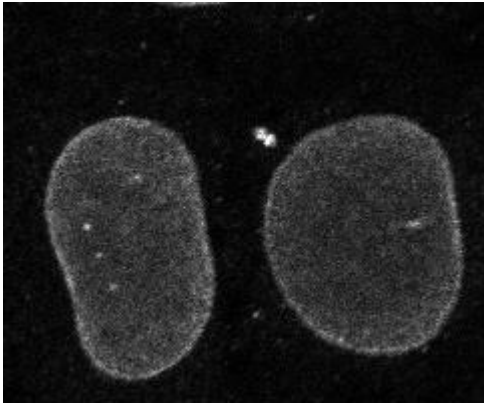
Lamin A + SNX6

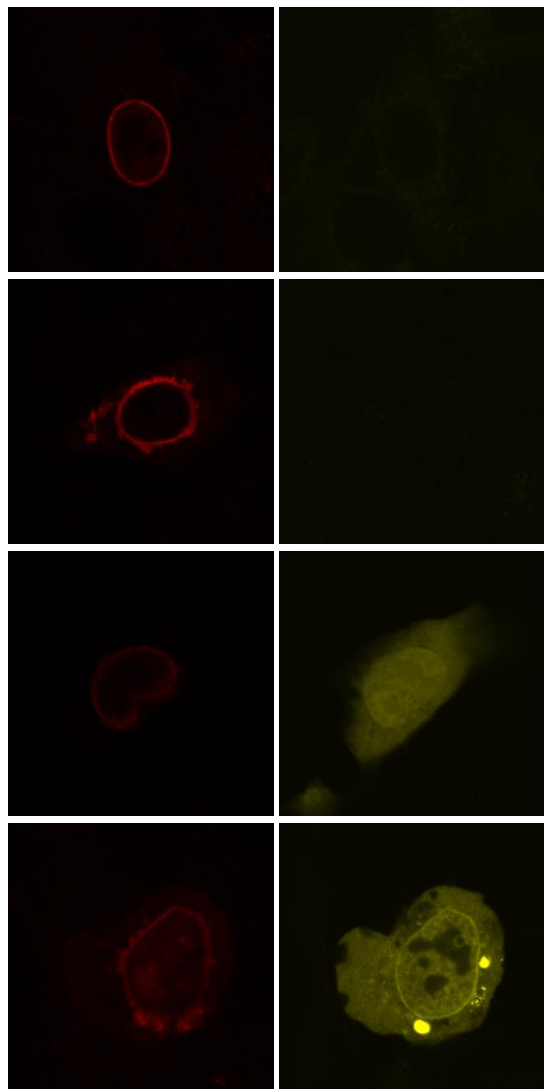




SNX6 overexpression affects endogenous lamin A/C distribution

Percentage of cells showing alterations in Lamin A localization



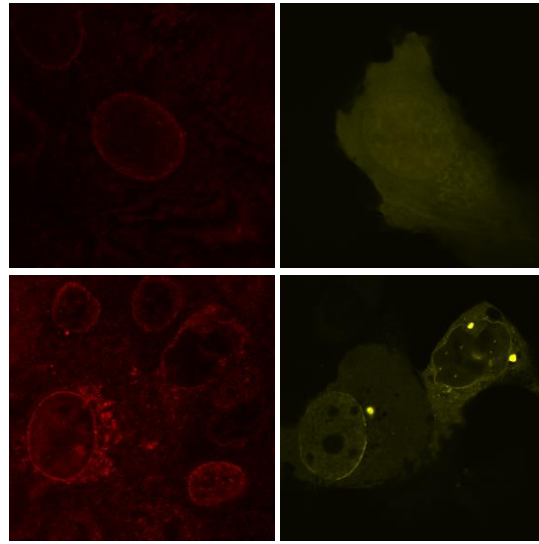


Anti-FLAG

HA

HA-SNX6

+ FLAG-Prelamin A

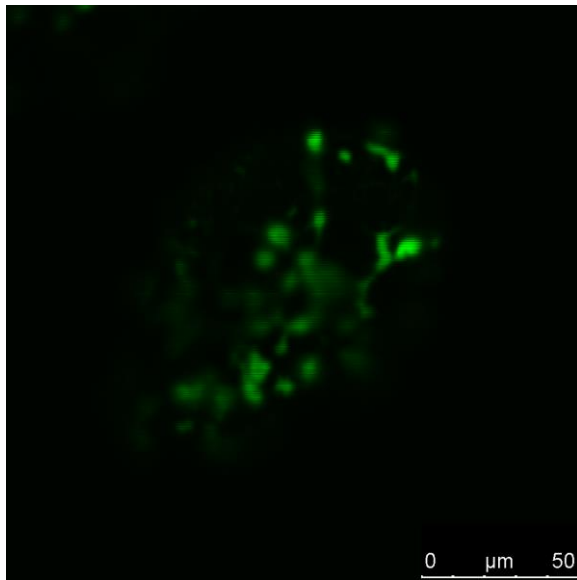


Anti-lamin A

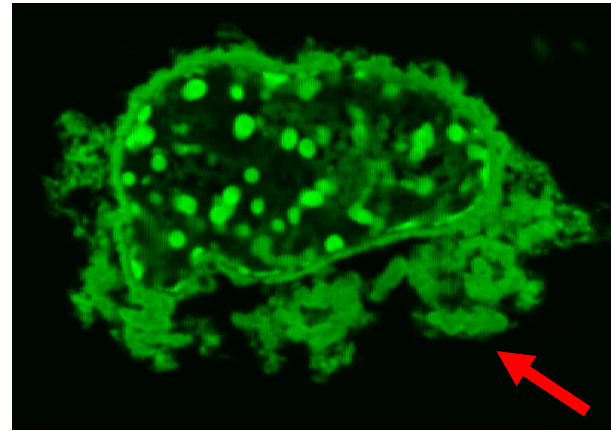
YFP

YFP-SNX6

+ FLAG-Prelamin A

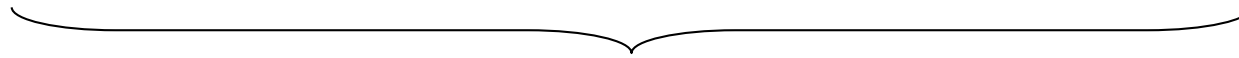


HA



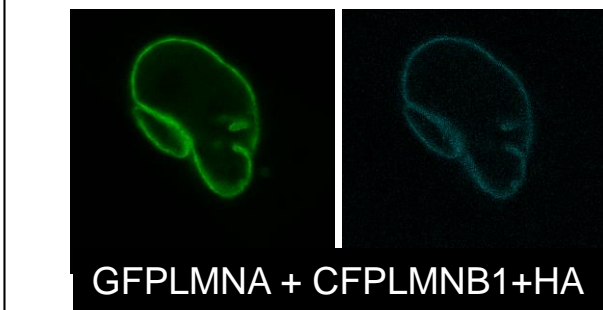
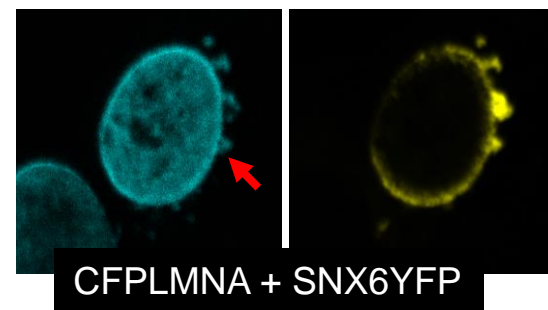
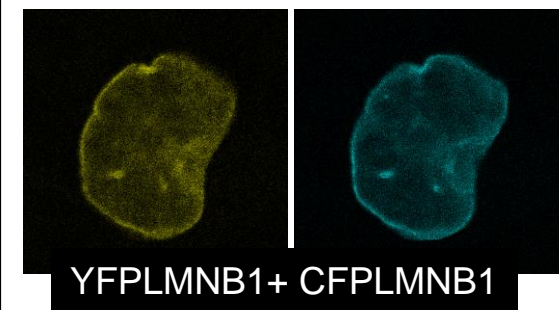
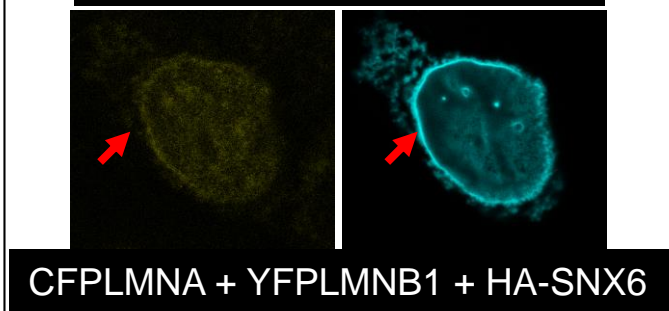
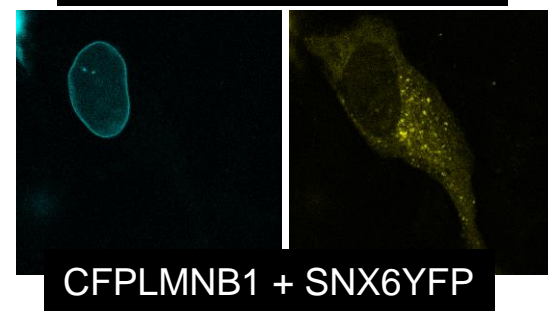
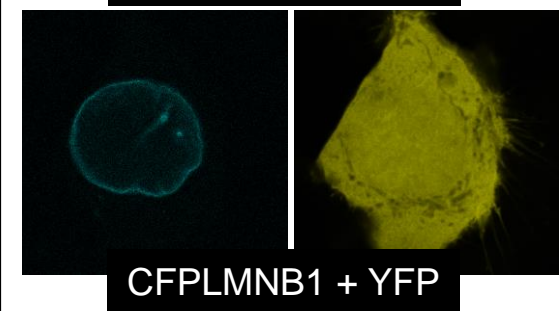
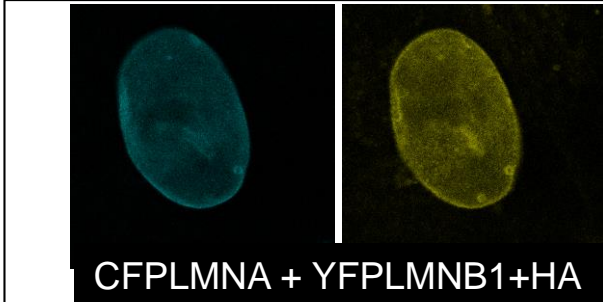
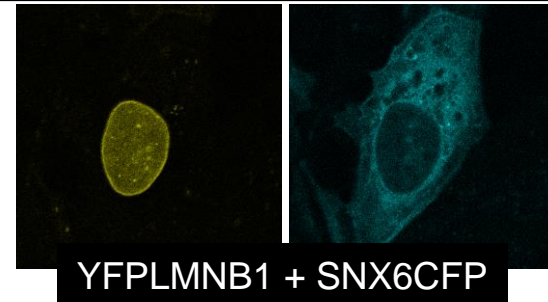
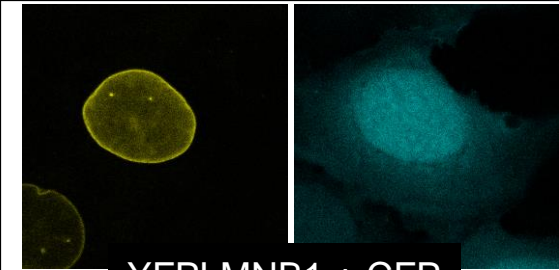
GFP-LMNC

HA-SNX6

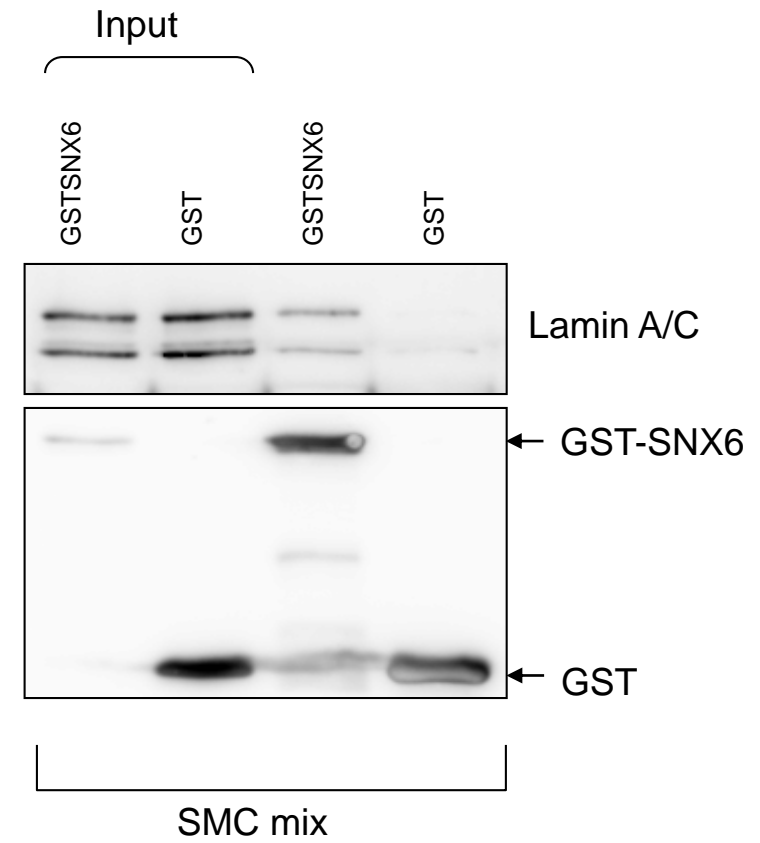
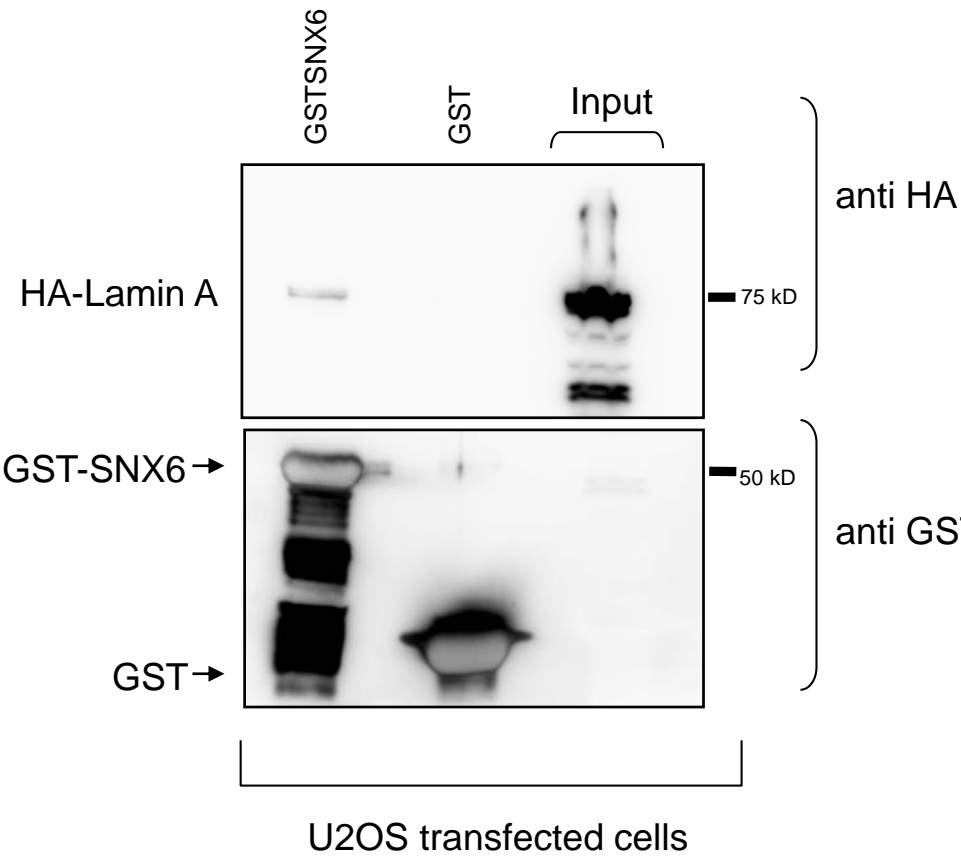


GFP-LMNC +

SNX6 overexpression disrupts lamin C localization

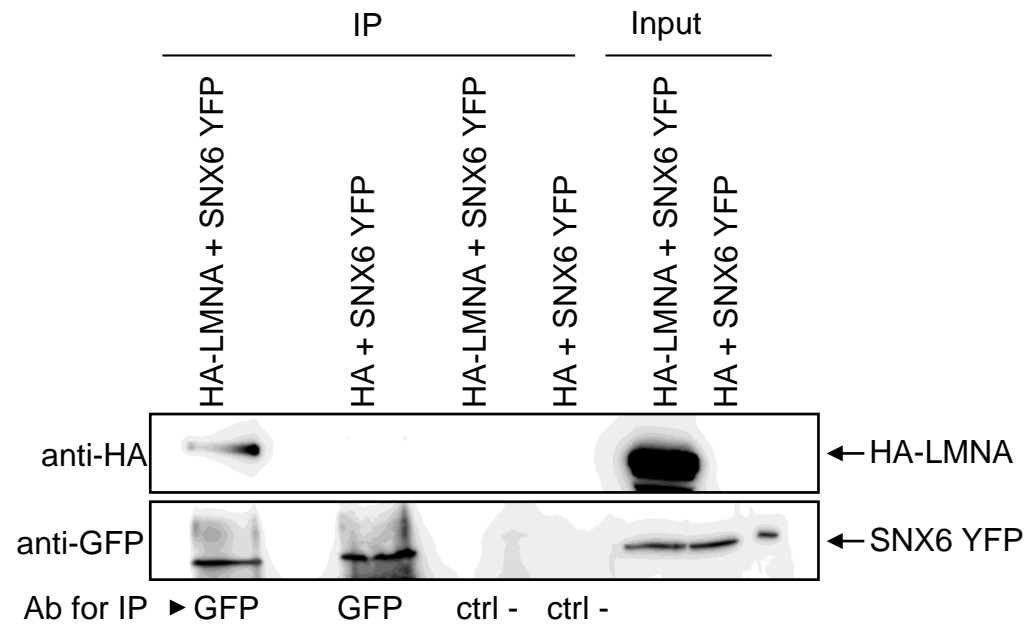


SNX6 does not disrupt lamin B1 localization

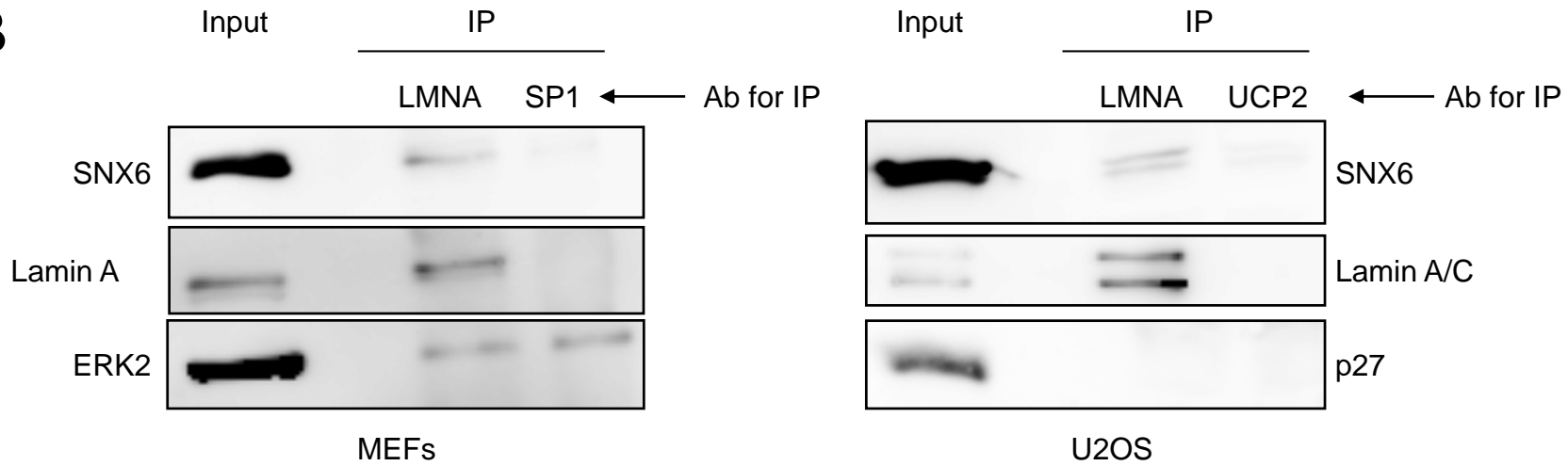


SNX6 interacts with Lamin A/C *in vitro*

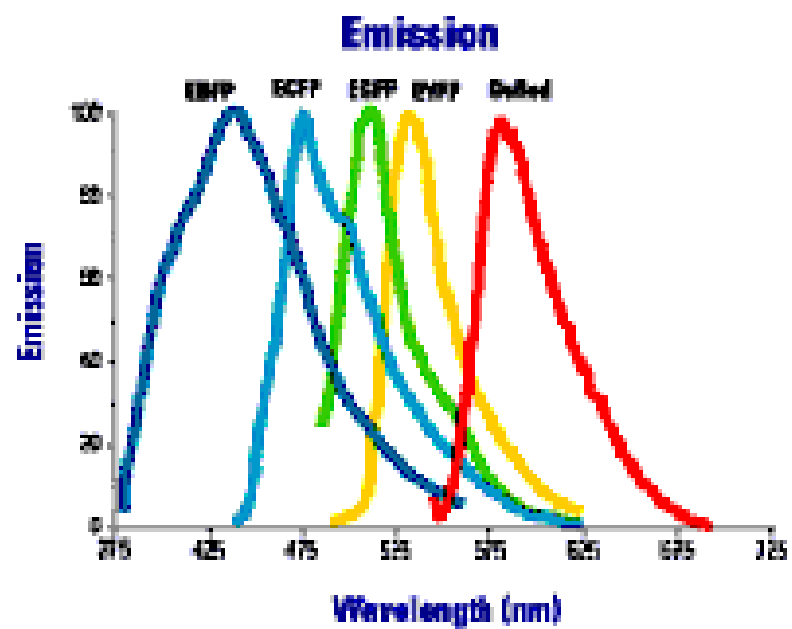
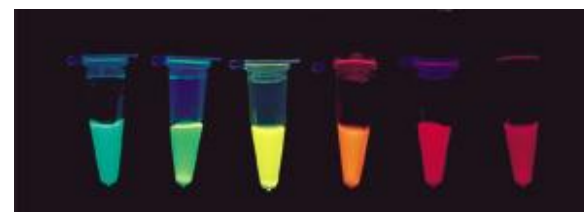
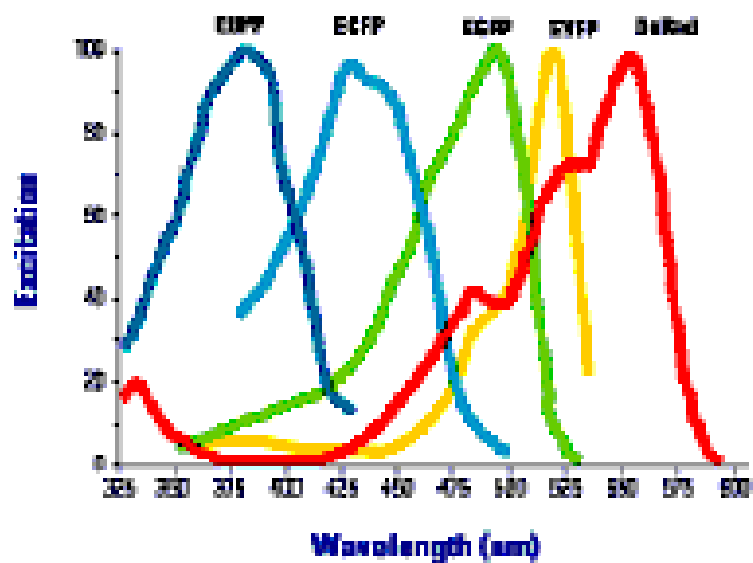
A



B



SNX6 interacts with Lamin A/C *in vivo*



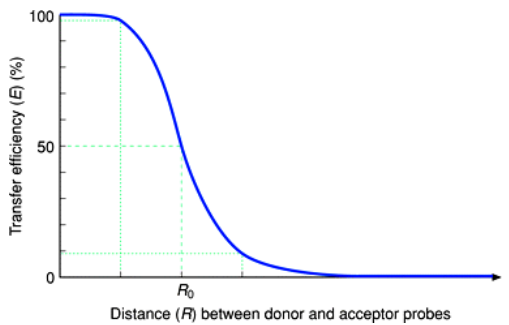
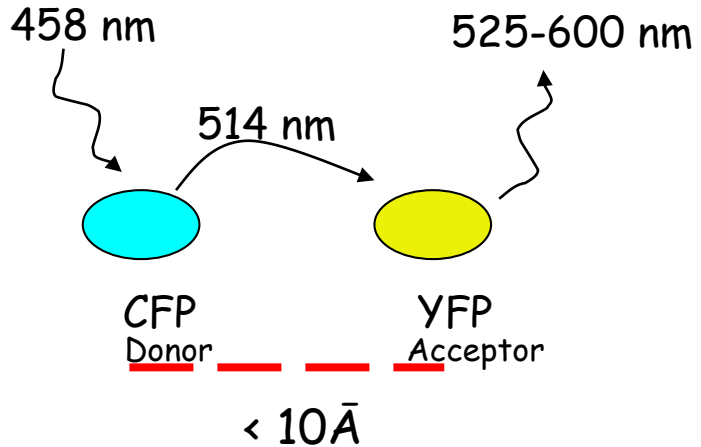
Fluorescence resonance energy transfer (FRET) microscopy imaging of living cells

FRET: radiationless transfer of energy between a donor and an acceptor chromophore molecule when they are within the range 10-100 Å.

Efficiency of transfer (Förster Equation):

$$E = 1 / (1 + R^6 / R_0^6)$$

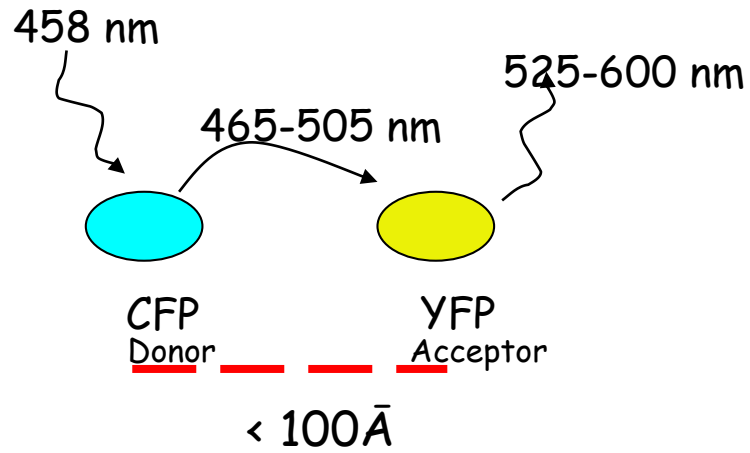
R_0 is the so-called Förster distance at which the efficiency of transfer is 50%



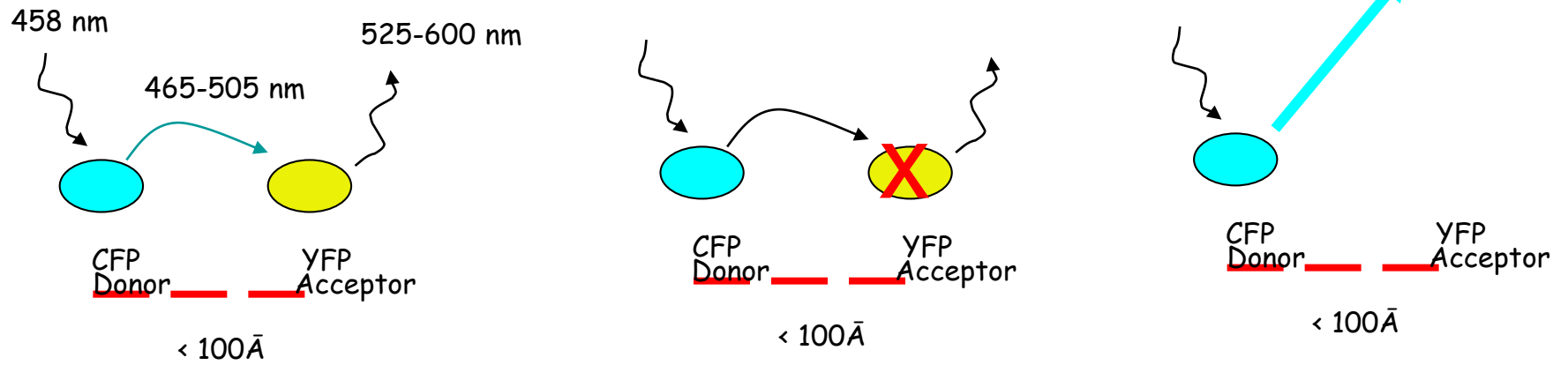
$$R_0^6 = (8.79 \times 10^{23}) \kappa^2 n^4 \Phi_d J_{da}$$

- κ^2 orientation factor
- n refractive index of the solvent
- Φ_d quantum efficiency of the donor
- J_{da} overlap of the donor emission spectrum

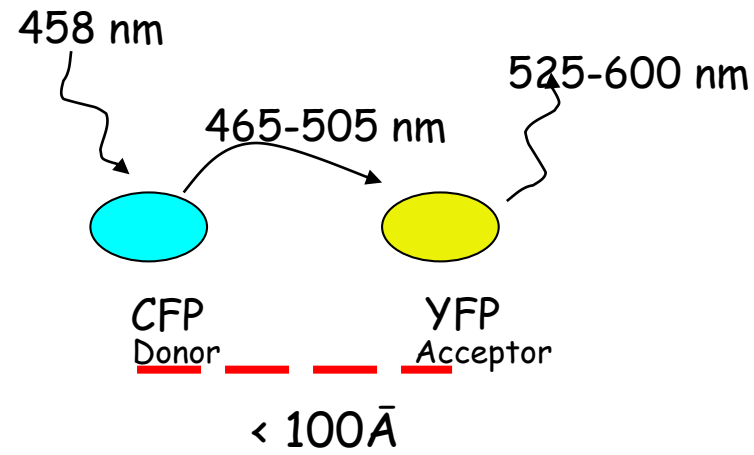
FRET sensitized emission.



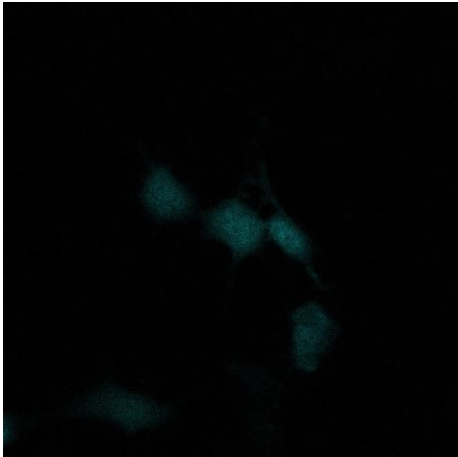
FRET Acceptor photobleaching.



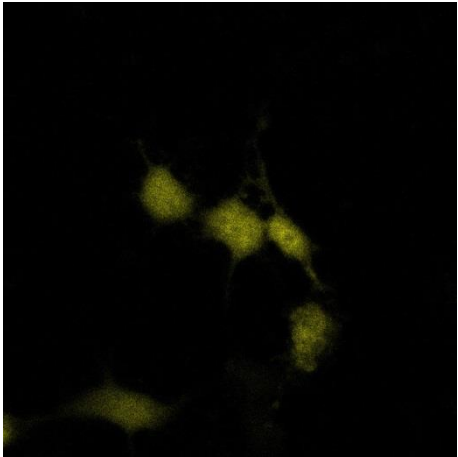
FRET sensitized emission.



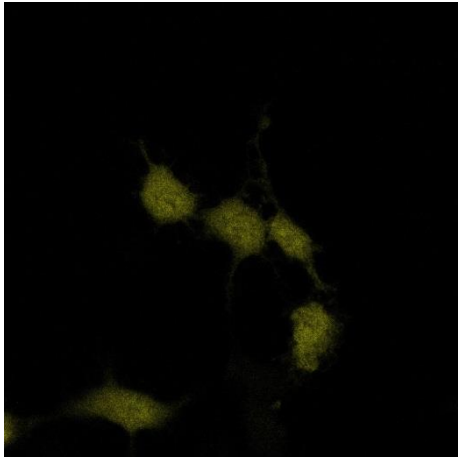
CFPYPF



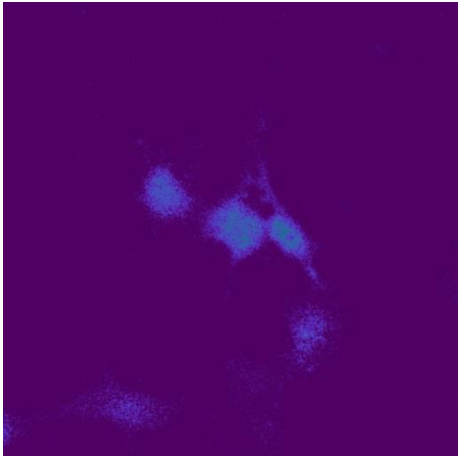
Donor (Donor excitation)



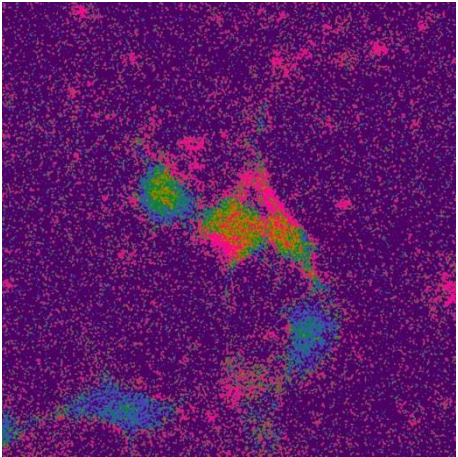
Acceptor (Donor excitation)



Acceptor (Acceptor excitation)



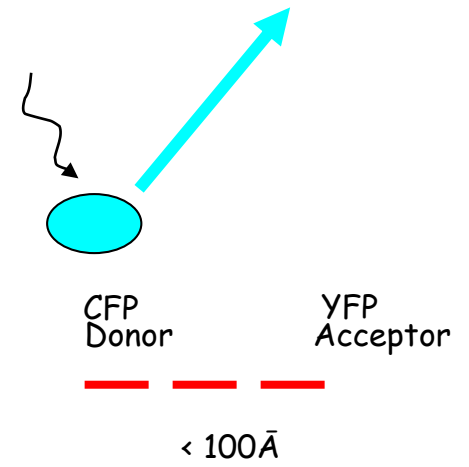
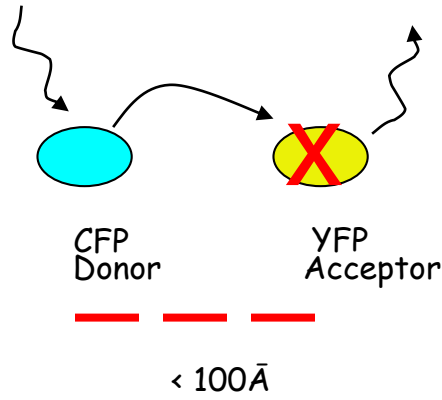
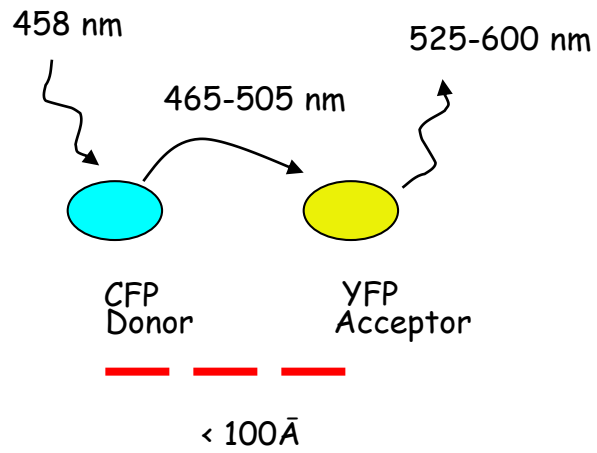
FRET



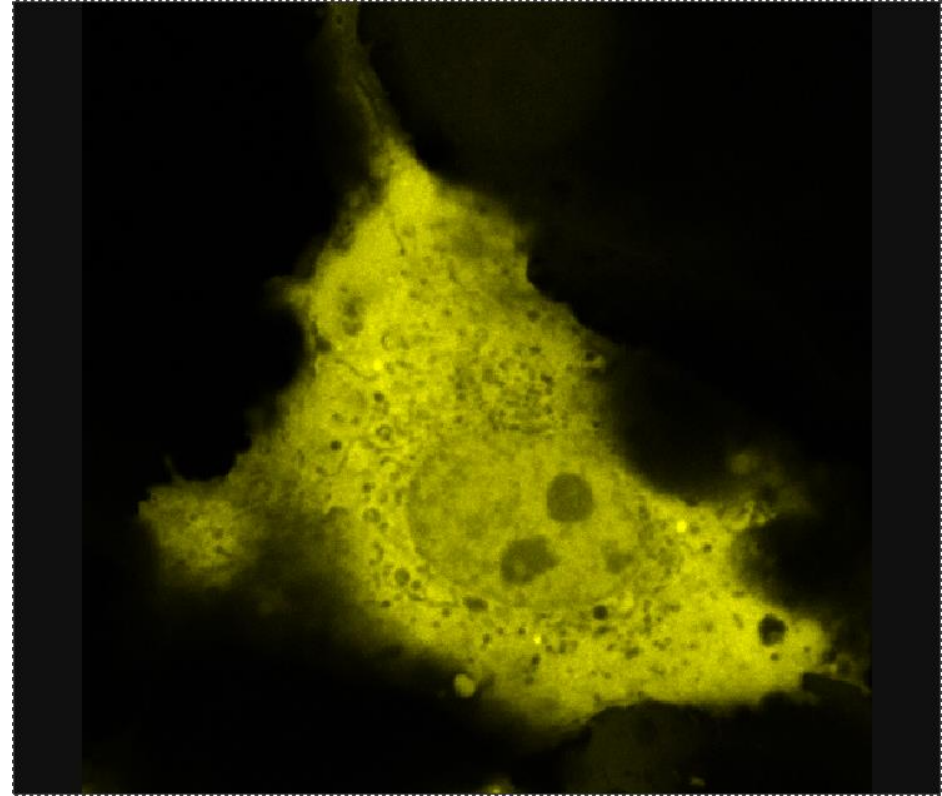
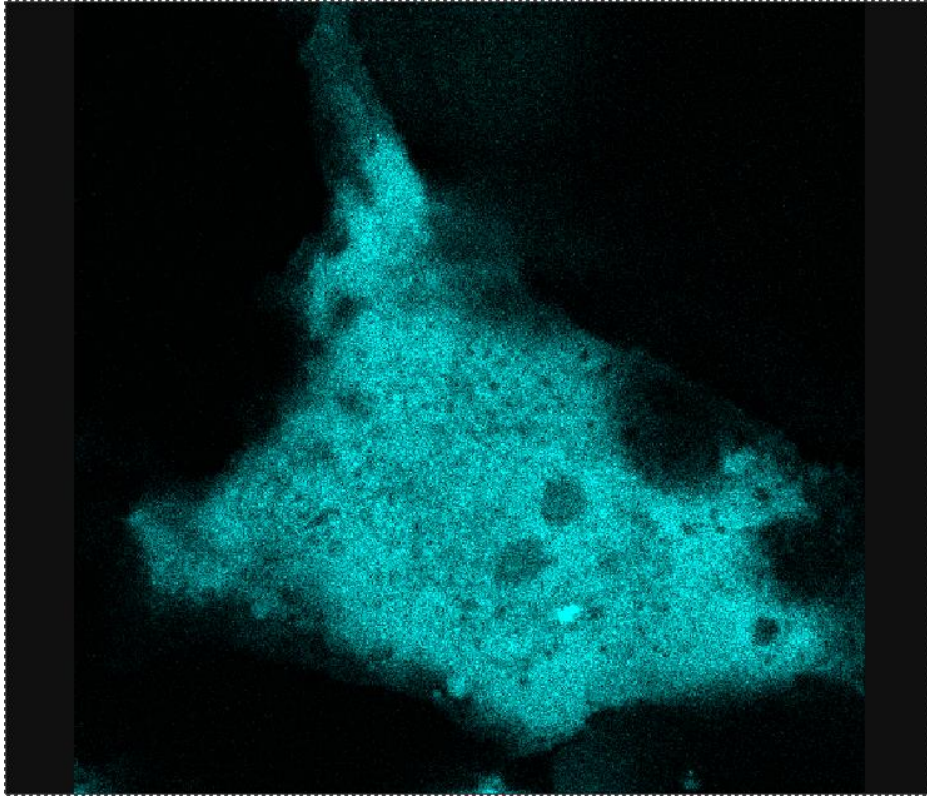
FRET Efficiency

ROI	ROI 1	ROI 2	ROI 3	ROI 4	ROI 5
FRET	515.97	683.81	732.80	258.39	191.21
FRETEff	0.43	0.70	0.65	0.23	0.19
A (ch1)	588.58	764.16	873.77	505.74	384.96
B (ch2)	1345.19	1471.53	1642.86	1022.42	850.95
C (ch3)	1191.97	970.64	1128.55	1127.08	1014.05

FRET Acceptor photobleaching.

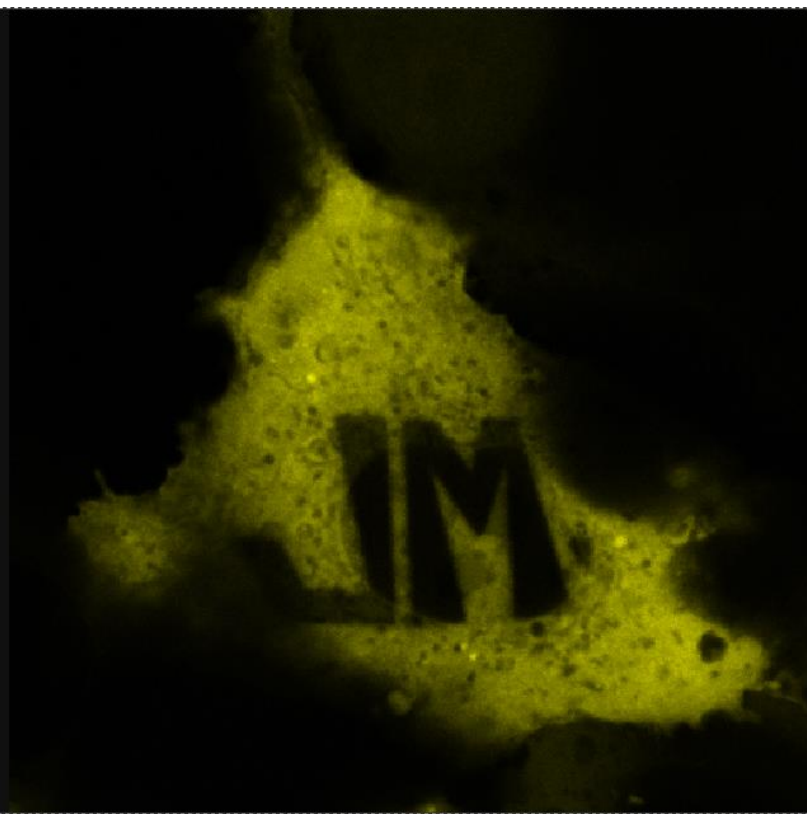


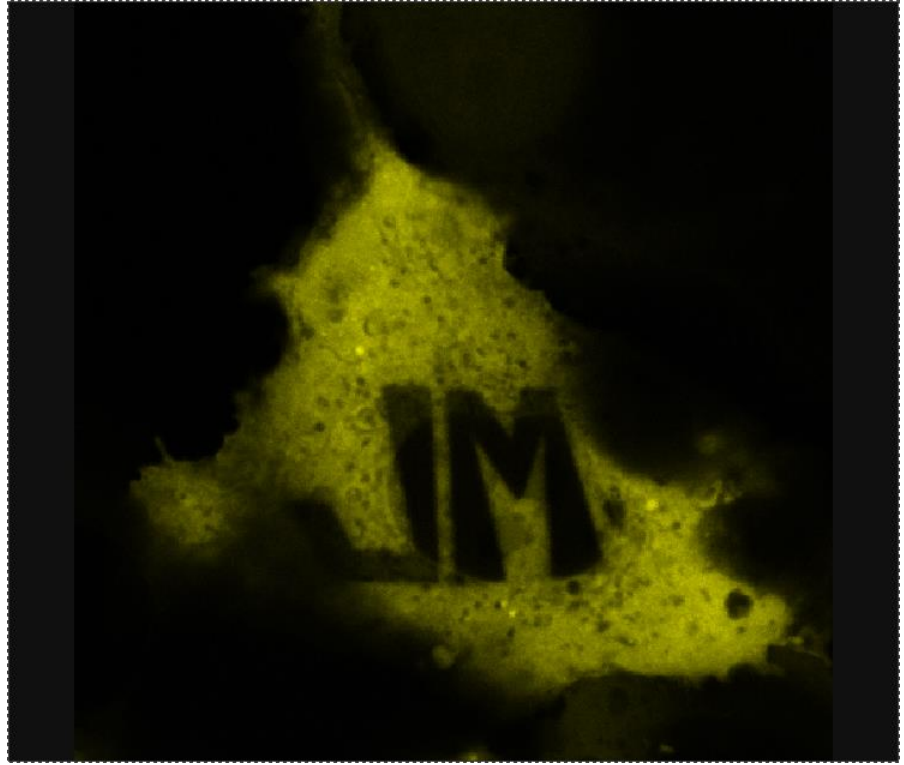
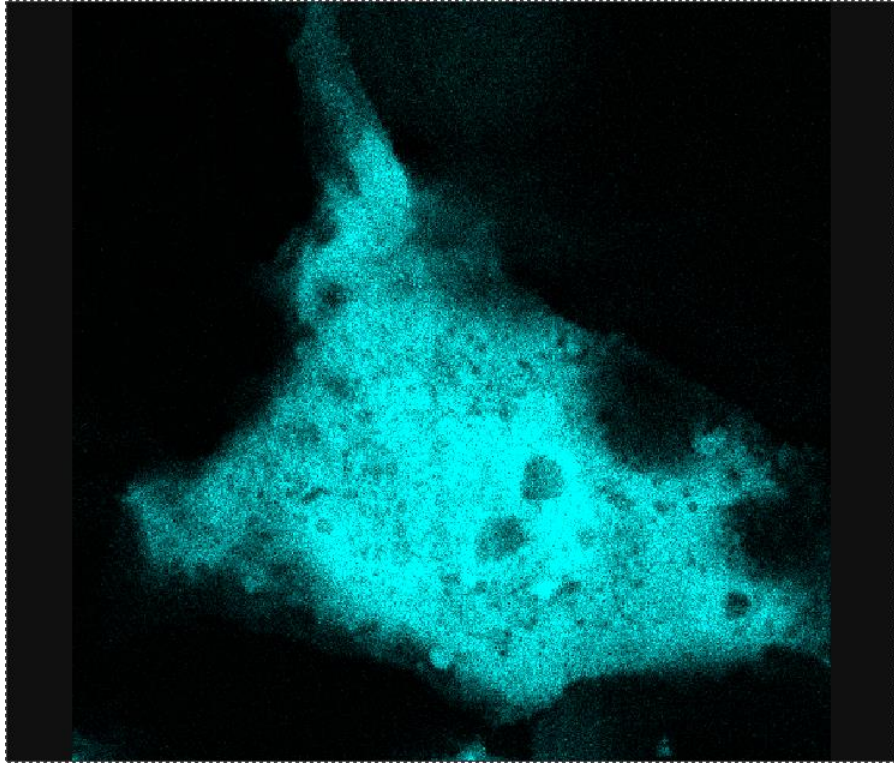
CFPYPF

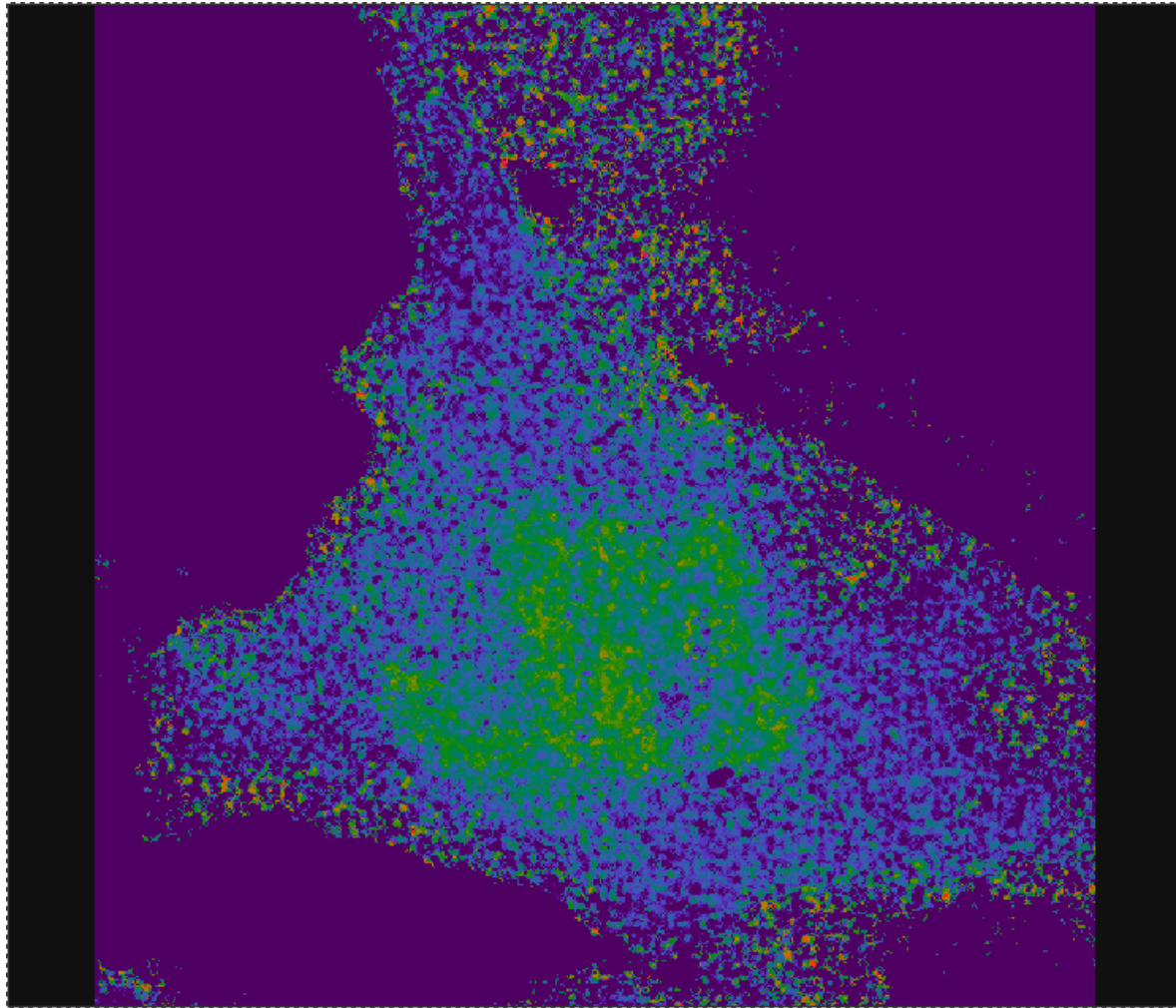


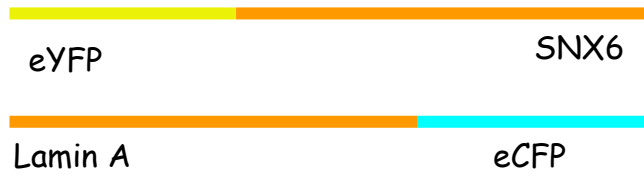
COS 7

LIM

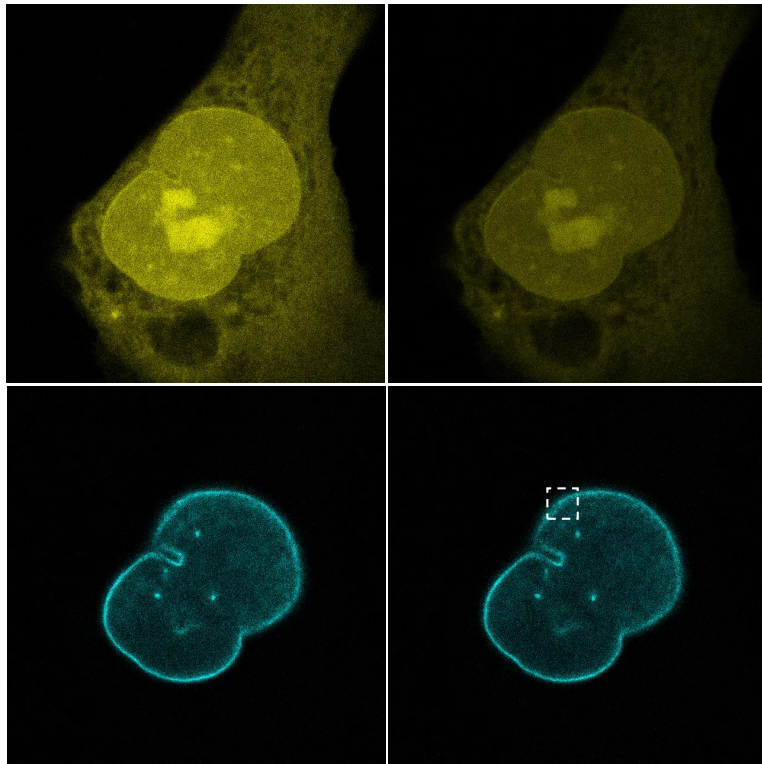






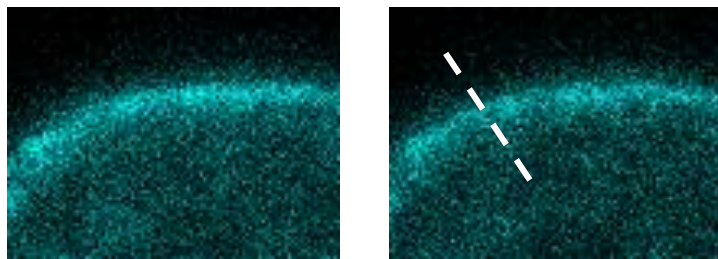


CFP-LMNA + YFP



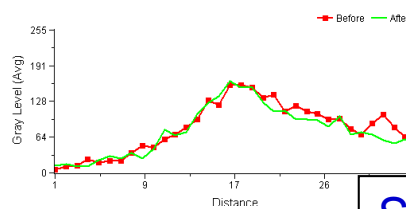
Before

After



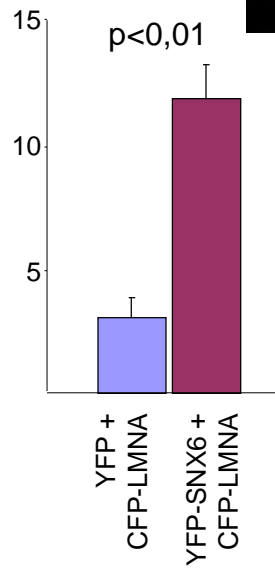
Before

After

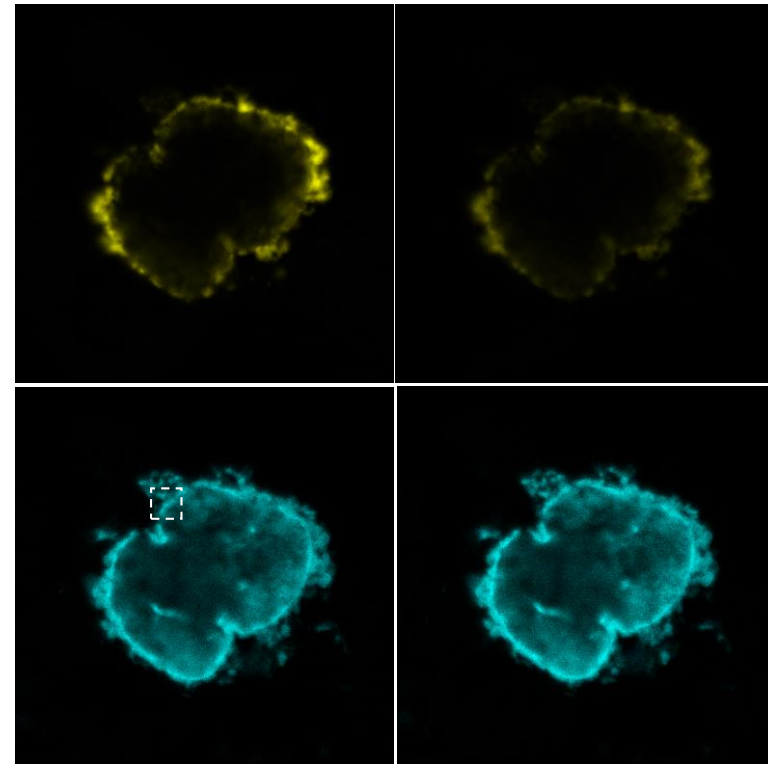


FRET

CFP fluorescence increment after photobleaching (%)

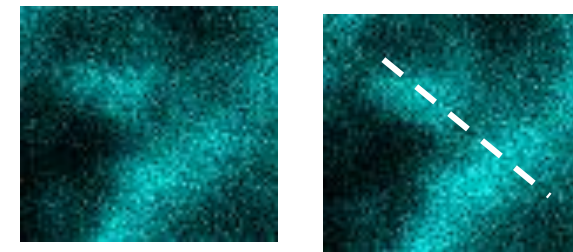


CFP-LMNA + SNX6-YFP



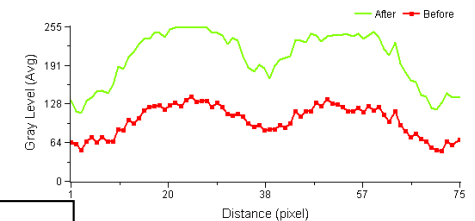
Before

After

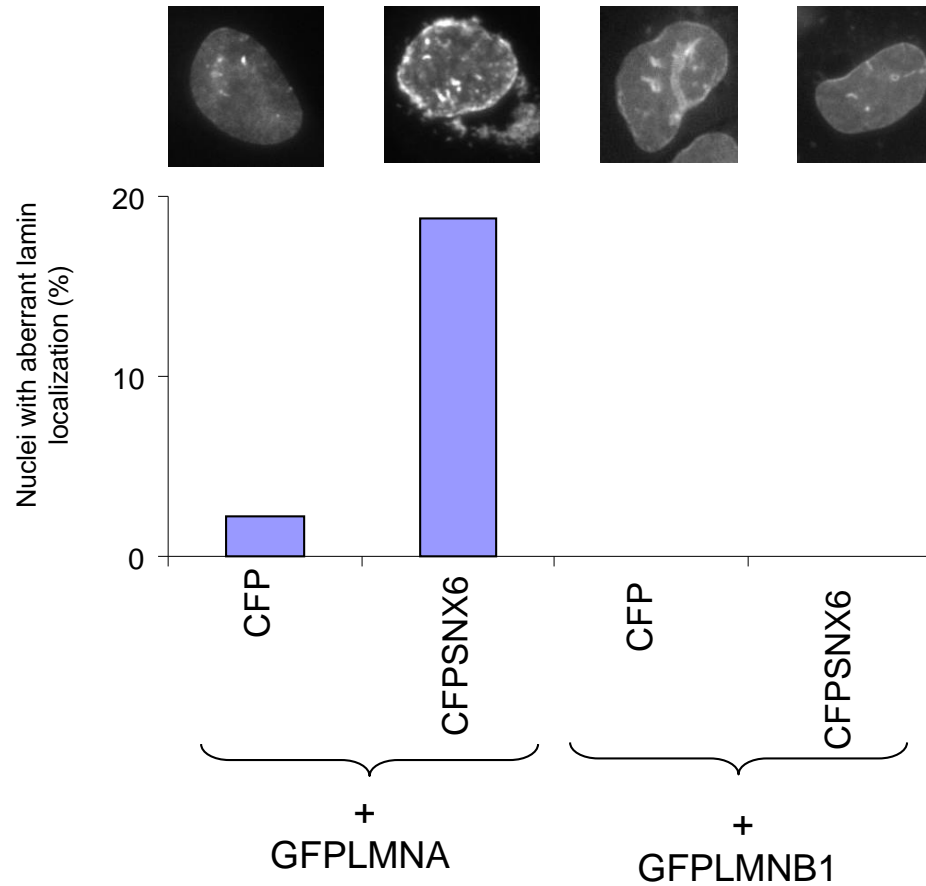


Before

After

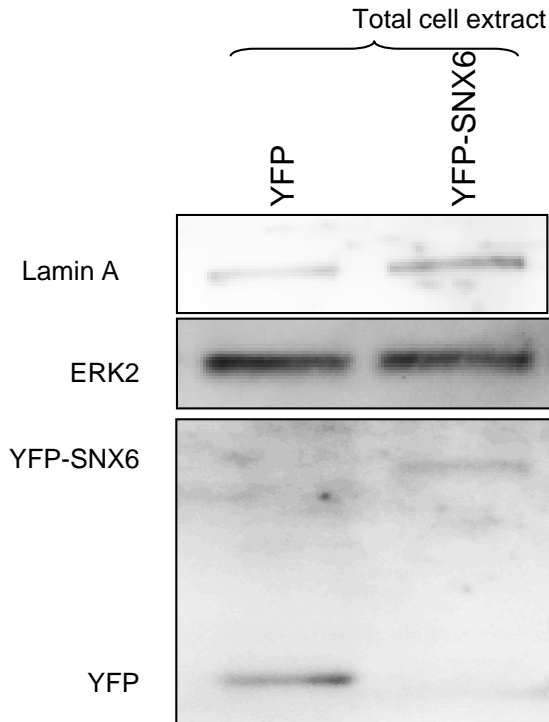
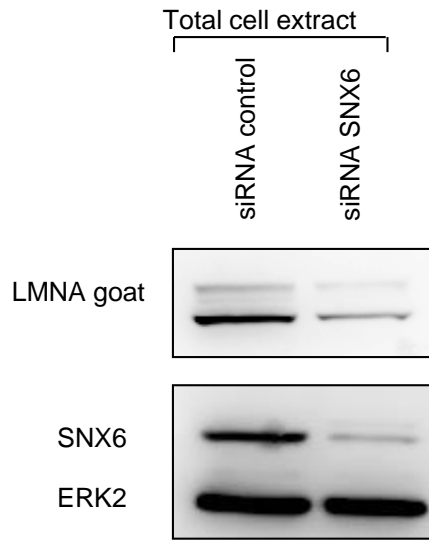
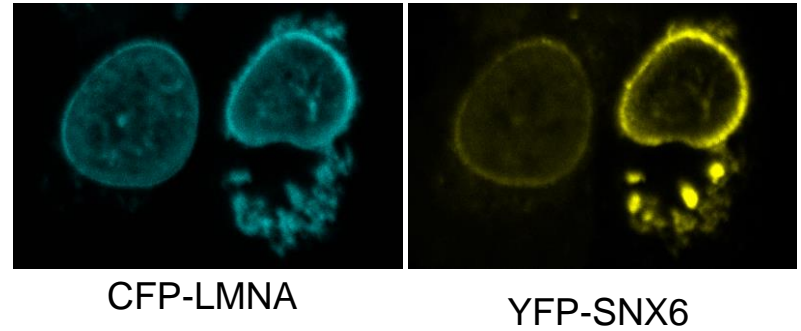


SNX6 interacts with Lamin A/C *in vivo*

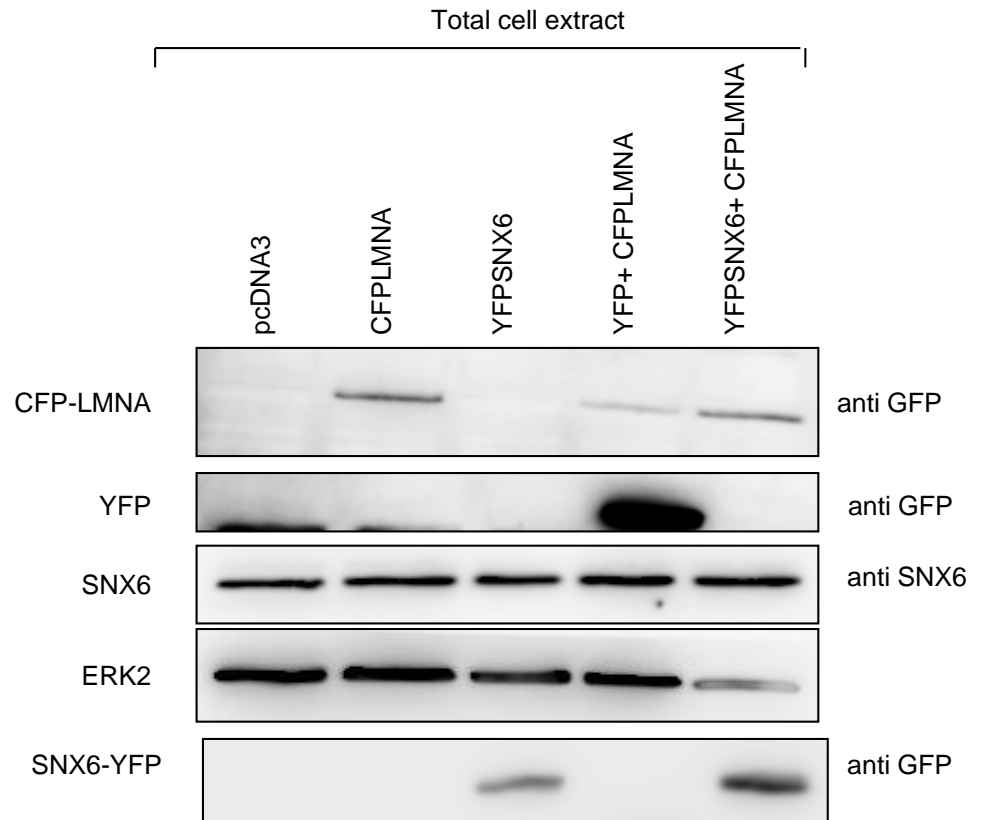


SNX6 does not disrupt lamin B1 localization

SYNTHESIS

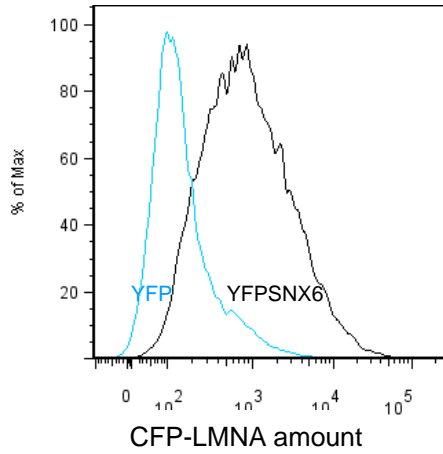


Anti GFP



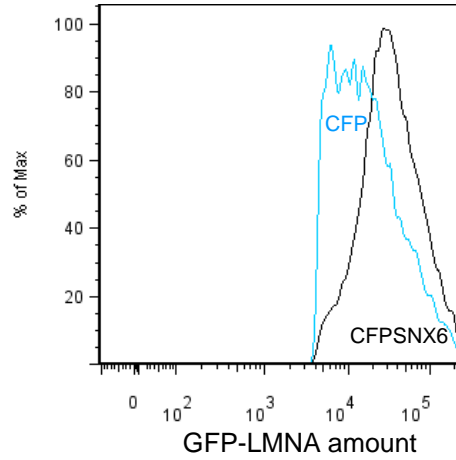
SNX6 overexpression increases the amount of Lamin A

FACs



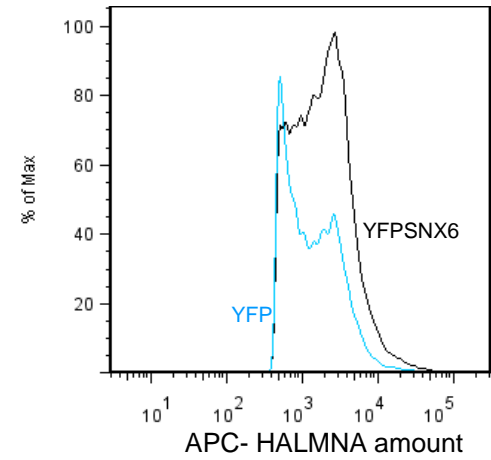
YFP
YFPSNX6

CFPLMNA +



CFP
CFPSNX6

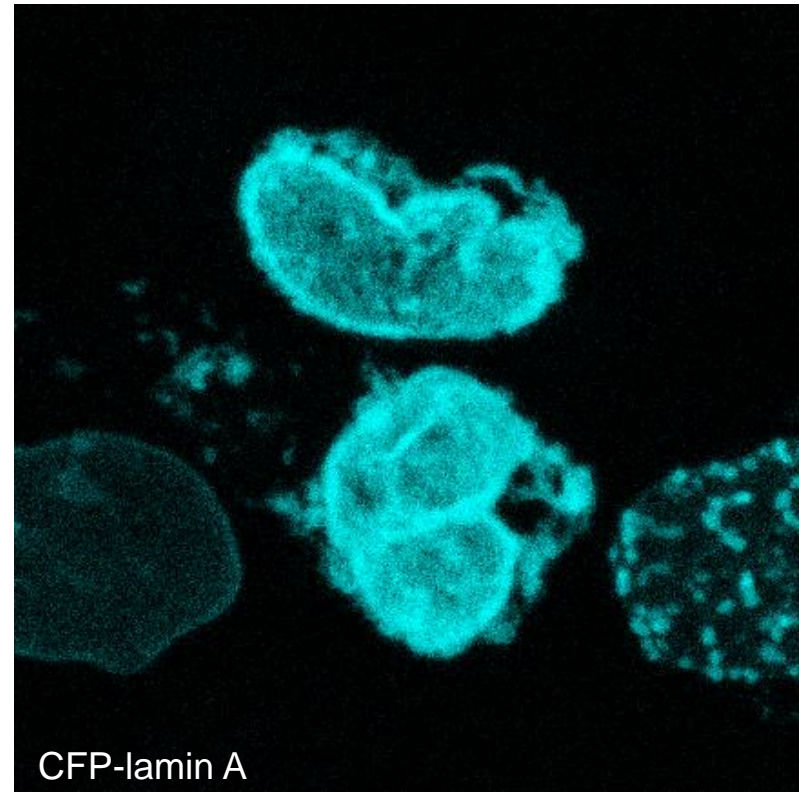
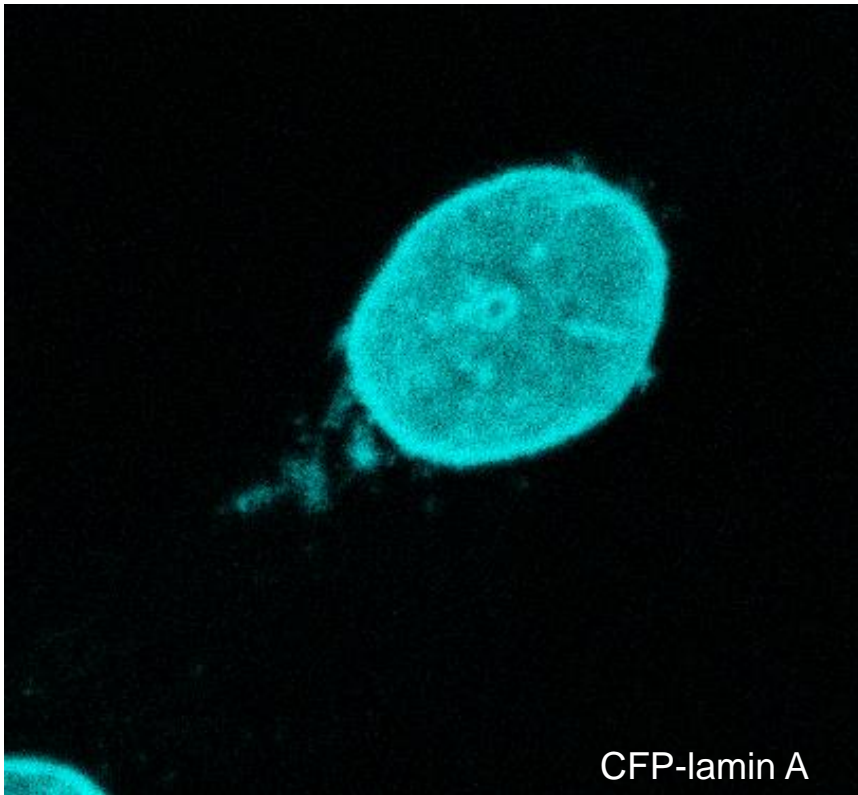
GFPLMNA +



YFP
YFPSNX6

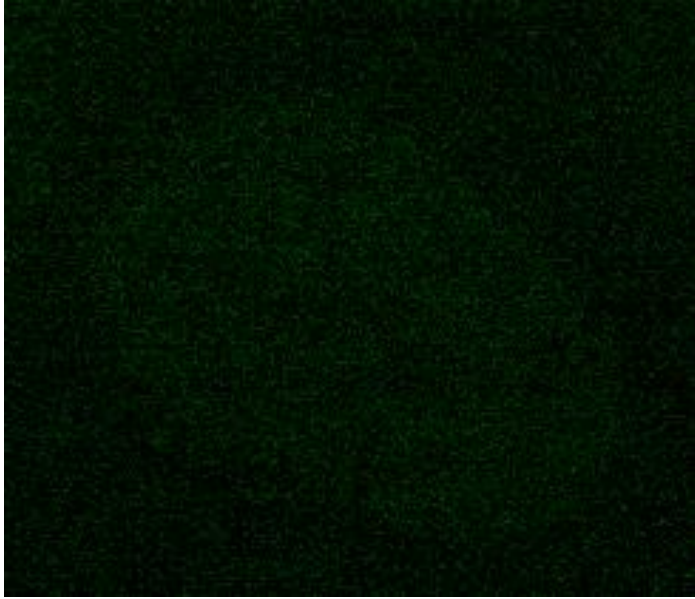
HA-LMNA +

SNX6 overexpression increases the amount of Lamin A

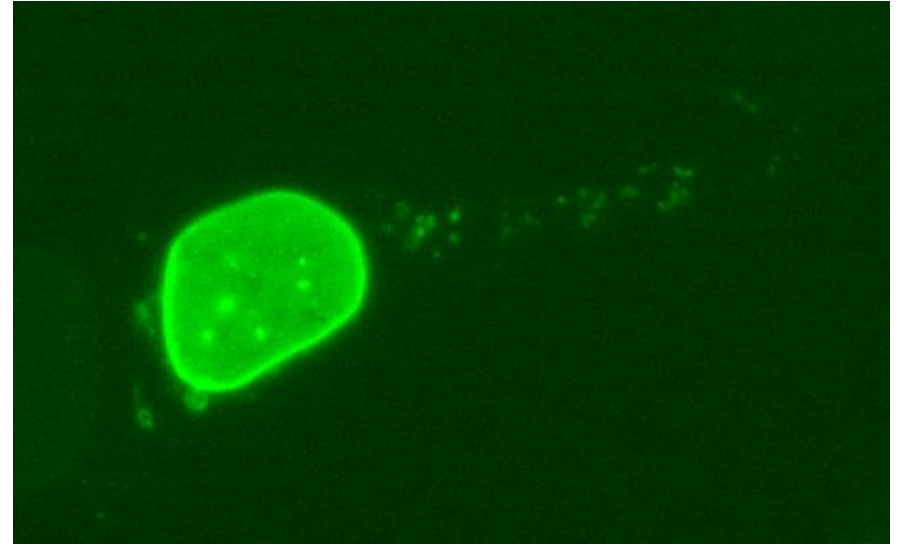


YFP-SNX6+CFP-lamin A. In vivo confocal microscopy. 10-20 h

GFPLMNA

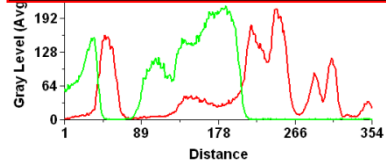
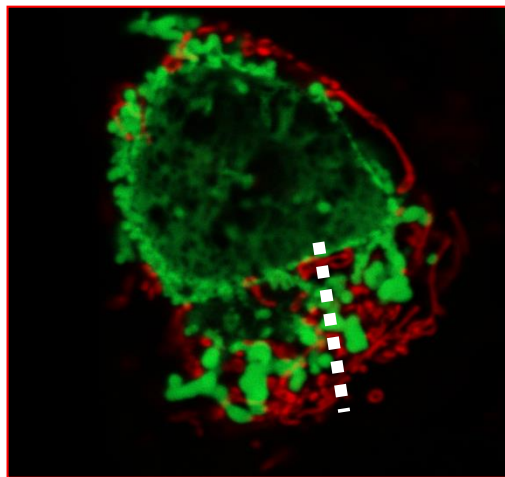


GFPLMNA only-transfected cells



HA-SNX6 transfected cell

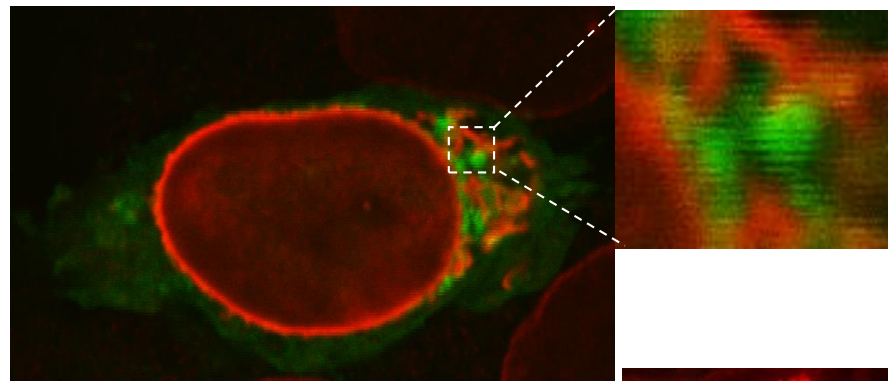
Mitochondria



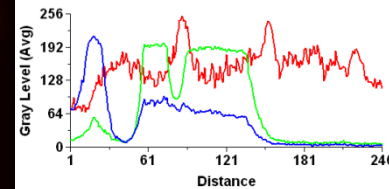
CFP-lamin A
Mitochondria

SNX6-Lamin A aberrant structures do not colocalize with the mitochondria or the golgi

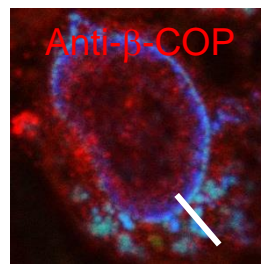
Golgi apparatus



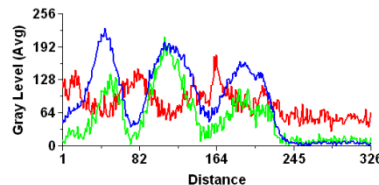
GPF-eNOS
CFP-LMNA
HA-SNX6



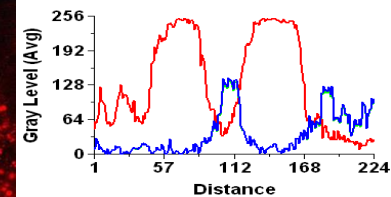
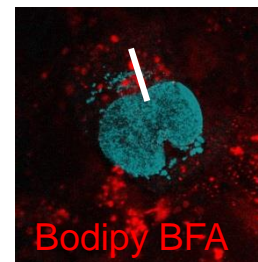
Rab7



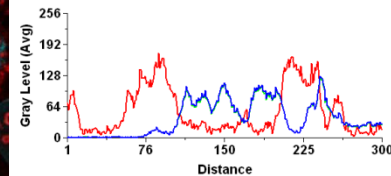
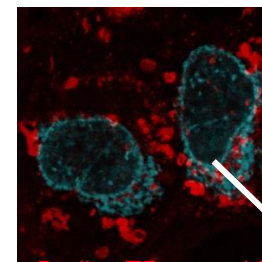
CFP-LMNA
YFP-SNX6



β-COP

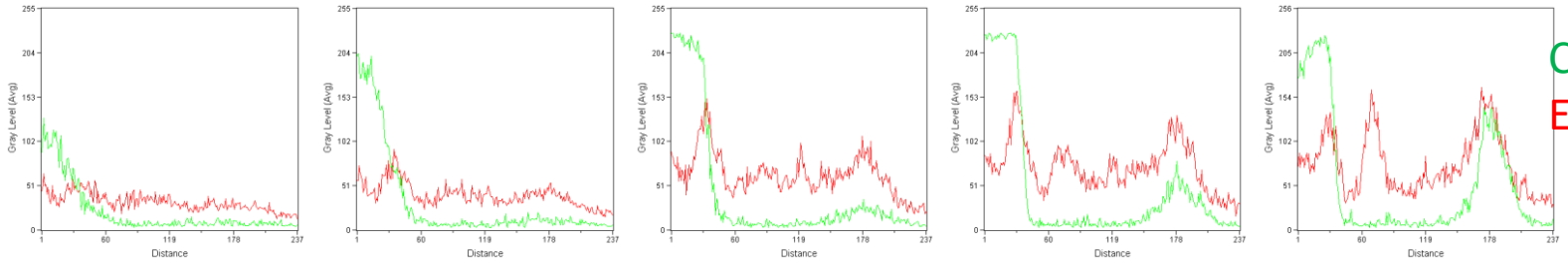
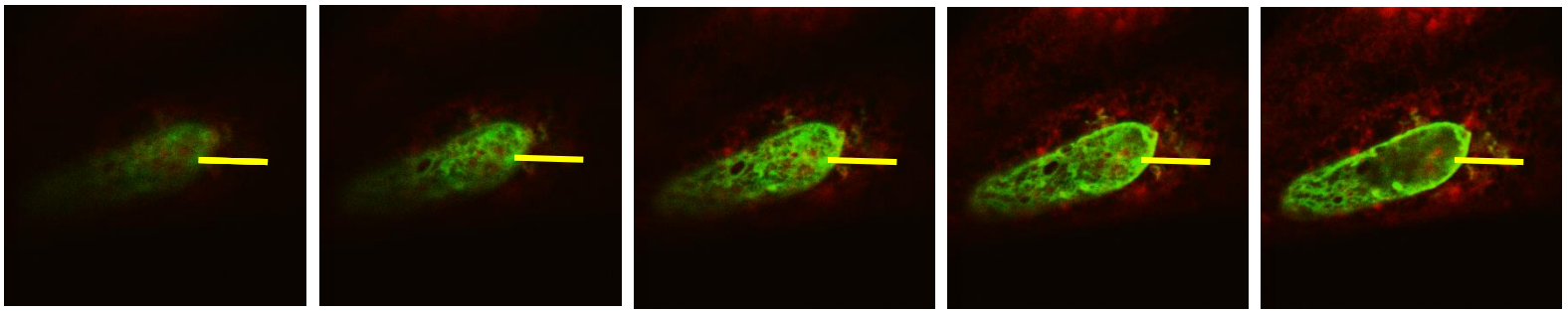


Bodipy BFA

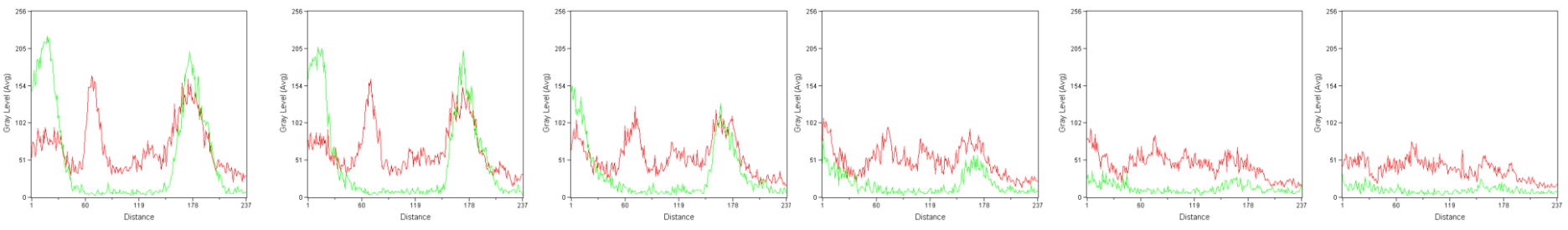
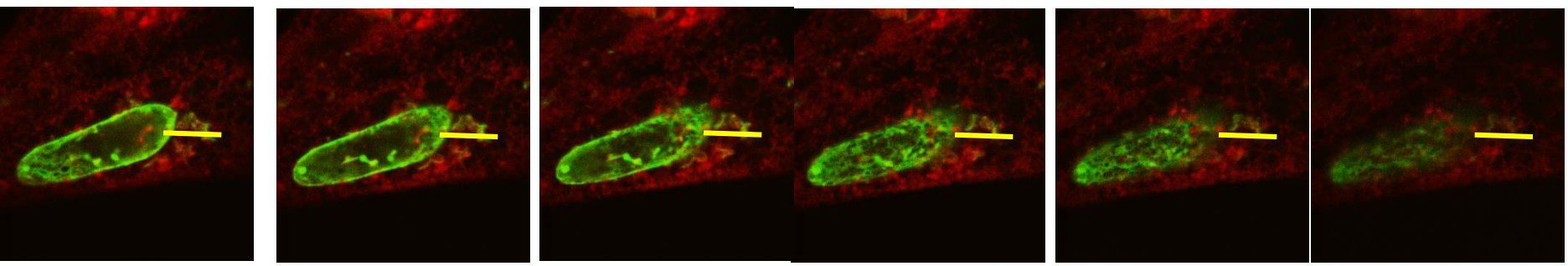


Bodipy TR ceramide

Bodipy TR ceramide

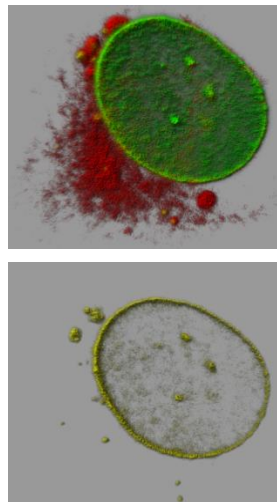
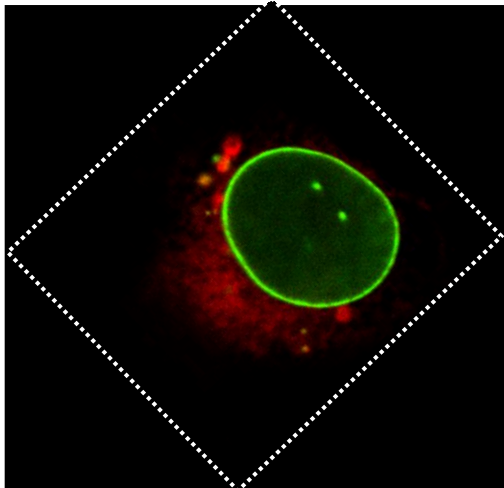
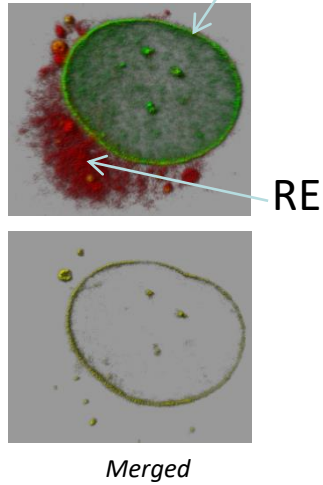
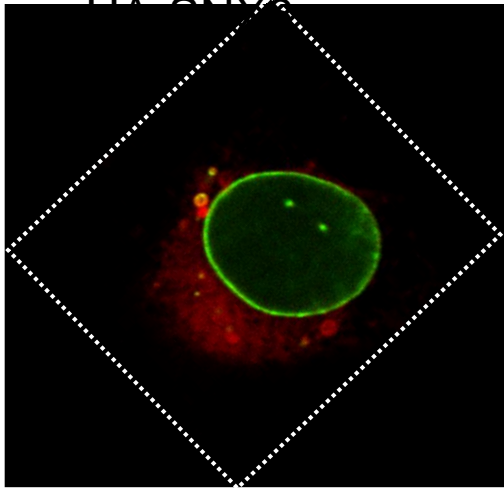


CFP-LMNA
ER-dsRED

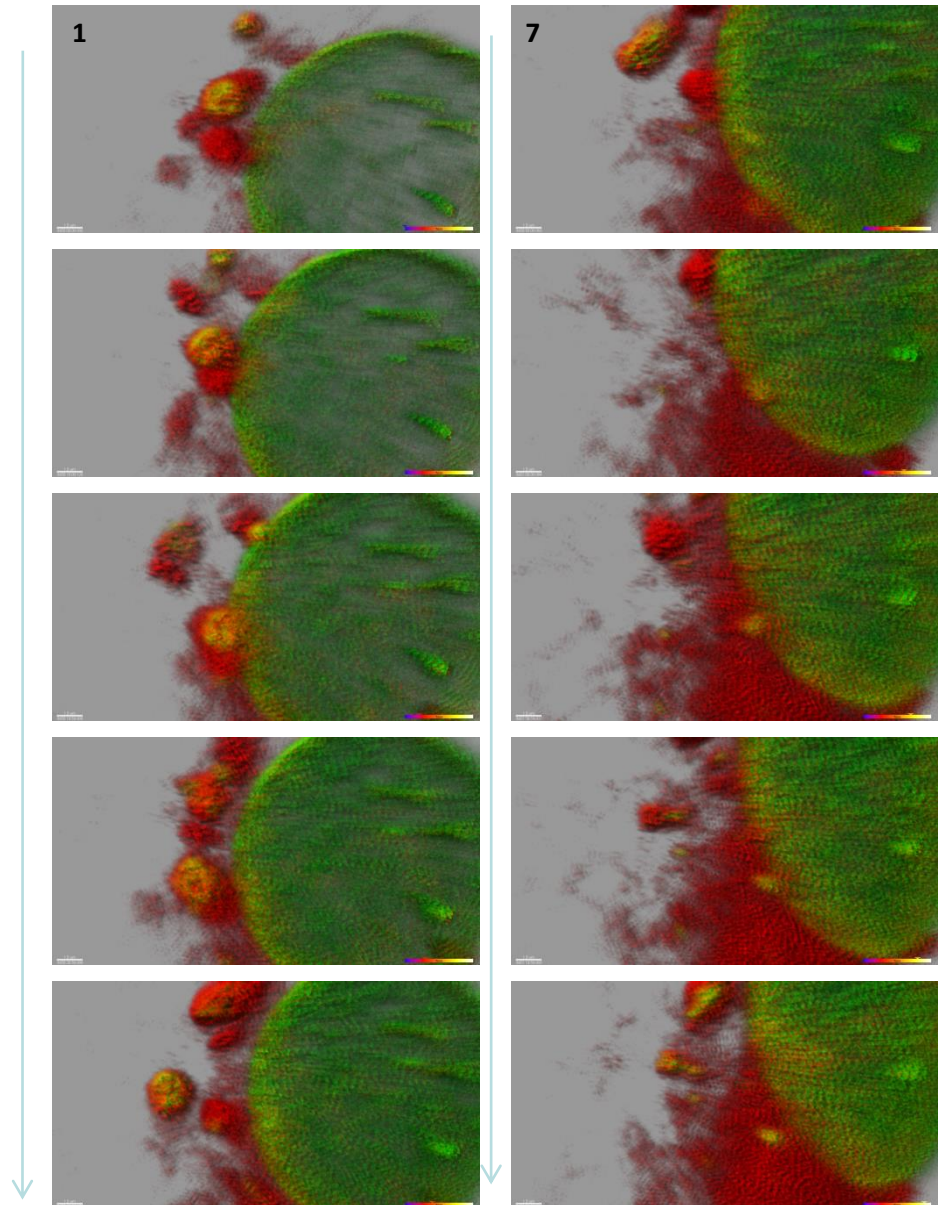


1. *In vivo*-microscopy

U2OS cells transfected with
RFP-SEC61 -- RE
GFP-Lamin A

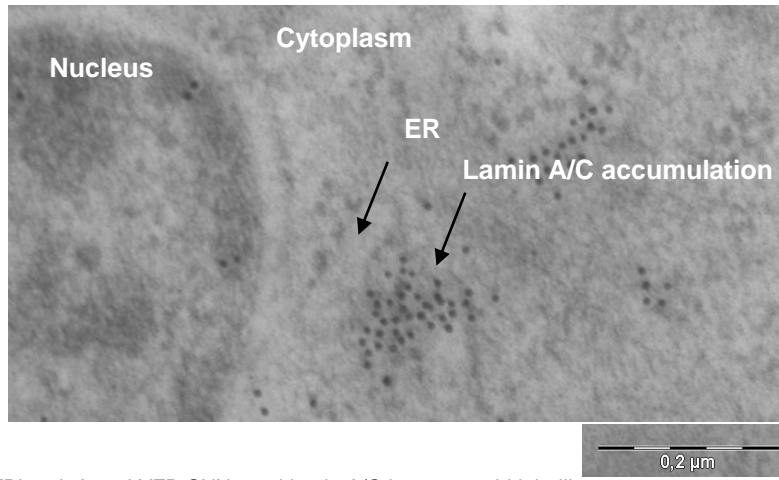


3D reconstruction

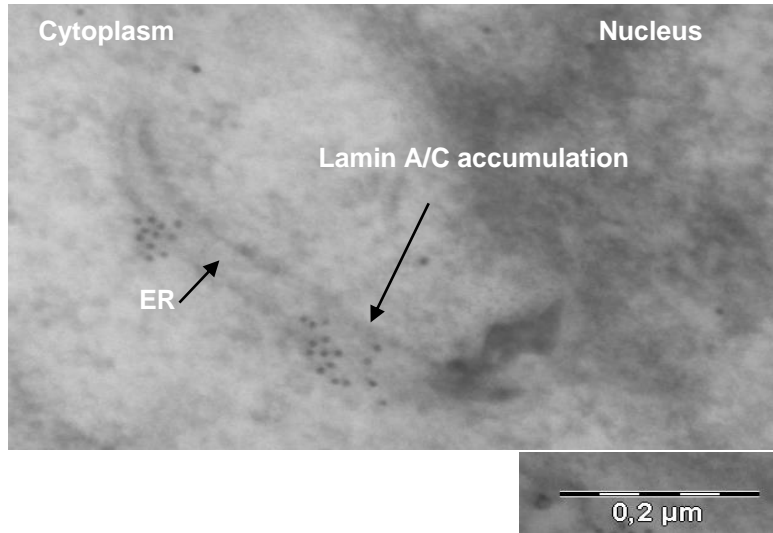


Crio-TEM

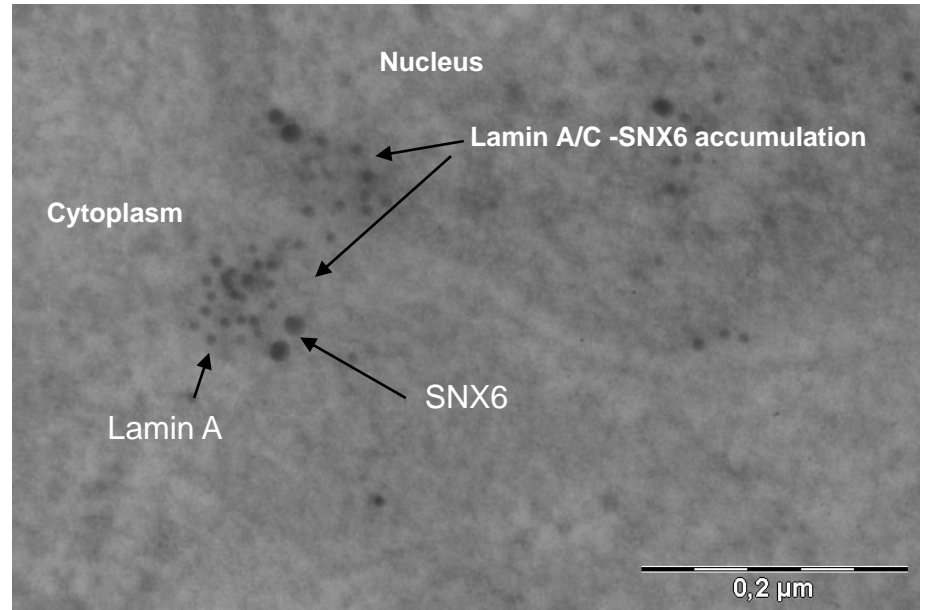
YFP-SNX6 transfected + anti lamin A/C immuno-gold labelling

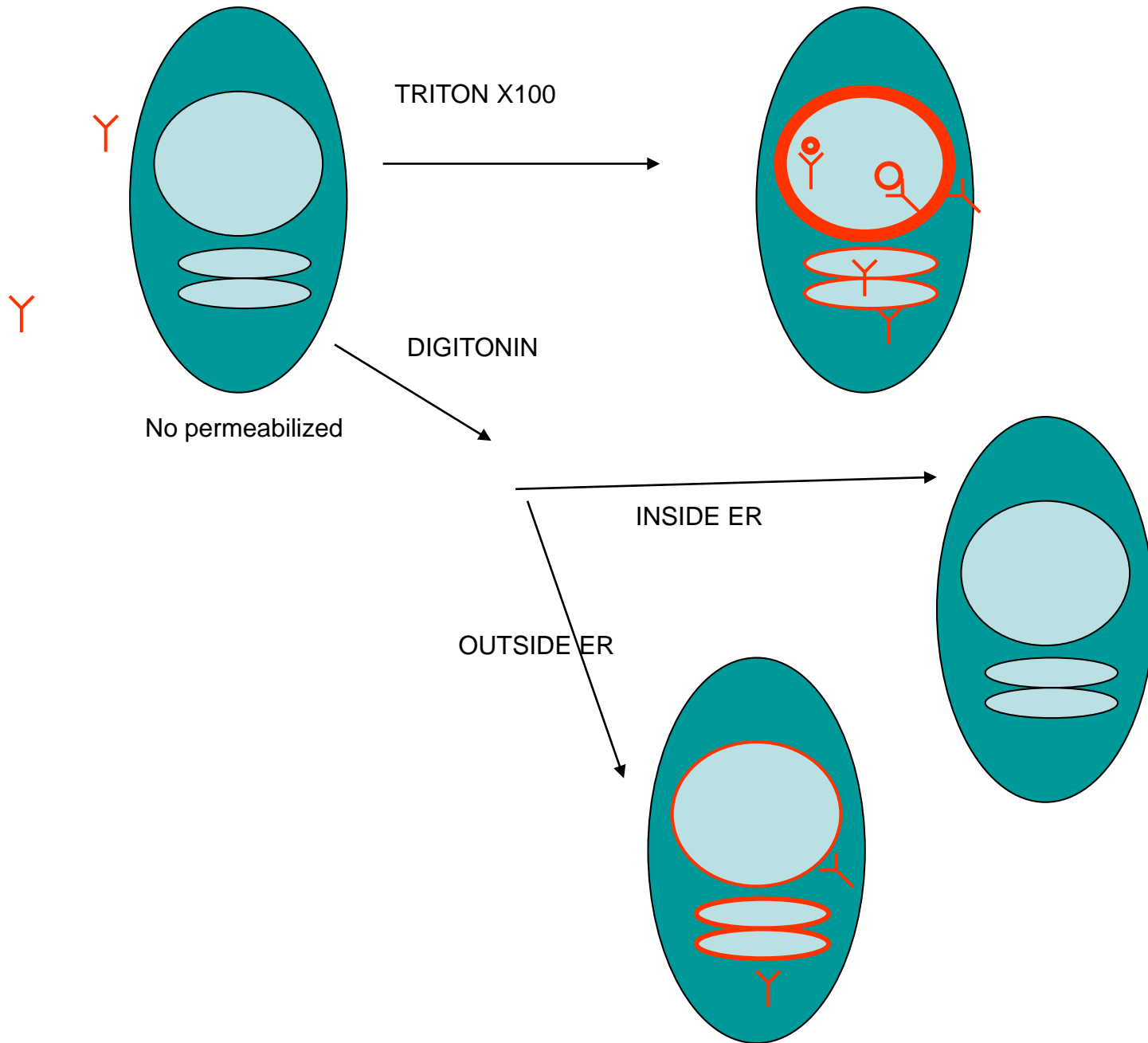


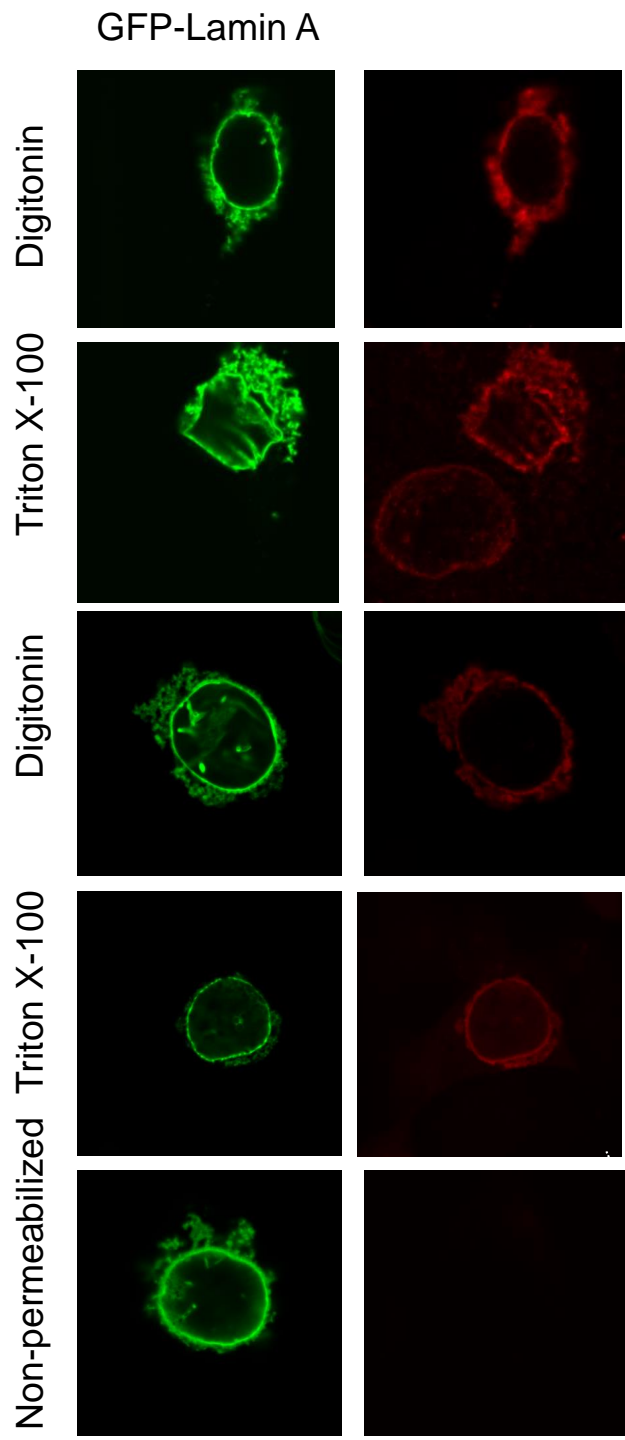
CFPLaminA and YFP-SNX6 anti lamin A/C immuno-gold labelling



CFPLaminA and YFP-SNX6 anti lamin A/C and SNX-6 immuno-gold labelling



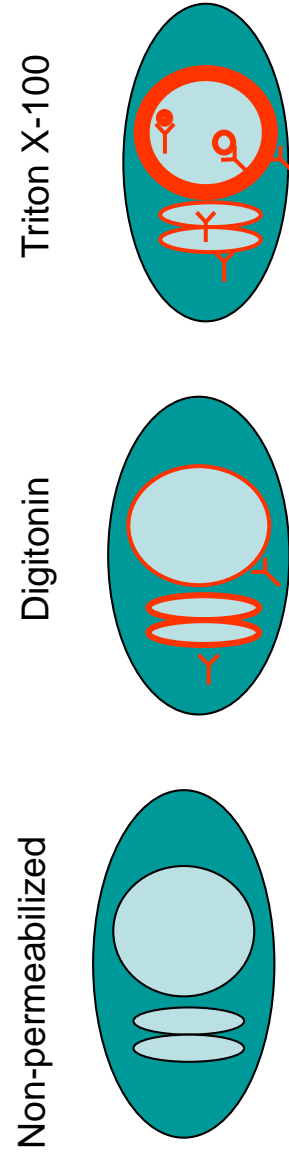




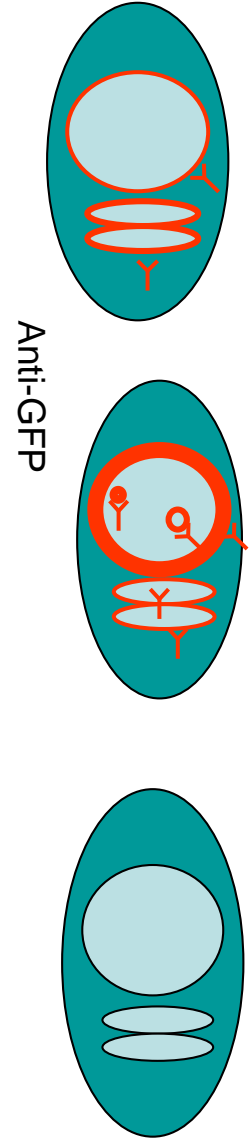
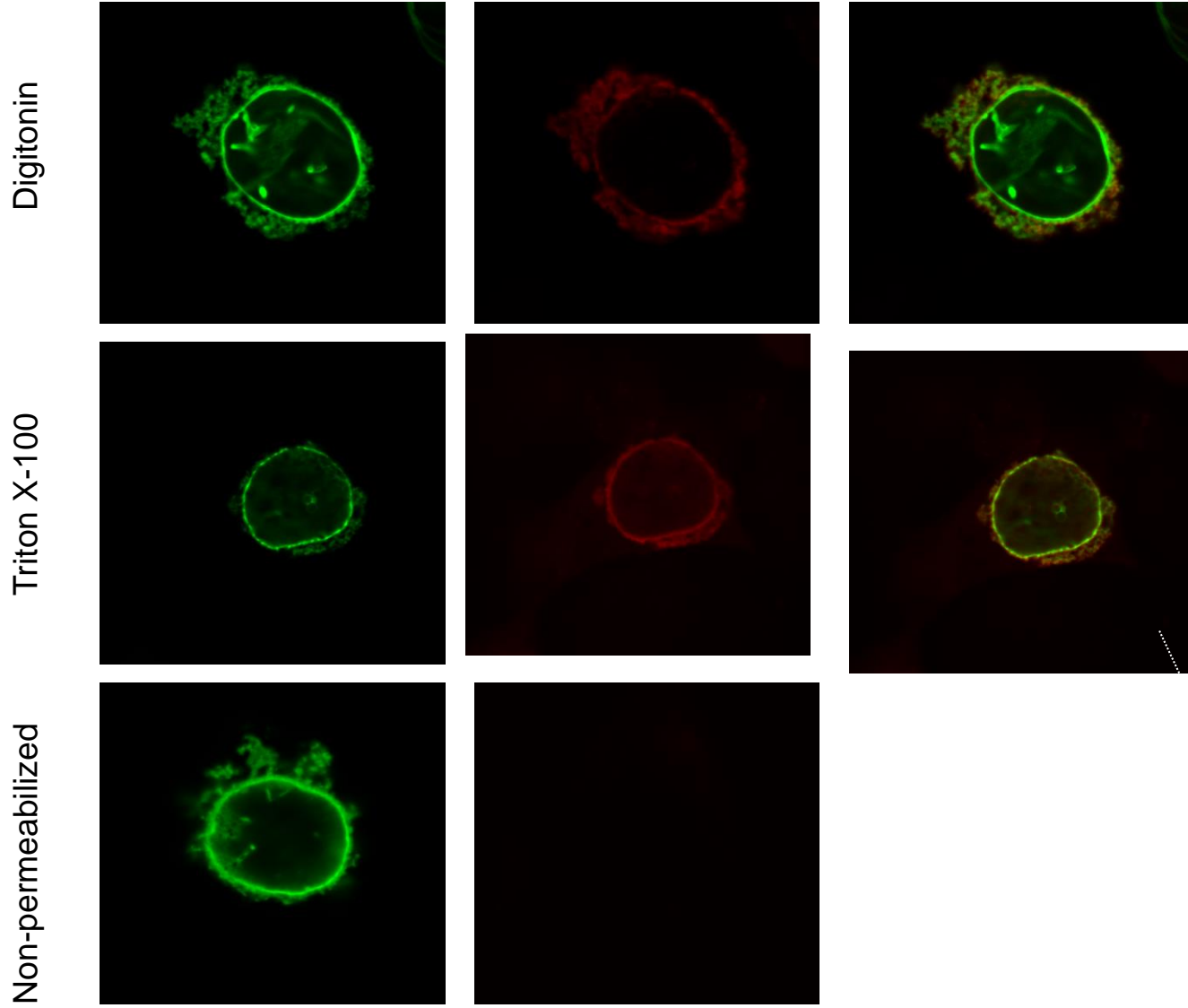
Anti-Lamin A/C

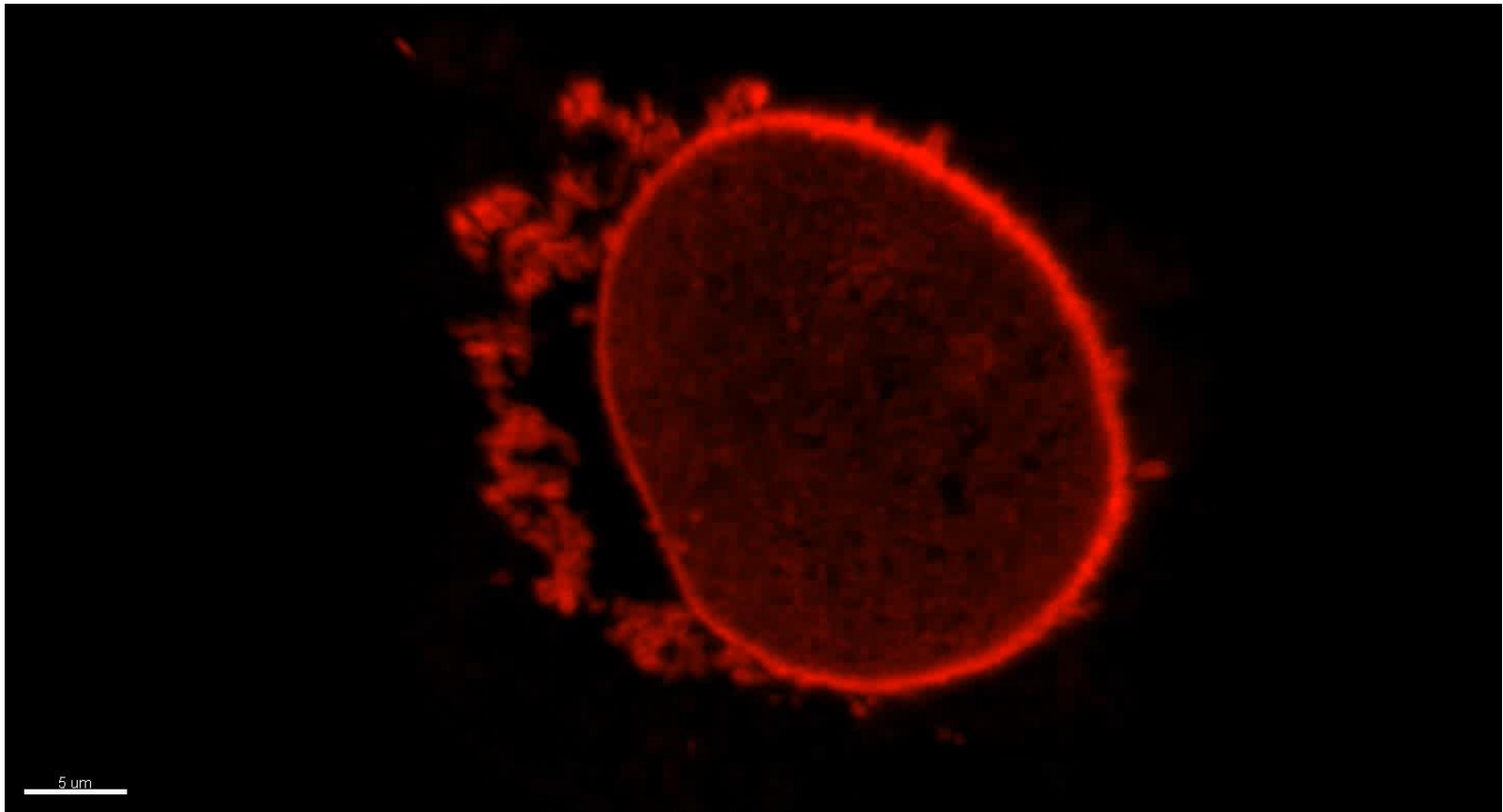
Anti-GFP

U2OS GFP-Lamin A
+HASNX6



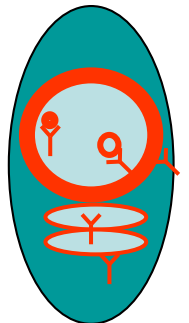
U20S GFP-Lamin A
+HASNX6

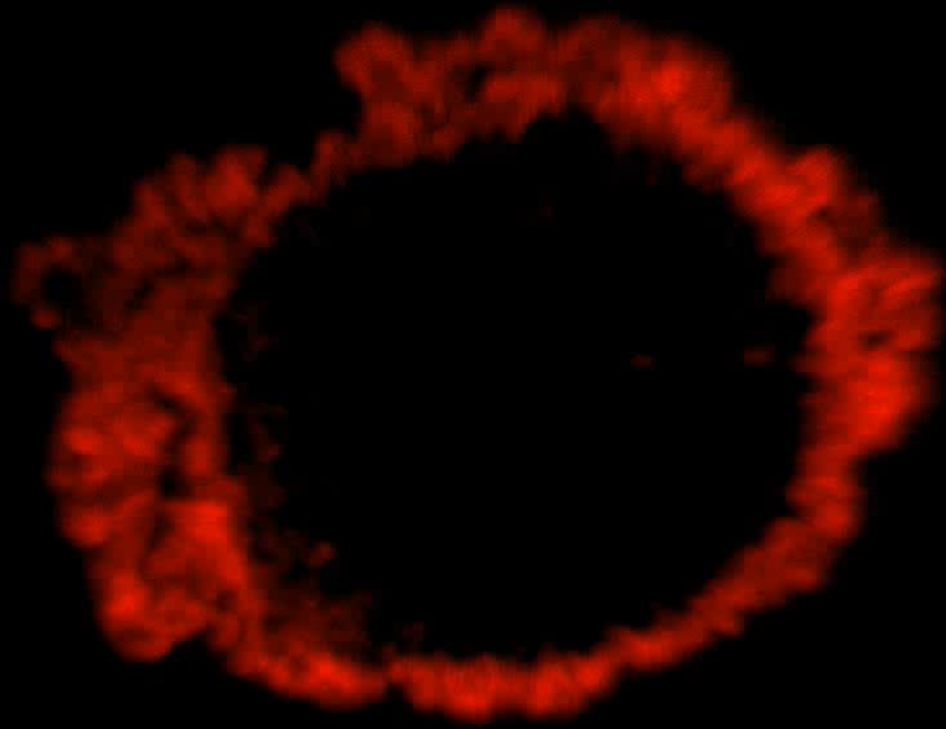




GFP-Lamin A – Green
Antibody anti-Lamin A – Red

Triton X-100

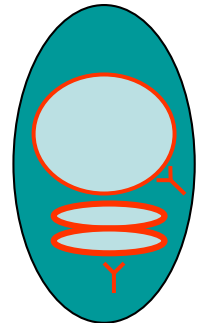




3 μ m

GFP-Lamin A – Green
Antibody anti-Lamin A – Red

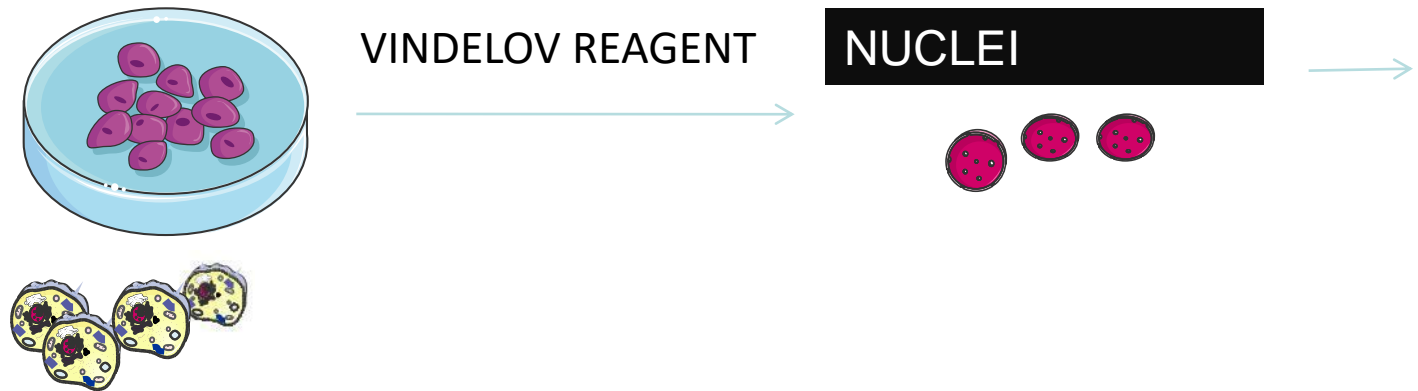
Digitonin



HOW ARE SNX6-LMNA ENTERING INTO NUCLEUS?

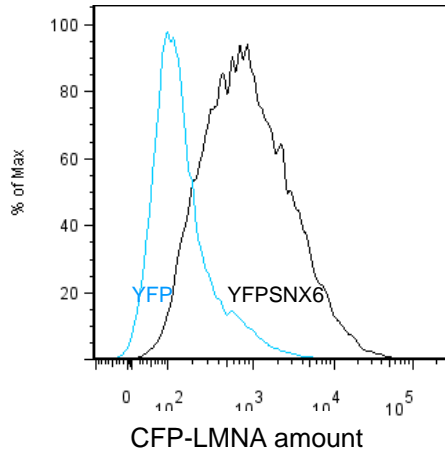
VIA ER?

U2OS transfection (LMNA-CFP, HA-SNX6 and RTN)



Cellular CFP-LMNA

FACs



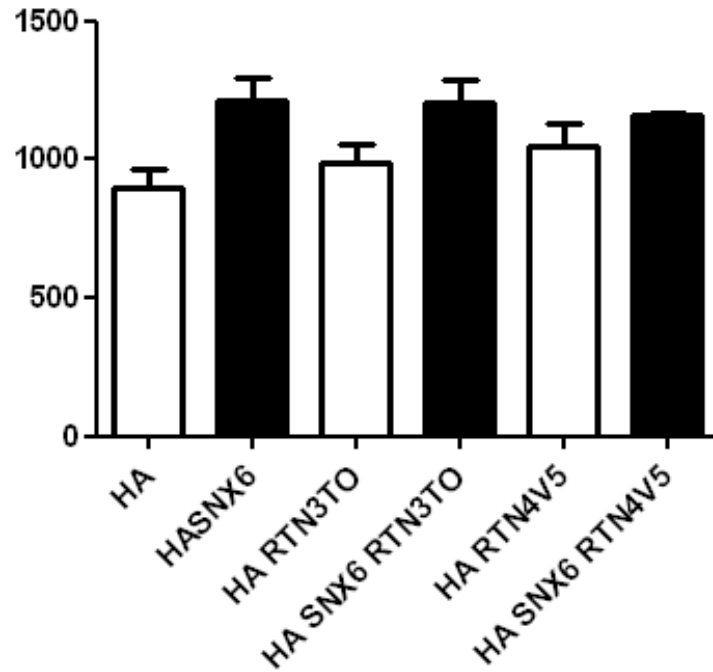
YFP

YFPSNX6

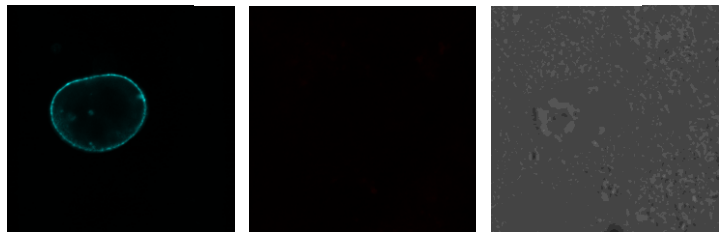
CFPLMNA +

Nuclear CFP-LMNA

MEAN INTENSITY

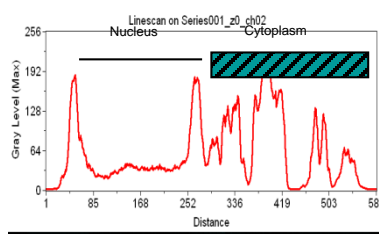


CFP-Lamin A + HA

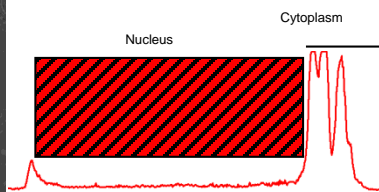
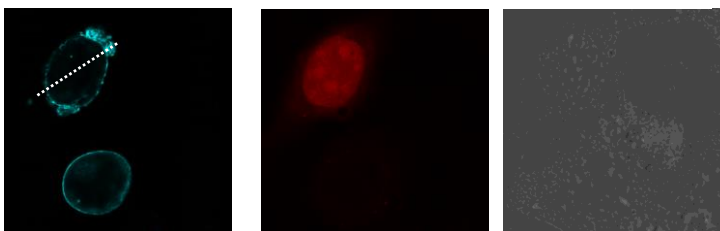


ACROSS NPC?

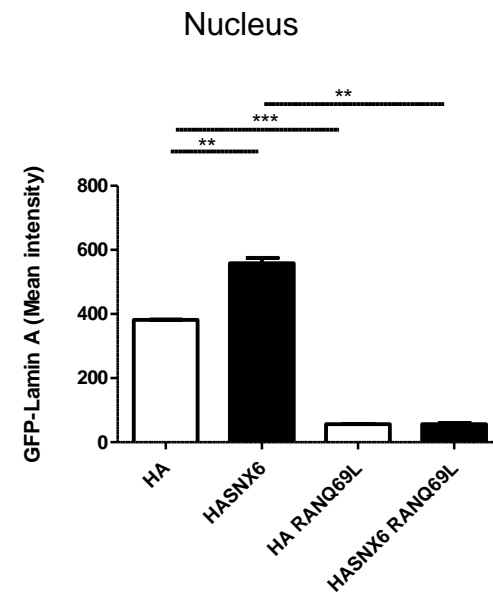
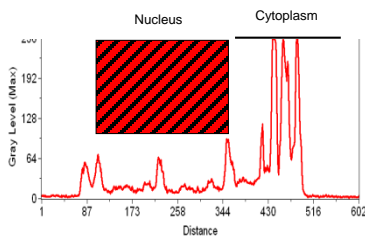
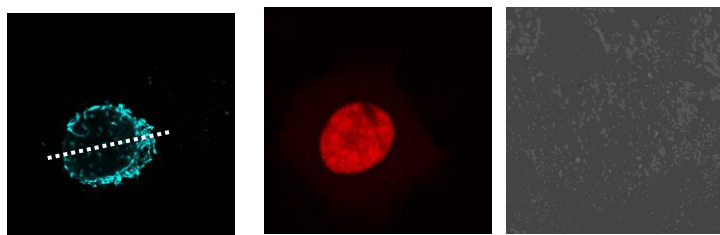
CFP-Lamin A + HASNX6

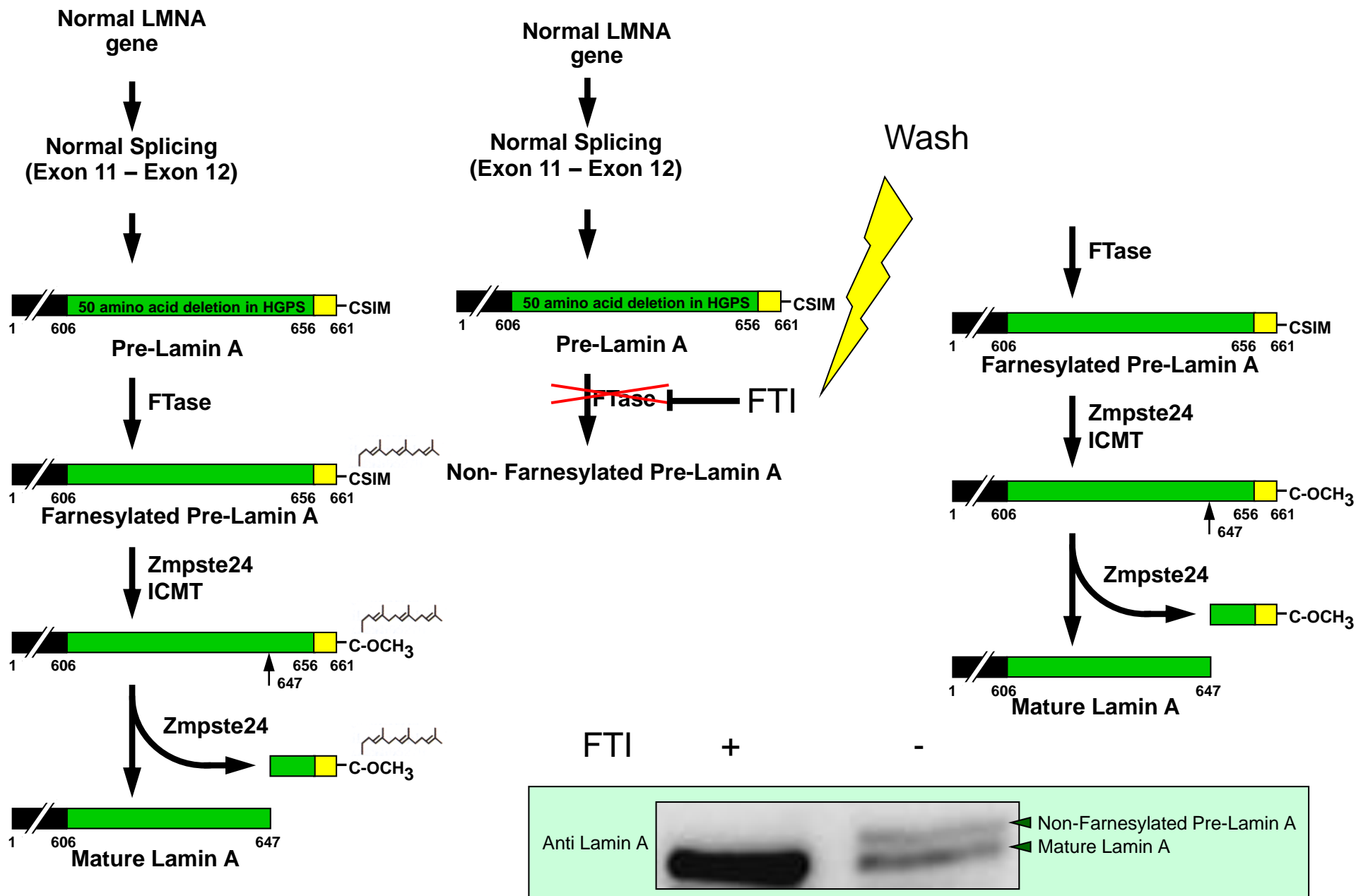


CFP-Lamin A + RAN Q69L



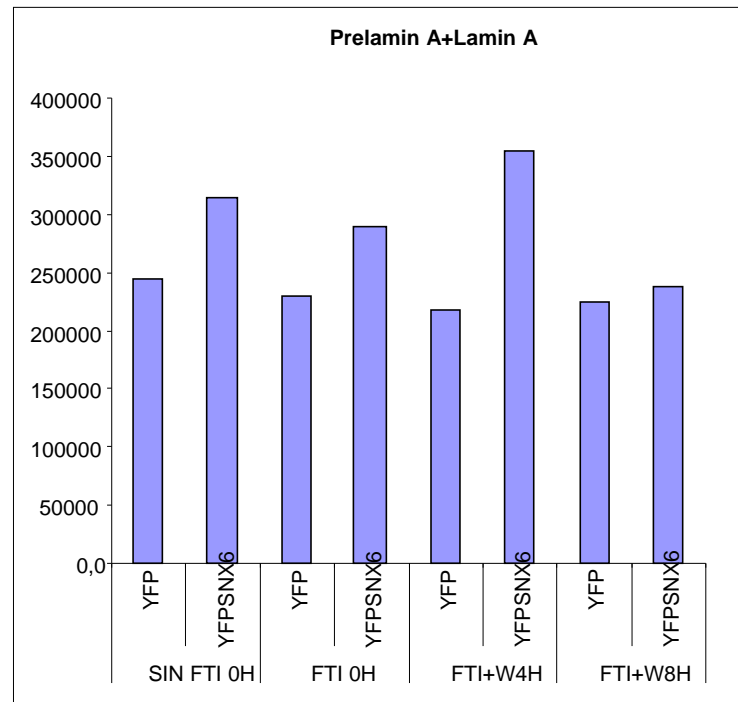
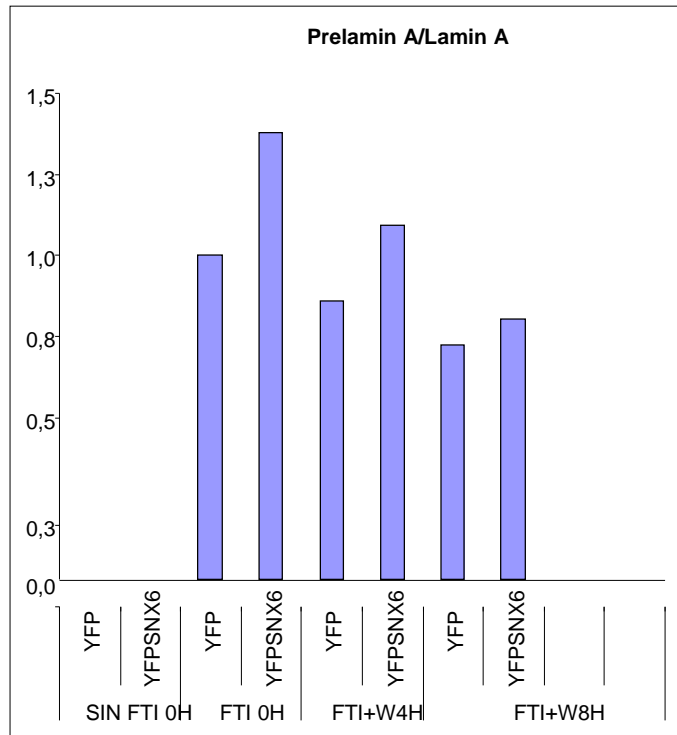
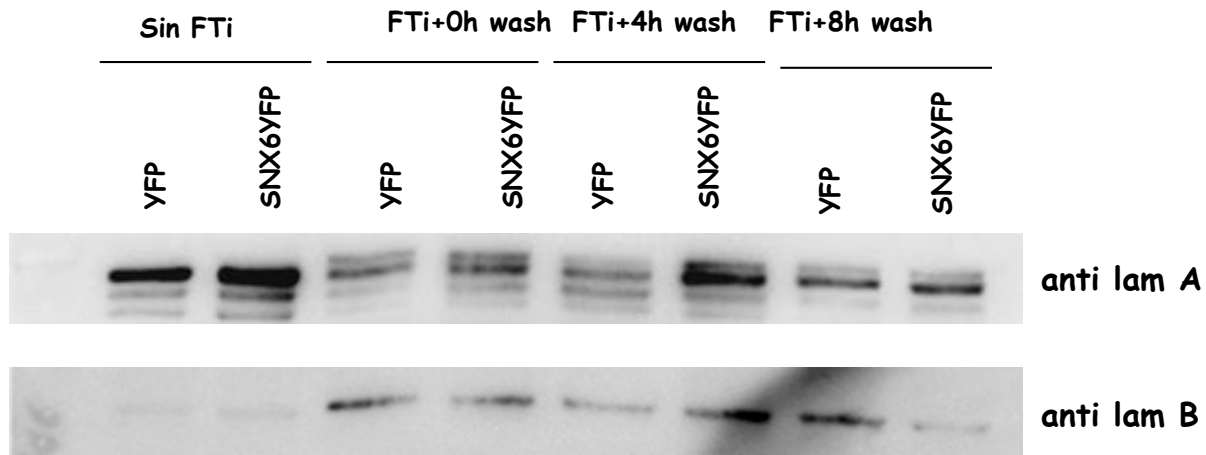
CFP-Lamin A + RAN Q69L+ HASNX6





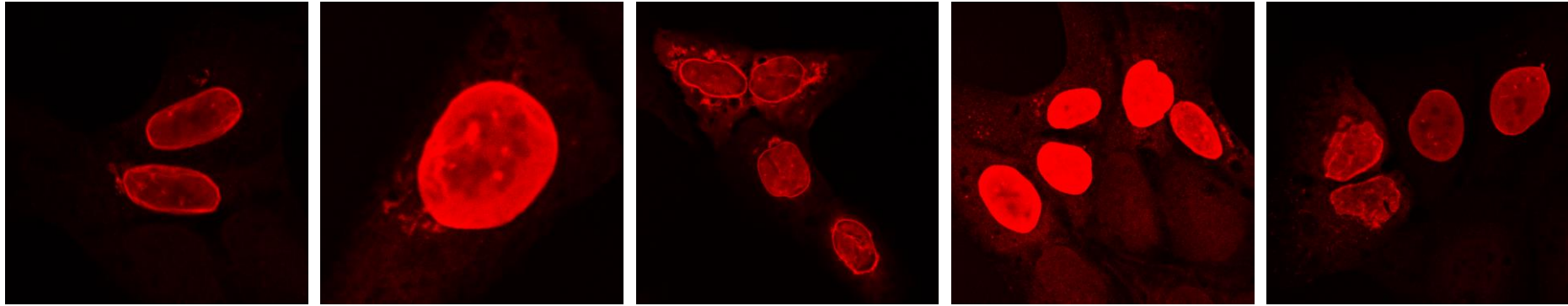
766

+CHX

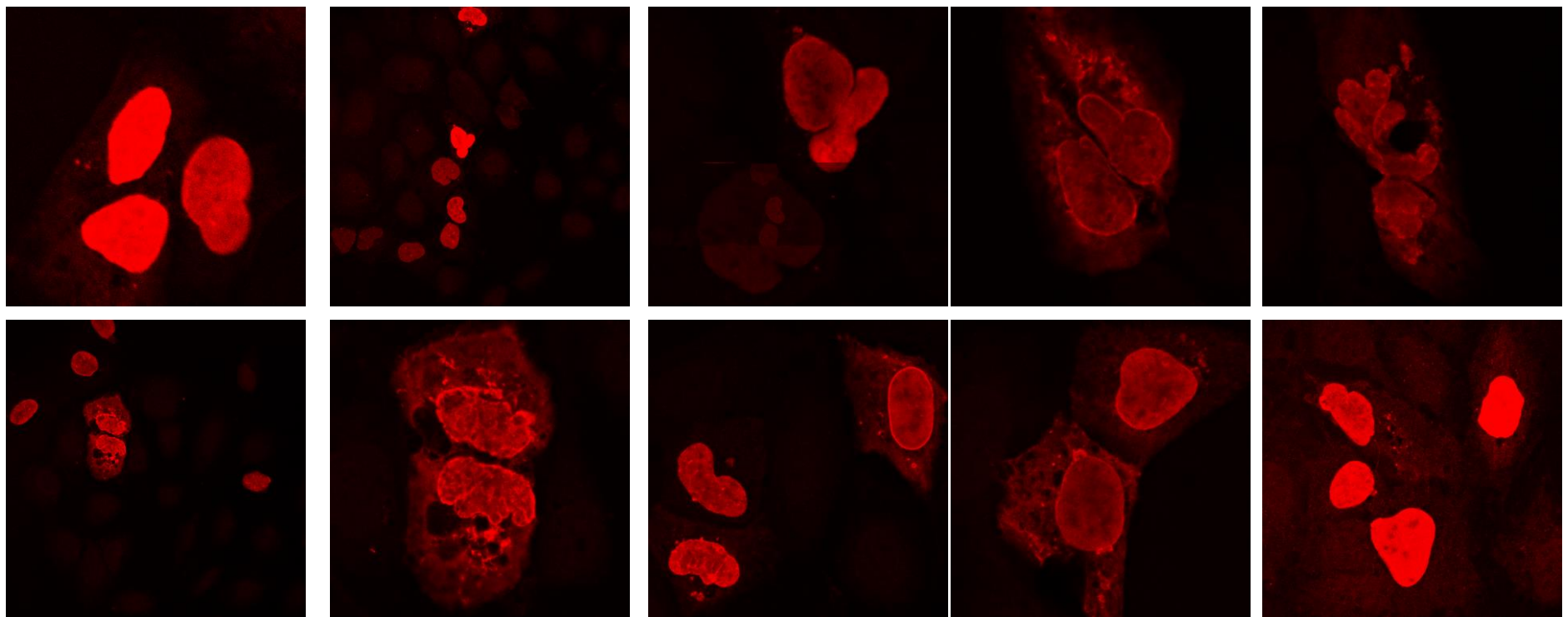


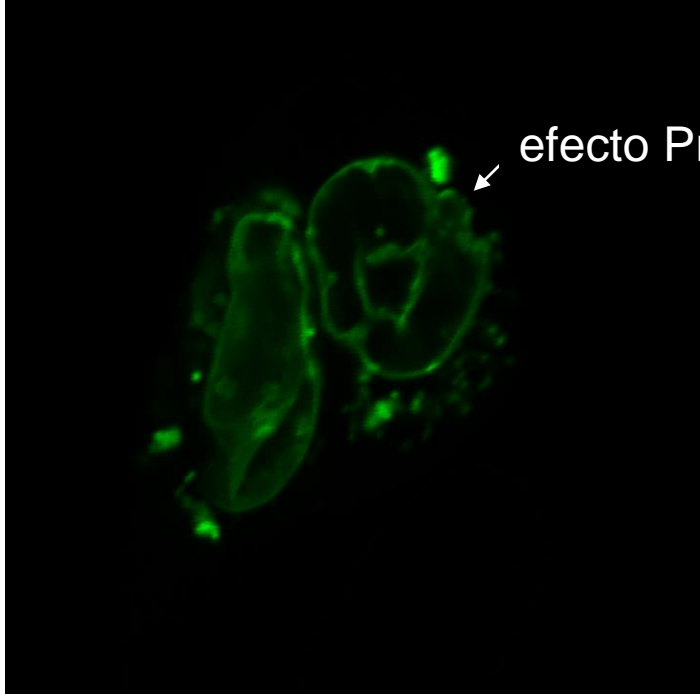
Flag-SNX6 +

HA-LMNA wt

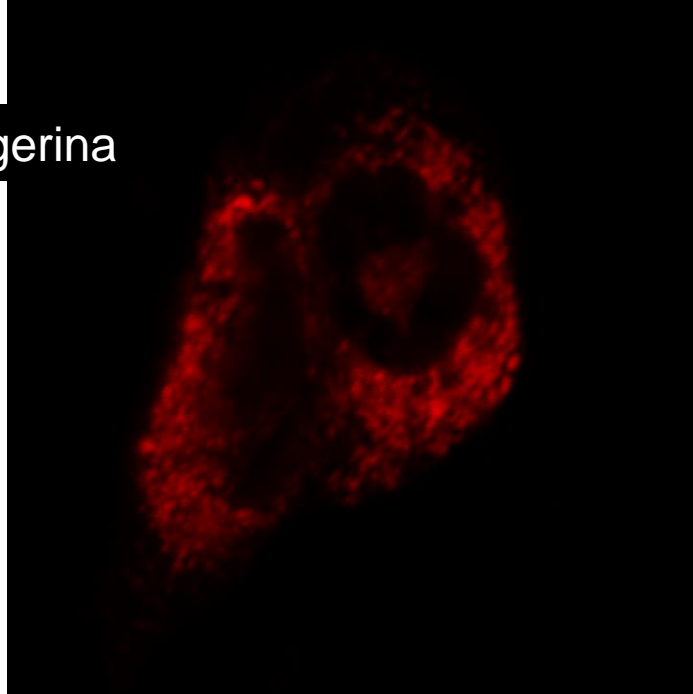


HA-PROGERIN

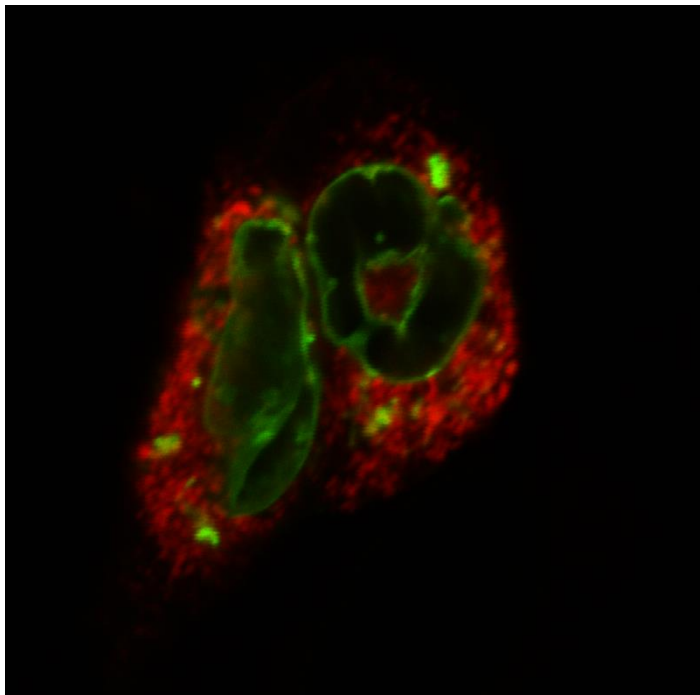




GPF-PROG



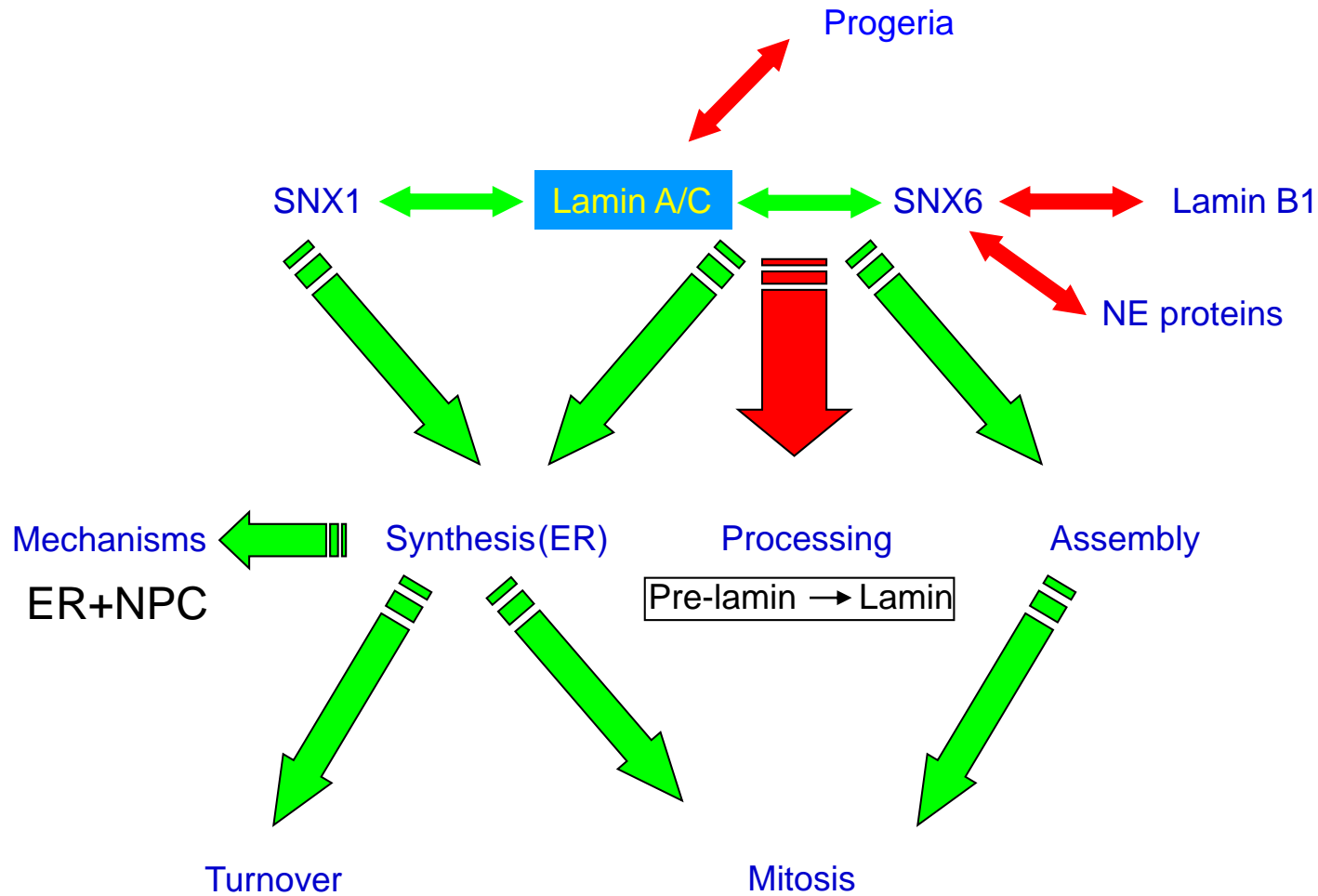
RE-dsRED



MERGE

GFP proge +HA SNX6 + RE-dsRED

CONCLUSIONS



NEXT...

RESEARCH ARTICLE

Sorting Nexin 6 Enhances Lamin A Synthesis and Incorporation into the Nuclear Envelope


Jose M. González-Granado¹, Ana Navarro-Puche¹, Pedro Molina-Sanchez¹, Marta Blanco-Berrocal¹, Rosa Viana², Jaime Font de Mora³, Vicente Andrés^{1*}

1. Department of Atherothrombosis, Imaging and Epidemiology, Centro Nacional de Investigaciones Cardiovasculares (CNIC), Madrid, Spain, **2.** Instituto de Biomedicina de Valencia (IBV), Consejo Superior de Investigaciones Científicas, Valencia, Spain, **3.** Fundación para la Investigación Hospital La Fe, and Instituto Valenciano de Patología, Facultad de Medicina, Universidad Católica de Valencia San Vicente Mártir, Valencia, Spain

*vandres@cnic.es



CrossMark
click for updates

 OPEN ACCESS

Citation: González-Granado JM, Navarro-Puche A, Molina-Sanchez P, Blanco-Berrocal M, Viana R,

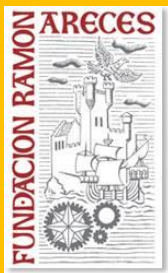
Acknowledgments

Laboratory:

- Dr. Francisco Sanchez-Madrid
- Dr. David Sancho
- Dr. Vicente Andrés
- Dr. José Luis Pablos
- Dr. Joaquín Arenas



Sigurd, Raquel, Virginia y Carmen



Programa Miguel Servet (ISCIII)

